

**KINETIC AND SIMULATION STUDIES OF THE
ESTERIFICATION OF ACRYLIC ACID WITH 2-
ETHYL HEXANOL IN A BATCH AND PACKED
BED REACTOR**

MOHD AMIRUL ASYRAF BIN AHMAD

UMP

Doctor of Philosophy

UNIVERSITI MALAYSIA PAHANG

UNIVERSITI MALAYSIA PAHANG

DECLARATION OF THESIS AND COPYRIGHT

Author's Full Name : MOHD AMIRUL ASYRAF BIN AHMAD
Date of Birth : 16th November 1988
Title : KINETIC AND SIMULATION STUDIES OF THE ESTERIFICATION OF
WASTEWATER CONTAINING ACRYLIC ACID WITH 2-ETHYL
HEXANOL
Academic Session : SEM 1 2019/2020

I declare that this thesis is classified as:

- CONFIDENTIAL** (Contains confidential information under the Official Secret Act 1997)*
- RESTRICTED** (Contains restricted information as specified by the organization where research was done)*
- OPEN ACCESS** I agree that my thesis to be published as online open access (Full Text)

I acknowledge that Universiti Malaysia Pahang reserves the following rights:

1. The Thesis is the Property of Universiti Malaysia Pahang
2. The Library of Universiti Malaysia Pahang has the right to make copies of the thesis for the purpose of research only.
3. The Library has the right to make copies of the thesis for academic exchange.

Certified by:

(Student's Signature)

(Supervisor's Signature)

New IC/Passport Number
Date:

Name of Supervisor
Date:

NOTE : * If the thesis is CONFIDENTIAL or RESTRICTED, please attach a thesis declaration letter.

SUPERVISOR'S DECLARATION

We hereby declare that we have checked this thesis and in our opinion, this thesis is adequate in terms of scope and quality for the award of the degree of Doctor of Philosophy

(Supervisor's Signature)

Full Name : DR CHIN SIM YEE
Position : ASSOCIATE PROFESSOR
Date :

(Co-supervisor's Signature)

Full Name : DR SUMAIYA BT ZAINAL ABIDIN @ MURAD
Position : ASSOCIATE PROFESSOR
Date :



STUDENT'S DECLARATION

I hereby declare that the work in this thesis is based on my original work except for quotations and citations which have been duly acknowledged. I also declare that it has not been previously or concurrently submitted for any other degree at Universiti Malaysia Pahang or any other institutions.

(Student's Signature)

Full Name : MOHD AMIRUL ASYRAF BIN AHMAD

ID Number : PKC15006

Date :

A large, semi-transparent watermark of the UMP logo is centered on the page. It consists of a shield shape with the letters 'UMP' in white, set against a background of teal and blue geometric shapes.

UMP

KINETIC AND SIMULATION STUDIES OF THE ESTERIFICATION OF
ACRYLIC ACID WITH 2-ETHYL HEXANOL IN A BATCH AND PACKED BED
REACTOR



MOHD AMIRUL ASYRAF BIN AHMAD

Thesis submitted in fulfillment of the requirements
for the award of the degree of
Doctor of Philosophy

UMP

Faculty of Chemical and Process Engineering Technology

UNIVERSITI MALAYSIA PAHANG

JANUARY 2020

ACKNOWLEDGEMENTS

My most gratitude to Allah S.W.T, the Almighty for giving me this gave the great chance to enhance my knowledge and to complete this research. May the peace and blessings be upon Prophet Muhammad S.A.W. I highly thank Allah gave me the opportunity to study and live in the Universiti Malaysia.

I would like to first thank my main supervisor, AP Dr Ir Chin Sim Yee who always gives intelligent suggestions and has always been patient throughout the course of my doctorate studies. Her thoughtful recommendations and assistance have contributed greatly to my work and growth as a researcher. Not to forget my co-supervisor, Dr Sumaiya Bt Zainal Abidin @ Murad, who had help me also throughout my studies with her thought in academic and also moral aspect.

I would also like to extend my gratitude to the other lecturers especially the members of the chemical reaction engineering academic panel for their guidance and comment regarding my research study.

A special thank goes to the technical staffs from the Laboratory of Faculty of Chemical and Natural Resources Engineering, who have helped me a lot especially in setting up the experimental equipment and assist in analysing samples.

I would like to express my heartfelt thanks to all my good friend who helped out for both academic and non-academics issues and made my life in Universiti Malaysia Pahang (UMP) enjoyable.

I must express my deep gratitude to UMP and Ministry of High Education (MOHE), Malaysia and Malaysia Science TORAY Foundation (MSTF) for the financial support throughout this research work via Graduate Research Scheme GRS150357 and GRS171501 respectively, Mitsubishi Chemical for sponsorship the catalyst throughout the research and MyPHD for sponsoring my financial.

Finally, I am indebted to my dear family especially my parent, Madam Azizah Binti Omar and Mr Ahmad Bin Hassan and all my relatives for their love, support and encouragement to pursue my doctorate studies. Special gratitude I would give to my mother who has taught me the importance of education and experience in life.

ABSTRAK

Air sisa yang mengandungi asid akrilik (AA) menjejaskan alam sekitar disebabkan oleh keperluan oksigen kimia yang tinggi. Pemulihan AA daripada air sisa secara esterifikasi dalam reaktor berpenyuling mungkin berbaloi. Kebiasanya, kajian kebolehlaksanaan proses perolahan ini dijalankan dalam proses batch bagi menentukan tindak balas kinetik. Hal ini tidak mencukupi untuk menentukan data asas penting lain seperti pemindahan jisim dan pencampuran yang juga sangat diperlukan semasa reka bentuk reaktor. Pertimbangan ini penting untuk melihat prestasi dan masalah seperti pembasahan pemangkin yang tidak lengkap, rintangan pemindahan jisim yang tidak baik, atau ketidakserataan taburan. Dalam kajian ini, kajian tentang pemangkin resin penukar ion heterogenous dan penyesuaian tettingkap operasi untuk tindakbalas pengesteran untuk memulihara AA dari sisa kumbahan dilaksanakan. Data asas seperti kinetik tindak balas, pemindahan jisim dan pencampuran untuk simulasi, reka bentuk dan pembinaan proses perolahan seperti reactor berpenyuling dan reaktor kromatografi untuk memulihara AA dari sisa kumbahan juga diperolehi. Reaktor pemangkin padat beraliran berterusan, sistem yang menyerupai bahagian reaktor dalam reaktor berpenyuling digunakan untuk pengesteran AA dengan 2-etil hexanol (2EH). Pemangkin resin kation yang mempunyai fungsi kimia asid sulfonik yang terbaik, SK104, SK1B, PK208, PK216, PK228, RCP145, dan RCP160, telah disaring dalam sistem batch. PK208 mendahului resin lain dan ia kemudiannya dipilih untuk digunakan dalam kajian seterusnya. Eley-Rideal (ER) merupakan model kinetik terbaik untuk mengaitkan kadar penghasilan 2EHA. Pengesterifikasian endoterma AA dengan 2EH ditunjukkan oleh peningkatan pemalar keseimbangan dengan suhu. Kesan parameter penting seperti kepekatan awal AA, suhu, nisbah molar bahan tindak balas (AA:2EH), kuantiti pemangkin, dan kuantiti penghalang pempolimeran telah dikaji dengan menggunakan reka bentuk 2 faktorial untuk melihat kesan pengaruh proses esterifikasi. Kepekatan awal AA dan suhu mempengaruhi proses esterifikasi AA dengan 2EH yang tertinggi. Memandangkan pengaruh kuantiti penghalang pempolimeran tidak ketara, faktor ini telah digugurkan untuk kajian seterusnya. Kuantiti penghalang pempolimeran yang terdapat dalam AA mentah mencukupi untuk menghalang pempolimeran AA. Taburan masa mastautin dikaji untuk memeriksa kelakuan pencampuran dalam sistem. Disebabkan masalah penyaluran yang teruk berlaku, sangkar pemangkin dipasang. Kajian penjerapan menggunakan campuran dedua tidak reaktif dilakukan untuk melihat keafinan resin terhadap setiap sebatian. Keafinan resin PK208 terhadap sebatian yang terlibat dalam sintesis 2EHA dalam tertib menurun ialah: air>AA>2EH/2EHA. Prestasi pemangkin resin PK208 untuk pengesteran antara AA dan 2EH kemudian dinilai dalam reaktor pemangkin padat (RPP) pada pelbagai suhu (55-90°C), kuantiti pemangkin (1-15 g), nisbah molar (1:1-1:5), dan kadar aliran suapan (1-5 ml/min). Keadaan terbaik yang memberikan penukaran tertinggi ialah 66.44mol% pada 95°C, dengan kuantiti pemangkin 5g, nisbah molar AA: 2EH 1: 3, dan aliran suapan 1 ml/min. Dibandingkan dengan sistem batch, pengaruh kepekatan awal AA tidak lagi ketara. Simulasi RPP yang dilakukan menggunakan model reaktor aliran palam menunjukkan hasil yang diramalkan tersasar sedikit dari data eksperimen, kerana berlakunya penyerakan dalam RPP seperti yang terbukti dengan kajian taburan masa mastautin. Data eksperimen RPP berpadanan dengan hasil simulasi yang dijana daripada model reaktor pemangkin padat yang mengambil kira penyerakan paksi di RPP. Justeru, tettingkap operasi yang dikenal pasti dan data asas telah membuktikan potensi RDC dalam menukar AA dalam air sisa dengan kecekapan yang lebih baik.

ABSTRACT

Wastewater containing acrylic acid (AA) imposes detrimental effect to the environment due to its high value of chemical oxygen demand. Recovery of AA from its dilute aqueous solution for heterogeneously catalysed esterification in a reactive distillation column (RDC) could be a promising approach. Typically, the feasibility study of these intensified processes was carried out in batch process to determine the reaction kinetics. It is insufficient to determine the other important fundamental data such as mass transfer and mixing which are also crucially required during the equipment design. This consideration is important to observe the probability of underperformance due to the problems such as incomplete catalyst wetting, severe mass-transfer resistances, or maldistribution. In the present study, the investigation on the suitable heterogeneous IER catalyst and appropriate operating window for the esterification reaction to recover AA from the wastewater was conducted. The fundamental data includes reaction kinetics, mass transfer and mixing for simulate, design, and construction of the intensified RDC and CR for the recovery of AA from the wastewater would also be obtained. The continuous flow tubular packed bed reactor (PBR), a system mimicking the reactive section in the intensified processes was used. The best sulfonic acid functional cation-exchange resin catalysts, SK104, SK1B, PK208, PK216, PK228, RCP145, and RCP160, were screened in a batch system. PK208 outperformed the other resins and it was used in subsequent studies. Eley-Rideal (ER) was the best kinetic model to correlate the production rate of 2EHA. Endothermicity of the AA esterification with 2EH was indicated by the increase of its equilibrium constant with temperature. The critical factor that contribute toward reaction performance include initial concentration of acrylic acid (AA), temperature, molar ratio of reactant (AA and 2EH), catalyst loading, and polymerisation inhibitor loading was studied using 2 factorial designs. Initial concentration of AA and temperature was found affected the esterification of AA with 2EH the most. Since the contribution of additional polymerisation inhibitor loading was not significant, this factor has been neglected to be studied in further experiment. The existing amount of the polymerisation inhibitor contained in raw AA is sufficient to avoid AA polymerisation. Residence time distribution (RTD) was studied to examine the mixing behavioural of system. Due to the severe channelling occurred, catalyst cage need to be install. An adsorption study using nonreactive binary mixtures was performed to observe the affinity of resin against each compound. The affinity of PK208 resin towards the chemical species involved in 2EHA synthesis in descending order is: water > AA > 2EH/2EHA. Catalytic performance of resin PK208 for the esterification between acrylic acid (AA) and 2-ethyl hexanol (2EH) was then evaluated in packed bed reactor (PBR) under various temperatures (55-90°C), catalyst loadings (1-15 g), molar ratios of AA to 2EH (1:1-1:5), and feed flow rates (1-5 ml/min). The best condition that gave highest yield, 66.44mol% was at 95 °C, with catalyst loading of 5 g, molar ratio AA:2EH of 1:3, and feed flow of 1 ml/min. In contrast to the batch system, the effect of initial concentration of AA was found to be not significant anymore. The PBR simulation performed using plug flow reactor model showed that the predicted results deviated marginally from the experimental data, owing to the occurrence of dispersion in PBR as proven by the residence time distribution (RTD) study. The PBR experimental data well matched with the simulation results generated from the packed bed reactor model considering the axial dispersion in PBR. Thus, the identified operating window and fundamental data validated the potential of RDC in converting the AA in wastewater with the better efficiency.

TABLE OF CONTENT

| | |
|--|------------|
| DECLARATION | |
| TITLE PAGE | |
| ACKNOWLEDGEMENTS | ii |
| ABSTRAK | iii |
| ABSTRACT | iv |
| TABLE OF CONTENT | v |
| LIST OF TABLES | ix |
| LIST OF FIGURES | x |
| LIST OF SYMBOLS | xii |
| LIST OF ABBREVIATIONS | xiv |
| LIST OF APPENDICES | xv |
| CHAPTER 1 INTRODUCTION | 1 |
| 1.1 Introduction | 1 |
| 1.2 Problem Statement | 3 |
| 1.3 Objectives | 4 |
| 1.4 Scopes of Study | 4 |
| 1.5 Significance of Study | 6 |
| 1.6 Organisation of This Thesis | 6 |
| CHAPTER 2 LITERATURE REVIEW | 8 |
| 2.0 Introduction | 8 |
| 2.1 Wastewater Containing Acrylic Acid | 8 |

| | | |
|------------------------------|---|-----------|
| 2.2 | Treatment Methods for the Wastewater Containing Acrylic Acid and Other Carboxylic Acids | 10 |
| 2.3 | Reactive Distillation Process | 14 |
| 2.4 | Residence Time Distribution and Mixing in RDC | 20 |
| 2.5 | Catalyst for the Esterification of AA | 21 |
| 2.5.1 | Homogeneous Catalyst for the Esterification of AA | 22 |
| 2.5.2 | Heterogeneous Catalyst for the Esterification of AA | 22 |
| 2.6 | Reaction Kinetics for the Heterogeneously Catalysed Esterification Reaction | 27 |
| 2.6.1 | Reaction Kinetics for the Esterification of Other Carboxylic Acids | 28 |
| 2.6.2 | Reaction Kinetics for the Esterification of AA | 29 |
| 2.7 | Summary | 31 |
| CHAPTER 3 METHODOLOGY | | 32 |
| 3.1 | Introduction | 32 |
| 3.2 | Materials | 33 |
| 3.3 | Catalyst Characterisation | 35 |
| 3.3.1 | Particle Size Distribution Analysis | 35 |
| 3.3.2 | Structural Analysis | 35 |
| 3.3.3 | Fourier Transform Infrared Spectroscopy (FTIR) analysis | 35 |
| 3.3.4 | Ion Exchange Capacity (IEC) Measurement | 36 |
| 3.3.5 | Leaching Test | 36 |
| 3.3.6 | Swelling Test | 37 |
| 3.4 | Experimental Studies of AA Esterification with 2EH in a Batch Reactor | 37 |
| 3.4.1 | Catalyst Screening | 37 |
| 3.4.2 | Mass Transfer Analysis | 39 |
| 3.4.3 | Screening of Important Operating Variable | 40 |

| | | |
|---|---|-----------|
| 3.4.4 | Recyclability | 41 |
| 3.4.5 | Kinetic Studies | 41 |
| 3.4.6 | Sample Analysis Using GC | 44 |
| 3.5 | Experimental Studies in a Packed Bed Reactor Studies | 44 |
| 3.5.1 | Residence Time Distribution (RTD) Studies | 46 |
| 3.5.2 | Adsorption Isotherm Studies | 48 |
| 3.5.3 | Experimental Study of the Effect of Important Operating Parameters in the PBR | 48 |
| 3.5.4 | Mass Transfer Parameter Calculations | 49 |
| 3.6 | Simulation Studies | 50 |
| 3.6.1 | Simulation of The Esterification Of AA With 2EH In A Tubular Reactor Using Aspen Plus V8 | 50 |
| 3.6.2 | Simulation of The Esterification of AA With 2EH In A Tubular Packed Bed Reactor With Dispersion | 52 |
| CHAPTER 4 RESULTS AND DISCUSSION | | 56 |
| 4.1 | Catalyst Characterisation | 56 |
| 4.1.1 | Measurement of Particle Size Distribution | 56 |
| 4.1.2 | Nitrogen Physisorption Analysis | 57 |
| 4.1.3 | Fourier Transform Infrared Spectroscopy (FTIR) analysis | 58 |
| 4.1.4 | Ion Exchange Capacity | 65 |
| 4.1.5 | Swelling and Leachability Analysis | 59 |
| 4.2 | Esterification of Acrylic Acid with 2-Ethyl Hexanol in a Batch System | 61 |
| 4.2.1 | IER Catalyst Screening Study | 61 |
| 4.2.2 | Parametric Studies Using 2 Factorial Design as Design of Experimental in Batch System | 63 |
| 4.2.3 | Mass Transfer Analysis | 68 |

| | | |
|-----------------------------|---|------------|
| 4.2.4 | Reusability Studies | 69 |
| 4.2.5 | Chemical Equilibrium Studies | 71 |
| 4.2.6 | Kinetic Studies in a Batch System | 74 |
| 4.3 | Esterification of AA with 2EH in a Packed Bed Reactor (PBR) | 80 |
| 4.3.1 | Residence Time Distribution (RTD) Studies | 80 |
| 4.3.2 | Adsorption Studies | 85 |
| 4.3.3 | Mass Transfer Parameter Studies (PBR System) | 89 |
| 4.3.4.1 | Effect of temperature | 91 |
| 4.3.4.2 | Effect of catalyst loading | 92 |
| 4.3.4.3 | Effect of molar ratio | 92 |
| 4.3.4.4 | Effect of feed flow rate | 93 |
| 4.3.4 | Esterification with Real Wastewater | 94 |
| 4.3.5 | Simulation Studies | 96 |
| CHAPTER 5 CONCLUSION | | 99 |
| 5.1 | Conclusions | 99 |
| 5.2 | Recommendation | 100 |
| REFERENCES | | 101 |

LIST OF TABLES

| | | |
|------------|--|----|
| Table 2.1 | Physico-chemical properties of AA | 9 |
| Table 2.2 | Advantages and disadvantages of potential methods for treatment of wastewater containing carboxylic acids | 14 |
| Table 2.3 | Applications of RDC for the esterification of pure carboxylic acid | 17 |
| Table 2.4 | The recovery of diluted carboxylic acid via esterification in RDC | 20 |
| Table 2.5 | Operating conditions of the homogeneously catalysed esterification of AA with different alcohol | 22 |
| Table 2.6 | Operating conditions of the heterogeneously catalysed esterification of AA with different alcohol | 26 |
| Table 2.7 | Kinetic studies for the esterification reaction of acrylic acid and other carboxylic acids with different type of alcohols | 30 |
| Table 3.1 | List of chemicals | 34 |
| Table 3.2 | Properties of selected ion exchange resin | 35 |
| Table 3.3 | List of main components in the experimental setup for the esterification reaction studies | 39 |
| Table 3.4 | Value for high and low level | 41 |
| Table 3.5 | Experimental design for 2 factorial analysis (half factorial) | 41 |
| Table 4.1 | Surface area and porosity of the tested acidic ion exchange resins | 58 |
| Table 4.2 | Degree of swelling for the tested acidic ion exchange resins | 61 |
| Table 4.3 | Two factorial result for experimental studies | 64 |
| Table 4.4 | P-values of responses against factors | 64 |
| Table 4.5 | The percentage contribution of factors on response variables | 65 |
| Table 4.6 | Analysis of variance (ANOVA) table for 2 factorial studies | 68 |
| Table 4.7 | Mears and Weisz-Prater parameter for experimental studies | 69 |
| Table 4.8 | The equilibrium conversion of AA (X_e) and the corresponding equilibrium constants (K_x) | 71 |
| Table 4.1 | The b_i variables and their standard errors, $\sigma(b_i)$ | 74 |
| Table 4.11 | Parameters of the kinetic models used | 76 |
| Table 4.12 | Adsorption parameters of the kinetic models used | 76 |
| Table 4.13 | The results of tracer study at 30°C | 84 |
| Table 4.14 | Liquid-solid external/internal mass transfer limitation effects in PBR | 89 |
| Table 4.15 | Kinetic and adsorption parameters for the models used to fit the experimental data | 94 |

LIST OF FIGURES

| | | |
|-------------|--|----|
| Figure 2.1 | (a) RDC and (b) traditional process for methyl acetate | 15 |
| Figure 3.1 | Summary of the research activities | 33 |
| Figure 3.2 | The experimental setup for the esterification reaction studies | 38 |
| Figure 3.3 | i) Packed bed reactor process flow diagram; ii) Packed bed reactor real photo | 45 |
| Figure 3.4 | Jacketed PBR cross sectional diagram | 46 |
| Figure 3.5 | Catalyst cage of tubular PBR | 47 |
| Figure 3.6 | Procedure of simulating the esterification of AA with 2EH in a tubular PBR using Aspen Plus software | 51 |
| Figure 3.7 | Summary of procedure of simulating packed bed reactor with dispersion using COMSOL Multiphysics software | 55 |
| Figure 4.1 | Particle size distribution for DIAION IER catalyst | 57 |
| Figure 4.2 | FTIR spectra for DIAION IERs catalyst (SK104, SK1B, PK208, PK216, PK228, RCP145, and RCP160) | 59 |
| Figure 4.3 | Yield of 2EHA for the reaction catalysed by different types resin catalysts for 4 h. Operating condition: Initial conc. AA: 100%; Temperature: 95°C; Catalyst loading of 10% w/w (catalyst/AA); molar ratio of AA:2EH is 1:3 | 62 |
| Figure 4.4 | Effect of the initial AA concentration (A), temperature (B), molar ratio of AA:2EH (C), catalyst loading (D) and polymerisation inhibitor loading (E) on the performance in term of yield of esterification AA with 2EH | 67 |
| Figure 4.5 | The 2EHA yield (%) after 4 h of reaction for 5 cycles of reaction (purity AA 99.9%; temperature of 368 K; catalyst loading of 10 wt% ; initial molar ratio acid to alcohol of 1:3) | 71 |
| Figure 4.6 | ln KA vs 1/T plot | 72 |
| Figure 4.7 | Schematic diagram of reaction of esterification of AA with 2EH followed ER | 76 |
| Figure 4.8 | Arrhenius plot for a) PH model; b) ER model; c) LHHW model | 77 |
| Figure 4.9 | Parity plot for the experimental and predicted rate of reaction of (a) PH; (b) ER and (c) LHHW (dotted linear line = $\pm 5\%$ deviation) | 78 |
| Figure 4.10 | Comparison between experimental and calculated (with ER model) of 2EHA concentration profiles. Molar ratio of AA to 2EH is 1:3, catalyst loading is 10 wt% and stirring speed at 500 rpm | 79 |
| Figure 4.11 | Exit distribution age for PBR [a) without cage; b) with cage; and c) with cage and catalyst at a flow rate of 5 ml/min] | 81 |
| Figure 4.12 | Exit distribution age for PBR [a) without cage; b) with cage; and c) with cage and catalyst at flow rate 3 ml/min] | 82 |

| | | |
|-------------|---|----|
| Figure 4.13 | Exit distribution age for PBR [a) without cage; b) with cage; and c) with cage and catalyst at flow rate 1 ml/min] | 83 |
| Figure 4.14 | Flow direction in PBR for design without cage, with cage and with cage and catalyst | 84 |
| Figure 4.15 | Breakthrough curves for AA/water binary mixtures [(a) 60/40, (b) 30/70 and (c) 70/30 % v/v] at 3 mL/min and 30 °C | 86 |
| Figure 4.16 | Breakthrough curves for AA/2EHA binary mixtures [(a) 60/40, (b) 30/70 and (c) 70/30 % v/v] at 3 mL/min and 30 °C | 87 |
| Figure 4.17 | Breakthrough curves for 2EH/2EHA binary mixtures [(a) 60/40, (b) 30/70 and (c) 70/30 % v/v] at 3 mL/min and 30 °C | 88 |
| Figure 4.18 | Yield (%) of 2EHA for the esterification of AA with 2EH at different reaction temperature with AA to 2EH feed molar ratio: 1:3; catalyst loading: 5 g; total feed flow rate: 3 ml/min | 90 |
| Figure 4.19 | Yield (%) of 2EHA for the esterification of AA with 2EH at different catalyst loading with temperature: 95°C; AA to 2EH feed molar ratio: 1:3; total feed flow rate: 3 ml/min | 91 |
| Figure 4.20 | Yield (%) of 2EHA for the esterification of AA with 2EH at different AA to 2EH feed molar ratio with temperature: 95°C; catalyst loading: 5 g; total feed flow rate: 3 ml/min | 92 |
| Figure 4.21 | Yield (%) of 2EHA for the esterification of AA with 2EH at different total feed flow rate with temperature: 95°C; catalyst loading: 5 g; AA to 2EH feed molar ratio 1:3 | 93 |
| Figure 4.22 | Parity plot for the experimental and predicted rate of reaction of (a) PH and (b) ER (dotted line stand for ±5% error) | 95 |
| Figure 4.23 | Yield (%) of 2EHA for the esterification of AA with 2EH at different AA concentration with temperature: 95°C; catalyst loading: 5g; AA to 2EH feed molar ratio 1:3; flow rate: 1 ml/min | 95 |
| Figure 4.24 | Simulation result with Aspen PLUS V8 software (x dotted) and experimental result (bar chart) | 97 |
| Figure 4.25 | Simulation result with COMSOL software (x dotted) and experimental result (bar chart) | 98 |

LIST OF SYMBOLS

| | |
|------------------|---|
| % | Percent |
| C_M | Mears parameter |
| $r_{A,obs}$ | Observed reaction rate |
| R_C | Catalyst particle radius |
| ρ_b | Bulk density of catalyst |
| C_{Ab} | Bulk concentration |
| k_C | Mass transfer coefficient |
| D_{AB} | Diffusivity of the solute A in solution |
| d_p | Diameter of the catalyst particle |
| μ_C | Viscosity of the solution |
| G | Gravitational acceleration |
| ρ_l | Density of the solution |
| C_{WP} | Weisz-Prater parameter |
| D_{eff} | Effective diffusivity |
| ΔG^o | Gibbs energy |
| ΔH_r^o | Free enthalpy of reaction |
| ΔH_{rxn} | Heat of reaction |
| \AA | Armstrong |
| A_{cs} | Adsorbate cross sectional area |
| a_i | Activity coefficient of component i |
| b_i | i^{th} adjustable variable |
| C_i | Concentration of component |
| d_p | Particle diameter |
| E_f | Activity energy of reaction |
| K_a | Thermodynamic equilibrium constant |
| K_{eq} | Equilibrium constant |
| k_f | Rate constant |
| k_{f0} | Pre-exponential factor |
| K_i | Adsorption equilibrium constant for species i |
| K_x | Apparent equilibrium constant |

| | |
|-------------|----------------------------------|
| M | Molecular weight of adsorbate |
| N | Number of experimental points |
| N_{Av} | Avogadro' s number |
| P/P° | Relative pressure |
| R | Gas constant |
| R^2 | Coefficient of determination |
| r_i | Rate of reaction of component |
| T | Reaction temperature |
| t | Reaction time |
| w | Catalyst weight |
| W_m | Weight of adsorbate |
| X_e | Degree of equilibrium conversion |
| x_i | Mole fraction of component i |
| γ_i | Gamma of component i |
| σ | Standard deviation |



UMP

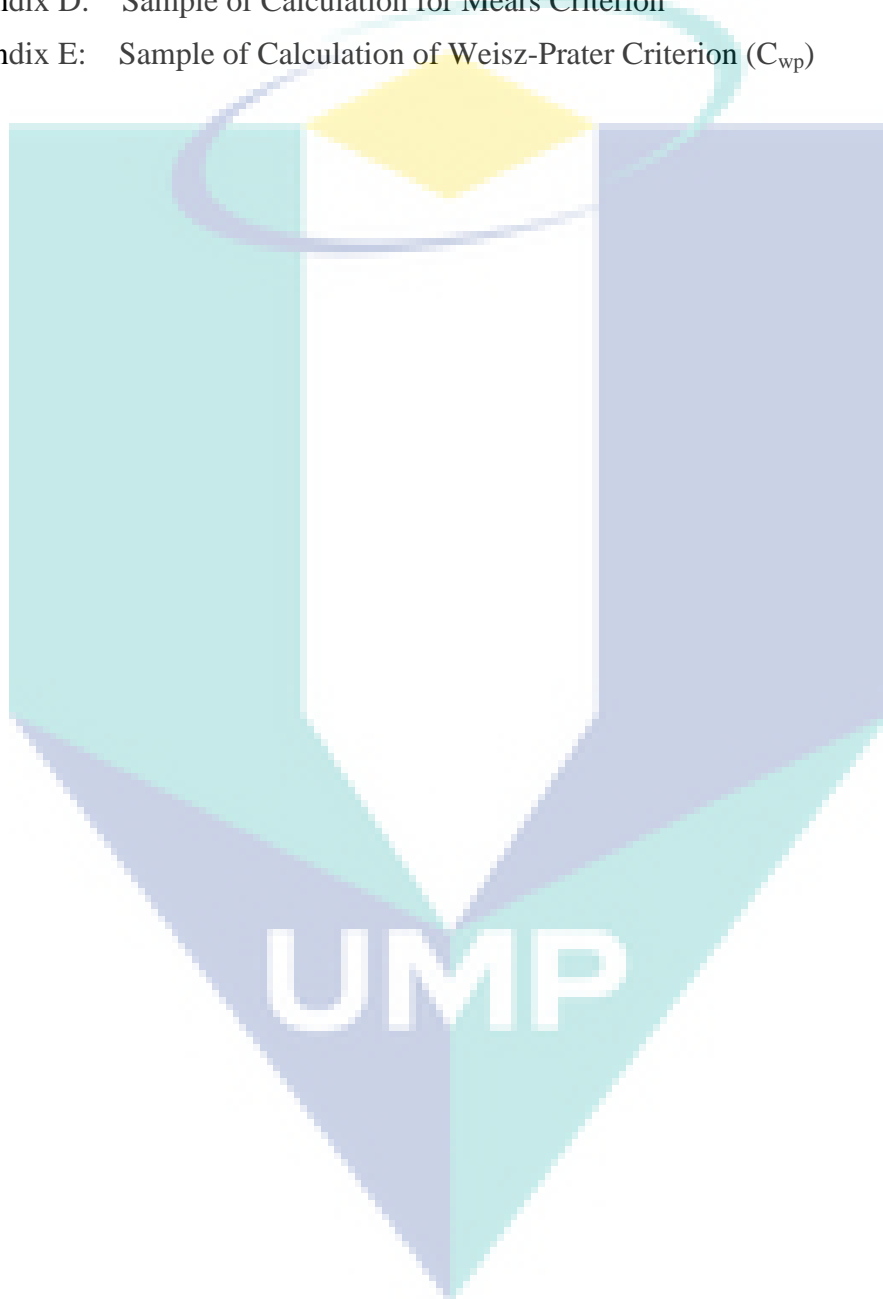
LIST OF ABBREVIATIONS



| | |
|--------|---|
| 2EH | 2 ethyl hexanol |
| 2EHA | 2 ethyl hexyl acrylate |
| AA | Acrylic acid |
| BET | Brunauer, Emmett and Teller |
| BJH | Barrett-Joyner-Halenda |
| COD | Chemical oxygen demand |
| EQA | Environment Quality Act |
| ER | Eley Rideal |
| FID | Flame ionization detector |
| FTIR | Fourier transform infrared |
| GC | Gas chromatography |
| IUPAC | International Union of Pure and Applied Chemistry |
| LHHW | Langmuir-Hinshelwood-Hougen-Watson |
| PH | Pseudo homogeneous |
| PVC | Poly(vinyl chloride) |
| RDC | Reactive distillation column |
| SMBR | Simulated-moving-bed reactor |
| TOC | Total organic carbon |
| UNIFAC | Universal functional activity coefficient |
| W | Water |

LIST OF APPENDICES

| | | |
|-------------|--|-----|
| Appendix A: | Standard Curve of AA | 119 |
| Appendix B: | Standard Curve Of 2EHA | 123 |
| Appendix C: | Unifac (VLE) For Esterification AA With 2EH | 128 |
| Appendix D: | Sample of Calculation for Mears Criterion | 129 |
| Appendix E: | Sample of Calculation of Weisz-Prater Criterion (C_{wp}) | 133 |



CHAPTER 1

INTRODUCTION

1.1 Introduction

Acrylic acid (AA) with its IUPAC nomenclature name propenoic acid is an organic compound with the formula $\text{CH}_2=\text{CHCOOH}$ (Figure 1.1). It is the simplest unsaturated carboxylic acid which consists a vinyl group connected directly to a carboxylic acid terminus that enabling its widely use as intermediate compound in various industrial processes such as in the production of paints, synthetic fibres, adhesives, papers and detergents. The molecule that follows the characteristics of both carboxylic acid and acrylate ester, making it suitable as an intermediate compound. AA is very toxic to the living species. The effective concentration for fish and invertebrates ranged from 27 to 236 mg/l (Staples et al. 2000).

In a typical acrylic acid and its derivatives manufacturing unit, the wastewater has AA concentration in the range of 4–20 wt% (Li et al., 2008). Such wastewater also consists of a very high chemical oxygen demand (COD) which inhibit the activity of the microbes used in the biological treatment. Therefore, the wastewater containing AA is conventionally being burned in the incinerator, a method that consumes a lot of energy due to the high heat capacity of water. Moreover, incineration also emits secondary waste gases that causes air pollution.

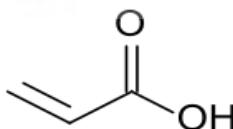


Figure 1. 1 Skeletal formula of AA

Several treatment methods, i.e. adsorption and a blend of wet oxidation followed by biological treatment, have been explored for the removal of AA from wastewaters (Kumar et al., 2008, 2010; Silva et al., 2004; Oliviero et al., 2000; Mishra et al., 1995). However, these methods are still suffering from the shortcomings of high operating cost during regeneration process. Adsorption consumes substantial amount of adsorbent, thus generating another type of waste hence resulting in high operating cost. Wet oxidation is one of the most effective methods to treat wastewater with high chemical oxygen demand (COD) but it requires elevated temperature and pressure. This leads to an increase of operational cost.

In recent years, the intensified processes such as reactive distillation column (RDC) or chromatography reactor (CR) have received much attention as the potential methods to recover acrylic acid in the form of acrylate esters. The AA in the solution is first converted to the acrylate ester before it is separated concurrently in the RDC or CR, or produce a hence generating additional income through the higher valued acrylate ester, while treating the wastewater.

RDC is a multifunctional reactor combining chemical reaction and distillation in a single column. The simultaneous separation of products and chemical reactions inside the column allows the reaction to take place efficiently, especially in esterification processes in which a maximum conversion is limited by reaction equilibrium (Park et al., 2006). Even though RDC has been successfully commercialized for the manufacture of certain high commodity chemicals such as Methyl Acetate and Methyl Tert-Butyl Ether, a very limited work was reported on the direct utilization of dilute carboxylic acid as the reactant to produce ester via the esterification process in RDC (Saha et al., 2000). Most of these studies was focusing on the recovery of dilute acetic acid through esterification process with different type of alcohols in a RDC (Saha et al., 2000; Xu et al., 1999 and Singh et al., 2006). While the CR combines reaction with adsorption in a single unit. It can be advantageous over RD for complex molecules that are difficult to separate by evaporation processes. Moreover, CR is operated at lower temperatures than RD being, in principle, preferable to prevent polymerization reactions (Dania et al., 2014).

1.2 Problem Statement

The important elements in the reactive distillation column (RDC) and chromatographic reactor (CR) processes design and development include catalyst selection, feasibility analysis, and equipment design.

The recovery of AA in the form of acrylate esters from the diluted solution such as wastewater using intensified processes is impractical to be carried out using a conventional homogeneous catalysed catalyst. Heterogeneously catalysed esterification of AA is required to avoid the generation of secondary waste. Furthermore, the incorrect operating window of these intensified processes would also lead to the failure of either the reaction or separation. For the past, the feasibility study of these intensified processes was typically and solely carried out using batch process to determine the reaction kinetics. Nevertheless, it is insufficient to determine the other important fundamental data such as mass transfer and mixing which are also crucially required during the equipment design. The RDC and CR designed and built without considering the mass transfer and mixing phenomena have high probability of underperformance due to the problems such as incomplete catalyst wetting, severe mass-transfer resistances, or maldistribution (Sundmacher & Kienle, 2003). Therefore, this fundamental data should be made available prior to the design and construction of this intensified equipment.

To the best of our knowledge, the research study about the recovery of AA from a diluted solution through esterification approach in a tubular packed bed reactor has not been reported so far. Esterification of diluted AA with 2 ethyl hexanol (2EH) catalysed by Amberlyst 15 in a batch reactor was only reported by Ahmad et. al (2014). The resultant product, 2-ethyl hexyl acrylate (2EHA) is widely used in the polymer industries for production coatings, adhesives, printing inks, binders for paints, super absorbent polymers, flocculants, fibers and plastics (Bauer et al., 1991). This previous study has proven that AA is feasible to be recovered via esterification in an intensified processes such as reactive distillation column (RDC) and chromatographic reactor (CR). This newly developed method could reduce the operating cost and increase the revenue of the AA production plant by recovering the otherwise incinerated AA-containing wastewater.

The present work aims to investigate the suitable heterogeneous IER catalyst and operating window for the esterification reaction to recover AA from the wastewater. The fundamental data includes reaction kinetics, mass transfer and mixing for simulate, design, and construction of the RDC and CR for the recovery of AA from the wastewater would also be obtained. The continuous flow tubular PBR, mimicking the reactive section in the RDC and CR. The types of catalyst in the present work have been streamlined to the cation ion exchange resin (IER) for screening purpose after a thorough review on its aspects in physical properties, cost and performance in the esterification of acrylic acid. Prior to the kinetics and parametric studies of the esterification of pure and dilute AA with 2EH, the mass transfer parameters and residence time distribution were identified.

1.3 Objectives

The objectives of this study are:

- To identify the suitable IER catalysts and operating window for the esterification of AA with 2EH in a batch reactor system.
- To investigate the effect of mixing, mass transfer and important operating parameters on the esterification of AA in a tubular packed bed reactor system.
- To develop the kinetic modelling for the esterification of AA with 2EH in batch reactor system
- To ascertain the suitable model for the simulation of the esterification of AA with 2EH in batch reactor and tubular packed bed reactor.

1.4 Scopes of Study

The following research scopes were defined to support the attainment of respective objectives:

a) The research scopes for achieving Objective 1 are:

- Characterise and screen different types of IER catalysts (gel type, microporous type, and highly porous type) based on its activity (yield), ion exchange capacity (IEC), leaching properties and recyclability.

- Perform statistical design of experimental using Design Expert 8 adopting factorial design for screening the critical factor that contribute toward reaction performance (AA initial concentration, temperature, catalyst loading, molar ratio of reactants and polymerisation inhibitors loading).
 - Determine the mass transfer parameter calculatedly from the design of experimental result.
- b) The research scopes required to achieve Objective 2 include:
- Perform the residue time distribution (RTD) analysis for the tubular PBR.
 - Evaluate mass transfer occurrence in the tubular PBR system.
 - Investigate the adsorption phenomenon in the tubular PBR system.
 - Perform statistical design of experimental using one-factorial-at-time approach to find the best condition of critical factor that contribute toward reaction performance (AA initial concentration, temperature, feed flow rate, reactants feed molar ratio, and reactor aspect ratio L/D).
 - Evaluate the reaction performance of the esterification of the real wastewater containing AA with 2EH in a tubular PBR.
- c) The research scopes required to achieve Objective 3 include:
- Develop the kinetic data modelling adopting pseudo-homogeneous (PH), Eley Rideal (ER), and Langmuir-Hinshelwood-Hougen-Watson (LHHW) model for batch system.
- d) The research scopes required to achieve Objective 4 include:
- Simulate the packed bed reactor system using Aspen Plus One V8 and COMSOL software adopting the plug flow reactor model and packed bed reactor with dispersion model by adopting the data obtain in kinetic studies, RTD, and mass transfer analysis.

1.5 Significance of Study

The outcome of the present research serves as a basis for the analysis of the prospect and feasibility of the AA recovery from the wastewater stream using intensification processes (e.g.: CR and RDC). The range of the important operating variables and the kinetic model identified in the present study can be adopted in the modelling and simulation for AA recovery through esterification. The feasibility can be examined based on the results obtained from the simulation study. The success of the present work would lead to a breakthrough of new treatment method for wastewater containing acrylic acid from the petrochemical industries. Hence, the environmental impact of the wastewater generated by petrochemical industries could be reduced.

1.6 Organisation of This Thesis

This thesis is divided into five chapters. Chapter 1 (Introduction) presents the application of AA and the impact of the wastewater containing AA in brief. The motivation and problem statement of the present study are initiated by the shortcomings of the existing methods used to treat the wastewater containing AA. The objectives, scopes and significance of study are then elucidated accordingly. The organization of the thesis is given in the last section.

Chapter 2 (Literature review) compares the existing treatment methods for wastewater containing carboxylic acid. Intensified process such as esterification via RDC and CR is identified as one of the promising methods to recovery AA from the wastewater stream. The operating conditions and catalysts used in the esterification reactions carried out in intensification processes are reviewed. The relevant kinetic models are assessed.

The materials, apparatus and equipment used in the present study are listed with their function in Chapter 3 (Methodology). Schematic diagrams of the experimental setup are drawn. The experimental procedures for the catalyst characterisation, catalyst screening, design of experimental and kinetic studies for both batch and tubular PBR system for esterification of AA and 2EHA, and simulation studies for the reaction are illustrated in detail.

Chapter 4 (Result and discussion) is divided into 4 main sections: In section 1, catalyst characterisation for fresh catalysts were performed and compared with the existing of technical data. The catalytic performance in batch system was studied and reported based on thermodynamicity in section 2. In order to develop an accurate kinetic model, the mass transfer effect was studied in this section. In the third section, the catalytic performance in tubular PBR system was studied and reported. OFAT studies were performed and kinetic data was determined in this section. RTD studies and adsorption studies of the tubular PBR were first examined to assure there are no channelling and huge distribution issues on the tubular PBR itself. Further on the kinetic data obtained was compared with the kinetic data obtained in batch system either comparable or otherwise. In the last section, the simulation studies were performed in both ASPEN PLUS and COMSOL software as the existing model could not fit the experimental data and it does not consider several issues that appear in the real tubular PBR.

In chapter 5, the conclusion and recommendations based on the current studies are given. The conclusions are drawn based on each individual study covered in the present research, while the recommendations are given based on the conclusions obtained by considering their significance and importance to the future research in the related field.



UMP

CHAPTER 2

LITERATURE REVIEW

2.1 Introduction

Chapter 2 describes the characteristics of wastewater containing acrylic acid and the problems associated with these wastewaters. The corresponding treatment methods of these wastewaters were compared and its drawbacks were identified. The potential intensified treatment or recovery methods were also proposed. Along the way from taking the proposed methods into practical process implementation, important fundamental data such as reaction kinetics, equilibrium, mass transfer and mixing are required to design the lab- and pilot-scale equipment. These data could provide valuable insights that increase the knowledge about the process and reduce the uncertainties that allow a confident design and construction of the plant. Emerging from the problem statement, the research gap was identified for the present study.

2.2 Wastewater Containing Acrylic Acid

Carboxylic acids such as acetic acid (HAc), propanoic acid, methacrylic acid and acrylic acid (AA) are the important building blocks used for the synthesis of value-added chemicals and polymers. Despite the extensive researches in bio-based production of carboxylic acids, it is commonly produced through the chemical synthesis using petro-based feedstock. Irrespective to the types of synthesis process, the isolation and purification of carboxylic acids from aqueous solution remain difficult, attributing to the strong affinity of carboxylic acids to water. As a result, wastewater containing carboxylic acids (< 10 wt%) is generated from the carboxylic acid production process (Bai et al., 2017).

Acrylic acid (AA), also known as 2-propenoic acid in IUPAC is a clear, colourless liquid with a pungent smell under normal condition. Table 2.1 summarizes the physical and chemical properties of AA. This substance has been classified as flammable. It is harmful by inhalation (in contact with skin and if swallowed), corrosive (can causes severe burns) and dangerous for the environment, which is very toxic to aquatic organisms.

Table 2.1 Physico-chemical properties of AA

| Properties | Value | Reference |
|-----------------------|---|----------------------|
| Physical state | liquid at 20°C | |
| Melting point | 14°C | Merck Index (1996) |
| Boiling point | 141°C at 1 bar | Merck Index (1996) |
| Density | 1.0621 g/cm ³ at 20°C | Merck Index (1996) |
| Vapour pressure | 3.8 hPa at 20°C – (dynamic method) | BASF AG (1994) |
| Surface tension | 59.6 mN/m c= 1 g/L – (ring method) | Hüls AG (1995) |
| Water solubility | miscible in all ratios | Merck Index (1996) |
| Dissociation constant | pK _a = 4.25 | Weast (1989) |
| Partition coefficient | log P _{ow} 0.46 at 25°C – (shake flask method) | BASF AG (1988) |
| Flash point | 48 – 55°C | CHEMSAFE |
| Auto flammability | 395°C – DIN 51794 | CHEMSAFE |
| Flammability | Flammable | Rohm and Haas (2006) |
| Explosive properties | not explosive | Rohm and Haas (2006) |
| Oxidizing properties | no oxidizing properties | Rohm and Haas (2006) |

AA has been in production over 30 years for commercial purposes mainly from petrochemical industry by two-step gas-phase oxidation of propylene (Falbe et al., 1995). In addition, AA can be prepared by hydrolysis of acrylonitrile (ECETOC, 1995). It is also produced naturally by several different types of algae. AA is an important intermediate for polymer industry. It has the major markets in the production of surface coatings, textiles, adhesives, paper treatment, and plastics beside polishes, leather, fibers, detergents, and super-absorbent material (Xu et al., 2006).

Fox et al. (1990) estimated the Western European production of AA in 1987 at about 342,000 tonnes. In 1995, the worldwide productivity of AA was more than 3

million tons annually and it was expected to grow 4 - 5% per year (Falbe et al., 1995; Rohe, 1995). The world demand for crude AA and glacial AA were forecasted to grow at 3.7% per year and 4% per year respectively from year 2006 to 2011 (ICB Chemical Profile, 2008). The acrylic acid global market in 2013 was approximately 5 million MT, which worth USD 8 billion, and was forecast to be growth rate at 4.2% annually during 2013–2018 (IHS Markit, 2015). In another report, the forecasts of the global market of AA is expected to garner USD18.8 billion by 2020, registering a grown of 7.6% during the period 2014-2020 (Sarah, 2014). World AA consumption would reach more than 8,100 kilo tons by 2020 (Sarah, 2014). Worldwide of AA market had accounted almost USD15,000 million in 2017 and is expected to growth up to USD35,000 million by 2026 at growth rate of 9.8% (Research & Markets, 2018).

With the massive production and usage, substantial amount of wastewater containing AA has been generated. The wastewater containing AA is normally within the range of 3,000 – 85,000 mg/L of chemical oxygen demand (COD) (Bhattacharyya et al. 2013). This wastewater has drawn the attention of the local authorities as AA could not be easily decomposed by organisms and hence leading to an adverse environmental impact on water quality and thus endanger public health and welfare when the large amount of acrylic acid accumulates (Yanase et al. 1985). Its effective concentration for fish and invertebrates ranged from 27 to 236 mg/l (Staples et al., 2000). It has been reported that 860 mg/L of acrylic acid caused a 50 % decrease in methnanogenic activity and IC₅₀ for acrylic acid was 200 mg/L (Staples et al., 2000). Acrylic acid may decrease the pH of aquatic systems to less than 5.0, which can be harmful to some aquatic organisms (DOW, 2014).

2.3 Treatment Methods for the Wastewater Containing Acrylic Acid and Other Carboxylic Acids

In a typical petrochemical industry for AA manufacturing, the wastewater has AA concentration in the range of 5–15 wt%. Such wastewaters also consist of high COD which renders the direct biological treatment difficult (Scholz, 2003). Stewart et al. (1995) found that AA could be treated using biological method at a dose of 100 mg/L or lower but not at higher concentrations due to the microorganism inhibition. In addition, the treatment of AA in aerobic biological systems is not feasible because of its extremely odoriferous effect (Demirer and Speece 1998; Tai et al. 2007).

Owing to the strong affinity of carboxylic acids to water, it is difficult to remove or recover carboxylic acids from dilute aqueous solution especially when the carboxylic acid concentration is < 10 wt% (Bai et al., 2017). At the present time, the wastewater containing carboxylic acid such as AA is always burned through an energy-intensive process in solely an incinerator (Bednarik and Vondruska, 2003) or an evaporator prior to incinerator (Kuila and Ray, 2011). It is a high energy consumption process and easy cause secondary pollution. Hence, the removal or recovery of carboxylic acids from dilute aqueous solution remains a great interest to researchers (Keshav et al., 2008; Uslu et al., 2016; Yuan et al., 2017; Bekatorou et al., 2016).

In the literature, various conventional techniques to remove or recover carboxylic acids from aqueous solutions have been reported. The removal techniques include adsorption and catalytic degradation. Adsorption is an effective physical treatment of wastewaters containing low concentration of carboxylic acids (< 720 mg/L) using commercially available adsorbents like activated carbon, alumina, silica, bentonite, piet, chitosan, and ion-exchange resins (Allen, 1996; Ayranci and Duman, 2006; Kumar et al., 2008; Mao and Fung, 1997). In spite of this, this process involves huge quantity of chemicals to regenerate absorbents. Meanwhile, the adoption of adsorption in the wastewater with high concentration of carboxylic acid like AA requires large amount of absorbent, leading to the issues of secondary waste generation and economic feasibility (Kumar et al., 2008; Bai, 2017). Catalytic degradation is used to mineralize the chemical compound via catalytic reaction such as ozonation, photocatalytic reaction, and wet oxidation. In recent years, oxidation process was claimed to be a more efficient process for the treatment of wastewater with AA but it required high pressure and temperature and thus increasing the operating cost. In addition, the use of catalyst in the oxidation also incurred additional cost (Shafaei et al., 2010).

In comparison to the carboxylic acid removal techniques, the carboxylic acid recovery methods are the more attractive and sustainable alternatives because value added products could be produced with least secondary waste generation, while treating the wastewater. The conventional recovery process alternatives encompass distillation, azeotropic and extractive distillation, pressure swing distillation (PSD), liquid-liquid extraction (LLX), membrane separation. The carboxylic acid content of the aqueous

solution is one of the important criteria used to choose a suitable separation technique. It was suggested that distillation may be chosen for the separation of HAc from an aqueous solution with an acid content of above 50 wt%, while LLX is a practical option if the acid content is below 50 wt% (Drake et al., 1985; Reyhanitash et al. 2018). Direct distillation is not suitable to be used to separate carboxylic acid from dilute aqueous solutions as high energy consumption is required to vaporize large amount of water with high specific heat capacity (Bai, 2017).

LLX, an affinity-based separation technique utilises the affinity agents that aiming on carboxylic acids to selectively recover them from the dilute aqueous solutions. Using relatively less energy requirement, an efficiency of more than 90% was recorded by LLX in the studies of carboxylic acids recovery from the dilute aqueous solution (Chang et al.,2009; Tuyun et al.,2011; Li et al.,2008; Rahmanian et al., 2008, Reyhanitash, 2018). Nonetheless, the selection of solvents and its regeneration processes remain the challenge to keep a practically high efficiency at low energy consumption and minimum environmental impact.

The membrane separation techniques of electrodialysis and pervaporation have been projected as the very attractive alternatives for the separation of carboxylic acids form very dilute aqueous solutions. Though the recovery efficiency of electrodialysis was high but it can only be achieved with the addition of pre-treatment such as active carbon filtration (for organic matter removal) and flocculation (for colloids removal) to avoid membrane contamination. This required the extra investment to be applied in industrial scale (Yu et al., 2002). Moreover, it consumed substantial amount of energy that resulting from the weak dissociated ability of the weak organic acid (Wang et al., 2006; Zhang et al.,2011; Xu and Yang, 2002; Grzenia et al., 2012; Schlosser et al., 2005 in Kienberger 2018). In the meantime, pervaporation method was suffering with the issues of obtaining the optimal practical flux that could remain the high recovery efficiency of carboxylic acid from the dilute aqueous solutions. A failure in looking for trade-off point between the flux and recovery efficiency would significantly affect the life time of the membrane (Hareesh K. Dave, Kaushik Nath, 2016; Choudhari et al. 2015).

In recent years, hybrid processes such as extractive distillation, pervaporative distillation, reactive distillation (RD) reactive extraction (RE) and reactive

chromatography have been successfully employed to intensify the recovery of carboxylic acid from dilute aqueous solutions (Li et al., 2004; Berg, 1992; Taylor and Krishna, 2000; Sharma and Mahajani, 2003; Hiwale et al., 2004 and Talnikar and Mahajan, 2014; Saha et al., 2000; Kiss, 2011, Arpornwichanop et al., 2008; Henczka and Djas, 2016; Reddy et al., 2015 in Kienberger 2018). Process intensification consists of energy integration of streams, stages or operations, to replace the required amount of heating and/or cooling provided with utilities. The combination of two or more operations or technologies within a single unit significantly reduces energy consumption and hence saving the operating cost.

RD, in particular heterogeneously catalysed RD process has been employed as a promising technique for the recovery of carboxylic acid with high purity and high yield from the wastewater and fermentation broth (Komesu et al., 2015). In RD process, chemical reaction and distillation separation are performed simultaneously within single fractional distillation unit. This process has become an attractive alternative to other hybrid processes due to following reasons: discarded the need of solvent and membrane that could cause downstream separation and fouling problems, avoided the azeotrope formation by changing substance properties through chemical reaction, improved conversion of reactants, reduced by-product formation and reduced recycling costs (Komesu et al., 2015; Painer et al., 2015; Lam et al, 2010; Vincente et al., 2004). Table 2.2 summarises the advantages and disadvantages of the carboxylic acid removal and recovery methods.

Currently, numerous reports were focused on the recovery of acetic acid, trifluoroacetic acid, lactic acid, adipic acid, myristic acid, succinic acid, chloroacetic acid and glycolic acid from the dilute aqueous solution by esterifying these carboxylic acids in the reactive distillation column (RDC) (Kumar and Mahajani, 2007; Mahajan et al., 2008; Sharma and Mahajani, 2003; Talnikar and Mahajan, 2014). On the other hand, the report about the recovery of AA from its dilute aqueous solution using RDC was scarce despite its potential.

Table 2.2 Advantages and disadvantages of potential methods for treatment of wastewater containing carboxylic acids

| Method | Advantages | Disadvantages |
|-----------------------|---|---|
| Incineration | Easy | Requires intense energy, releases green-house gases |
| Adsorption | High efficiency (almost above 90% removal) Low energy consumption | No recovery, restricts to wastewater with low AA concentration application (in ppm level), requires bulk usage of absorbent |
| Catalytic degradation | More efficient Low cost process | Operating cost is relatively high |
| Extraction | High efficiency (more than 90%) | Separation of solvent/extractant |
| Distillation | High efficiency | Consumes large amount of energy |
| Biodegradation | Cheap | Application restricted when COD high, takes time, and low chemical resistance |
| Electrodialysis | Moderate efficiency (current efficiency only about 30-40 %) | Required necessary pre-treatments |
| RD | Convert carboxylic acid to value added ester products while treating the wastewater Ease of separation | Higher energy consumption Low conversion in diluted compound |

2.4 Reactive Distillation Process

Reactive distillation column (RDC) has been explored as a potentially important process for several reactions. Along with esterification and etherification, other reactions like hydrogenation, hydrodesulphurisation, isomerisation, and oligomerisation are some of the unconventional examples to which RDC has been successfully applied on a commercial scale. Moreover, hydrolysis, alkylation, acetalization, hydration, and transesterification have also been identified as potential candidates for RDC (Harmsen, 2007). In addition to the application of RDC for the esterification of pure carboxylic acid, RDC has also been used to esterify the carboxylic acid from the dilute aqueous solution, aiming to recover the carboxylic acid by converting it to a value added ester product (Saha et al., 2000; Singh et al., 2006; Arpornwichanop et al., 2008; Arpornwichanop et al., 2009 in Kienberger, 2018)

RDC was adopted with the purpose of shifting the equilibrium of the esterification, a reversible reaction to increase the reactant conversion and product yield. One of the most remarkable commercial process in 1980s is the RDC for the production of methyl acetate. Conventionally, this homogeneously acid catalysed process used multiple reactors with a large excess of one of the reactants to achieve high conversion. The formation of methyl acetate-methanol and methyl acetate-water azeotropes required the use of a series of atmospheric and vacuum distillation columns or extractive distillation. Figure 2.1 compares the conventional process and reactive distillation process for the production of methyl acetate. The complex and capital intensive process containing two reactors and eight distillation columns in **Figure 2.1(b)** is compared with a simple and compact RDC process as shown in **Figure 2.1(a)**. Nearly 100% conversion of the reactant is achieved with only one column required in the RDC process with reduced capital and operating costs (Siirola, 1995).

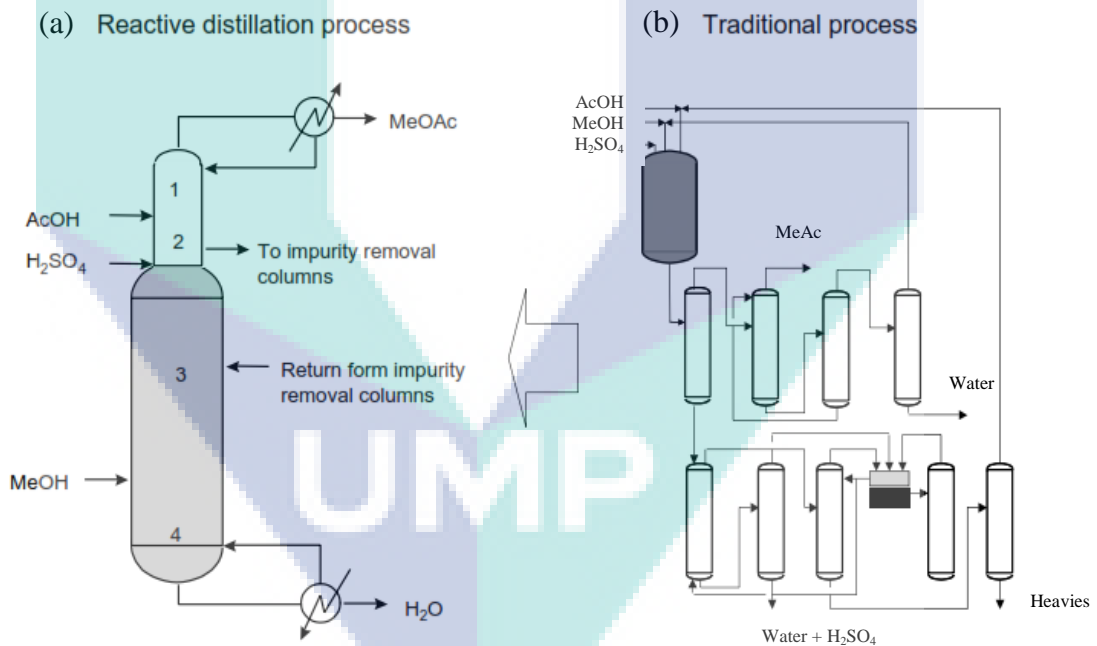


Figure 2.1 (a) RDC and (b) traditional process for methyl acetate

2.4.1 Esterification of pure carboxylic acids in RDC

Numerous research works were carried out to study the esterification of pure carboxylic acid with alcohol in RDC. Most of these studies of RD used carboxylic acid

with high purity (Kumar and Kaistha, 2009; Lutze et al., 2010; Hanika et al., 2001; Zhicai et al., 1998; Calvar et al., 2007).

Emerging from the homogeneously catalysed RD process for the synthesis of methyl acetate in 1980s, various heterogeneously catalysed RD processes for methyl acetate production using ion exchange resins and other solid acidic catalysts were investigated extensively. These works covered the experimental, modelling and rigorous simulation studies. The most significant operating parameters which influenced methyl acetate purity were reflux ratio, mole ratio of methanol to acetic acid, reboiler temperature and feed position of reactants. It was also found that the results from the simulation analysis using equilibrium stage model well matched the experimental results (Agreda et al., 1990; Dirk-Faitakis et al., 2009; Kumar and Kaistha, 2009; Mallaiiah and Reddy, 2016). RDC was also used for the production of other acetate esters such as ethyl acetate, isopropyl acetate, and butyl acetate (Calvar et al., 2007; Zhicai et al., 1998). The conversion achieved was only in the range of 50 – 55%, a much lower amount in relative to the conversion of acetic acid obtained in the RD process for methyl acetate synthesis.

Apart from acetate esters, the RDC was also adopted for the synthesis of acrylate esters like butyl acrylate and 2-ethyl-hexyl acrylate. Niesbach et al. (2013, 2012) esterified acrylic acid in a pilot scale RD column with n-butanol in the presence of phenothiazine inhibitor. Katapak SP-11 packings were used to accommodate A-46 and Amberlyst 131 solid acid catalysts. The work presented systematic process intensification approach through experimentation, model validation and process analysis. A non-equilibrium model was used to validate the experimental data. The validated model with the incorporation of the packing characteristics was then adapted to optimise the industrial scale RD process. Coupling the RD with a decanter was found to be the most economic process. Moraru and Bildea (2017) also used the identical RDC configuration in their studies on the design, control and economic evaluation of a RD-based process. Decanter separated the un-reacted n-butanol from the water by-product. N-butanol was recovered and recycled to the RDC while obtaining a high purity water stream. The RDC was operated under vacuum condition to minimise AA polymerisation. It was equipped with Sulzer Katapak SP-12 consisting of catalyst granules immobilized in wire gauze layers. The economic analysis revealed that a cost

of RD process was 43.5% lower than those of classic batch processes for the production of butyl acrylate. The same group of researchers validated the use of Amberlyst 70 catalysed RD process was also feasible for the production of 2-ethylhexyl acrylate. This process achieved complete conversion of reactants, and obtained 99.5 wt% acrylate ester and 99.9 wt% wastewater. In comparison to the conventional reaction–separation–recycle process, the utility and remuneration costs of the RD process were lower with a factor of approximately 3 (Moraru and Bildea, 2018). The applications of RDC for the esterification of various types of pure carboxylic acids and alcohols are listed in **Table 2.3**.

Table 2.3 Applications of RDC for the esterification of pure carboxylic acid

| Reaction | Catalyst | Reference |
|--|---------------------------|------------------------------|
| Production of methyl acetate from acetic acid and methanol | Sulphuric acid | Agreda et al. (1990) |
| Production of isopropyl acetate from isopropanol and acetic acid | para-toluenesulfonic acid | Lee and Kuo (1996) |
| Production of butyl acetate from butanol and acetic acid | Sulphuric acid | Zhikai et al. (1998) |
| Production of 2-methyl propyl acetate from 2-methyl propanol and acetic acid | acidic ion exchange resin | Hanika et al. (2001) |
| Production of ethyl acetate from ethanol and acetic acid | Amberlyst 15 | Calvar et al. (2007) |
| Production of methyl acetate from acetic acid and methanol | Amberlyst 35 | Dirk-Faitakis et al., (2009) |
| Production of butyl acrylate from butanol and acrylic acid | Amberlyst 46 | Niesbach et al. (2012) |
| Production of butyl acrylate from butanol and acrylic acid | Amberlyst 131 | Niesbach et al. (2013) |
| Production of methyl acetate from methanol and acetic acid | Indion 180 | Mallaiah and Reddy, (2016) |
| Production of 2 ethyl hexyl acrylate from 2 ethyl hexanol and acrylic acid | Amberlyst 70 | Moraru and Bildea, (2018) |

2.4.2 Esterification of diluted carboxylic acid in RDC

Recovery of carboxylic acids from its dilute aqueous solution by using it as a reactant for esterification in a RDC could be a promising approach. This approach has received much attention as the dilute acetic acid, trifluoroacetic acid, formic acid and lactic acid can be recovered to produce a higher valued ester (Kumar and Mahajani, 2007; Mahajan et al., 2008; Sharma and Mahajani, 2003; Talnikar and Mahajan, 2014), which in turn saving raw material cost and solving environment problem.

The recovery of acetic acid from dilute aqueous solution (30% acetic acid) via esterification in a RDC was investigated by Saha et al. (2000). They used n-butanol and iso-amyl alcohol to esterify the acetic acid using catalyst Indion 130. Acetic acid conversion of 58% was reported. It was discovered that the deactivation of this cation exchange resin was the major process constraint. The deactivation was attributed to the fouling and precipitation of non-specific matrix constituents at elevated temperature. On the other hand, simulation analysis was performed by Arpornwichanop et al. (2009) for the production of n-butyl acetate from dilute acetic acid and n-butanol in three RD configurations. These include single-column RD, distillation–RD hybrid system and pervaporation–RD hybrid system. The single-column RD was identified as the optimum system as it provided the minimum total annual cost. The reaction of acetic acid in aqueous solution (50 wt%) with butanol in a single RD has resulted acetic acid conversion of 99 mol% and butyl acrylate purity of 98 mol%. Nevertheless, the total annual costs increased significantly when the dilute feed of 35 wt% acetic acid was employed.

The recovery of acetic acid from aqueous water through esterification in RDC was examined by Painer et al. (2015) in the presence of formic acid. The aqueous formic acid–acetic acid mixtures were esterified using methanol in batch mode and continuous mode. Under the continuous mode, almost all the formic acid was converted but the highest conversion achieved for acetic acid was only approximately 71%, implying that the separation and isolation of acetic acid can be done either by esterification or alternatively distillative separation. Nonetheless, esterification in RDC was still preferable from the economic point view.

Trifluoroacetic acid (TFA) is widely used in the industries and the resulting streams are dilute aqueous mixtures of the TFA with the concentrations of upto 20%. This TFA has been recovered by use of RD. RD has been proven a suitable process intensification technology applicable for this recovery because it yielded a quadruple TFA conversion, comparing to the conversion obtained in batch reactor (approximately 20%) (Mahajan et al., 2008, Talnikar et al., 2016).

RD was also employed for the recovery of lactic acid from aqueous solutions (Komesu et al., 2015). Kamble et al. (2012) and Barve et al. (2009) attempted to recover lactic acid from the dilute aqueous solution (20 wt%) through esterification

using ethanol in RDC. High yield of ethyl lactate was achieved with the aid of multiple unit operations which requiring additional cost. In the study of Komesu et al. (2015) for the recovery of lactic acid in RDC, they used dilute aqueous solution with 12 wt% of lactic acid, a model solution of fermentation broth that typically contained 1.6–16 wt% of lactic acid. The effect of ethanol/lactic acid molar ratio, reboiler temperature and catalyst concentration on the ethyl lactate production was investigated. High yield of ethyl lactate (~100%) was produced while lactic acid was three times more concentrated than the initial concentration, evidencing that the RD is technically feasible for lactic acid purification. Table 2.4 summarizes the studies about the recovery of carboxylic acid from the dilute aqueous solution using RDC.

To the best of our knowledge, the research study about the esterification of acrylic acid in the wastewater has not been reported so far. Esterification of diluted AA with 2EH catalysed by Amberlyst 15 in a batch reactor was only reported by Ahmad et al (2014). This previous study has proven that AA is feasible to be recovered via esterification in a RDC. This newly developed method could reduce the operating cost and increase the revenue of the AA production plant by producing the additional acrylic ester. The important elements for the RDC processes design and development include catalyst selection, feasibility analysis, and column design. Fundamental data such as reaction kinetics, mass transfer and mixing are the crucial information required during the column design. This data provide the basis of the pilot scale studies upon scaling up the RDC.

As a continuity of the earlier studies, the present work adopted the continuous flow tubular packed bed reactor, a system similar to the reactive section in the RDC for the esterification of acrylic acid with 2-ethyl hexyl acrylate. The mass transfer parameters and residence time distribution were also identified. The present study was a very important step to implement a future RDC process for the recovery of acrylic acid from the wastewater through esterification.

Table 2.4 The recovery of diluted carboxylic acid via esterification in RDC

| Process | Catalyst | Alcohol | Reference |
|---|------------------------------|-----------------|------------------------------|
| Recovery of diluted acetic acid (35-60 wt%) in RDC (economic studies)-simulation | Amberlyst 15 | n-butanol | Arpornwichanop et al. (2009) |
| Recovery of trichloroacetic acid | T-63 (cation-exchange resin) | 2-propanol | Mahajan et al., 2008, |
| Recovery of diluted acrylic acid (10%-90wt%) in batch and RDC | Amberlyst 15 | 2 ethyl hexanol | Talnikar et al., 2016, |
| Recover lactic acid and acetic acid from the wastewater in RDC | Autocatalysed | Methanol | Kamble et al. (2012) |
| Recover lactic acid from the dilute aqueous solution (20 wt%) in RDC | Autocatalysed | Ethanol | Barve et al. (2009) |
| Recovery of diluted lactic acid from diluted streams in RDC | Sulphuric acid | Ethanol | Komesu et al. (2015) |
| Recovery of diluted acrylic acid from diluted stream in batch | Amberlyst 15 | 2 ethyl hexanol | Ahmad et. al (2014) |
| Recovery of formic acid and acetic acid from wastewater using reactive distillation | Autocatalysed | Methanol | Painer et al. (2015) |
| Recovery of diluted acetic acid from diluted streams (30% w/w) | Indion 130 | n-butanol | Saha <i>et al.</i> (2000) |

2.5 Residence Time Distribution and Mixing in RDC

In the process from taking an innovative idea into practical implementation for the recovery of AA from the dilute aqueous solution using RDC, the simulations are used to guide the conceptual process design and the experimental work, while the experiments data is used to validate the simulation model. The validated model can be used then for process scale-up, sensitivity analysis studies, process control and optimization. These steps could provide valuable insights about the process within a shortest time to minimise the uncertainty that allow an assured design and construction of the RDC (Kiss, 2018).

Commonly, RDC is simulated using equilibrium (EQ) modelling or rate-based modelling. The equilibrium modelling approach assumes vapour and liquid are in equilibrium. This may not be applicable to the actual operation since a real column rarely operates at equilibrium. In addition, the equilibrium modelling can be insufficient to describe the complex physical and chemical interactions in the RD process. The degree of separation depends on the mass and energy transfer between the contacted phases on a tray, or within a packed section of the column. As a consequence, the more accurate rate-based models have been developed to avoid the over-design and under-design of RDC and thereby reducing the capital and operating costs. The rate-based models take into account the followings: (1) vapor–liquid equilibrium only at the interface between the bulk liquid and vapour phases; (2) estimated mass and energy flux across the interface using transport-based approach; (3) the hydrodynamic situation of either a tray or a packed column (Taylor and Krishna, 2000; Baur et al., 2000; Katariya et al., 2008; Kiss, 2010, 2011; Peng et al., 2003 and Shah et al., 2012).

The advantageous of rate-based models could be significantly offset if the information of mass transfer and hydraulic characteristics of the RDC internals are limited. A number of researchers have proven that the hydrodynamic of the RD column cannot be neglected especially when the process is kinetically controlled. Shah et al. (2012) discovered that the use rate-based model considering axial dispersion for the simulation of RDC for polyester synthesis could give a more accurate predicted result in comparison to the conventional rate-based modelling approach. Residence time distribution (RTD) curve is one of the very important information for the establishment of flow regimes and determination of the hydrodynamic parameters. The analysis of the RTD experiments allows the determination of axial dispersion coefficients for the catalyst packing. The axial dispersion model is the most widely spread residence time distribution concept for modelling and designing conventional chemical reactors and RDC, especially the heterogeneous catalysed reaction process (Kołodziej et al., 2005; Shah et al., 2012).

2.6 Catalyst for the Esterification of AA

Catalyst is used for the esterification process to accelerate the chemical reaction by reducing the activation energy required. Catalysts can be divided into 3 types; there are homogenous catalysts, heterogeneous catalyst and biocatalyst. Typically,

homogeneous and heterogeneous catalysts are used in the esterification of AA with different types of alcohol.

2.6.1 Homogeneous Catalyst for the Esterification of AA

Saha and Sharma (1996) employed H_2SO_4 as the catalyst for the esterification of AA with an excess of cyclohexene, 1-hexene, 1-octene, 1-decene, 1-dodecene, 2-octene at 333-383 K. H_2SO_4 was also used as a catalyst for the esterification of AA with 2-ethylhexanol (Fomin et al., 1991, Nowak, 1999), hexanol (Sert et al., 2013) and n-octanol (Nowak, 1999) in an isothermal semi-batch reactor. All these studies recorded the reaction conversion of more than 95% in the presence of polymerization inhibitor, hydroquinone (0.2 wt%) and excess alcohol at a temperature between 333-403 K.

Despite the higher activity of homogeneous catalyst, it is toxic, corrosive and difficult to be recovered from the process. These drawbacks has led to an increase in operating and capital costs (Farnetti et al., 2004; Essayem et al, 2007). Heterogeneous acidic catalysts such as zeolite, alumina or resin could be an alternative to replace the homogenous catalysts (Chen et al., 1999; Saha and Sharma, 1996; Komon et al., 2013). Table 2.5 show the significant findings of the esterification of AA using several heterogeneous catalysts and alcohols.

Table 2.5 Operating conditions of the homogeneously catalysed esterification of AA with different alcohol

| Temperature (K) | Molar Ratio (Acid to alcohol) | Catalyst and the loading | References |
|-----------------|-------------------------------|------------------------------|------------------------|
| 353-403 | 1:2-1:10 | Sulphuric acid; 0.1-1.0 % wt | Nowak (1999) |
| 333-403 | 1:2-1:10 | Sulphuric acid; 0.1-1.5 % wt | Nowak (1999) |
| 338-358 | 1:1 | Sulphuric acid, 3% v/v | Sert et al. (2013) |
| 473 | - | Amberlite resin | Essayem et al., (2007) |

2.6.2 Heterogeneous Catalyst for the Esterification of AA

The heterogeneous catalyst could offer superior advantages over the homogeneous catalyst in reducing equipment corrosion, easing of product separation and catalyst recovery (Essayem et al, 2007; Paul and Samuel, 1995). The synthesis of acrylate esters through a more environmental process employing heterogeneous catalysts like supported tungstophosphoric acid (TPA) and ion exchange resin (IER) have been the research subject in recent years.

The study of Sert and Atalay (2012) showed that zirconia supported TPA is a highly active and thermal stable catalyst in the esterification of AA. The results indicated that 25 wt % TPA loading and calcination temperature of 650 °C were the best catalyst preparation conditions since the maximum conversion values of AA were achieved for different alcohols (33%, 31%, and 27% for butanol, iso-butanol, or hexanol respectively). These esterification processes were carried out in a batch reactor operated at a temperature of 358 K for 5 h, using the reactants with the molar ratio of 1. Phenothiazine was charged into the reaction vessel as inhibitor.

Up to the present time, IER was found as one of the most commonly used solid acid catalysts for the production of various types of acrylate esters through esterification reaction. The IER catalysed esterification of AA was primarily carried out using butanol (Darge & Thyron, 1993; Sert et al., 2013; Karakus et al., 2014), 2-ethyl hexanol (Komon et al., 2013, Ahmad et al., 2014; Chin et al, 2015) and other alcohols such as methanol, hexanol and propylene glycol (Altioka & Odes, 2009; Buluklu et al., 2014). Strong acidic IER is functionalised with sulfonic acid group that performs in the same way as that of homogeneous sulfuric acid catalyst through the dissociation of acid, H species. Commercially, the ion exchange resins are available in spherical resin beads. The capacity of these IER as catalyst counts on its highly porous nature that directly influences the rate of overall catalytic process. In general, the overall rates are determined by the rate of pore diffusion and rate of chemical reaction. The IER catalysts can be categorised into gel type resins and macroporous type resins on the basis of its pore structure to minimize the pore diffusion resistances. The microporosity (< 2 nm) and high surface area of the gel type resins can only be exhibited when it swells. It usually possesses very low crosslinking agent, di-vinyl benzene (DVB) content since swelling is a very important effect to the gel type resins. It can only be used in the esterification reactions that involved the swelling-solvents (Van de Steene et al., 2014). On the other hand, the micropore areas of the macroporous (2-50 nm) type resins are embedded in macroporous bead. It has relatively lower surface area but swelling is not an important effect to demonstrate its catalyst capacity. Therefore, the macroporous type resins are widely applied in the esterification reactions involve aqueous, nonaqueous and nonpolar solvents (Bhandari et al., 2016).

Sert et al. (2013) and Karakus et al. (2014) compared macro-reticular type IER (Amberlyst 15 (A15)) with gel type IER (Amberlyst 131 (A131) and Dowex 50WX400 (WX400)) in terms of its activity in the esterification of AA with n-butanol and iso-butanol carried out in a batch reactor. The higher activity of gel type IER was ascribed to the larger number of accessible active sites when these IER swelled remarkably in the presence of the by-product water. A131 outperformed A15 because of its higher ion exchange capacity and recyclability. The highest AA conversion of 50% was achieved for both the esterification using n-butanol and iso-butanol at 358 K in the presence of 10 g/L of catalyst. However, the esterification using iso-butanol needed higher butanol-to-AA molar ratio to achieve the same conversion within 4 h, owing to a lower reaction rate caused by the steric hindrance effect of iso-butanol structure. In comparison to IER includes A15, A131 and D50WX400, A131 was also proven as the best catalyst for the esterification of AA with hexanol (Buluklu et al., 2014) as the best catalyst. Unlike the esterification of AA with butanol, a higher hexanol to AA ratio (3 mol/mol) or catalyst loading (20 g/L) was required to achieve conversion of $\geq 50\%$ when esterifying AA with hexanol at 358 K.

Despite the reported inferior activity of A15, this porous IER was packed and evaluated by Constantino et al. (2015) in a fixed-bed adsorptive reactor for the esterification reaction of AA with 1-butanol. The reactor operated at a reaction temperature of 363 K with an equimolar reactants ratio solution and a feed flow rate of 0.9 mL/min. The coexistence of reaction and separation resulted a higher maximum butyl acrylate concentration (38%) than the equilibrium concentration. In spite of the higher ion exchange capacity of A36, Altioikka & Odes (2009) verified that A15 was a better catalyst because it resulted higher selectivity in esterifying AA with propylene glycol. This comparison study was carried out at the following operating condition: Temperature of 353 K, reactant ratio of 1, catalyst and inhibitor loadings of 5.5 wt% and 0.3 wt% respectively.

The IER catalysts were also used to catalyse the esterification of AA with 2 ethyl hexanol for the synthesis of 2 ethyl hexyl acrylate, another acrylate ester of industrial significance. The activities of macroporous type resins (Amberlyst 39 (A39), Amberlyst 46 (A46) and Amberlyst 70 (A70)) were compared with gel type resin A131 in the esterification of AA with 2 ethyl hexanol (Komon et al., 2013). A131 exhibited

the lowest activity because its active sites could not be fully exposed and accessed under a minimum swelling condition in a non-polar reaction system. In spite of A70 lower number of the acid centers, it overtook the others the macroporous resins in terms of activity in the reaction performed at a temperature of 373 K with initial 2 ethyl hexanol to AA mole ratio of 1, inhibitor and catalyst loadings of 0.2 wt% and 5 wt% respectively. The highest conversion and yield of 76% and 71.6% respectively were recorded after 360 mins. The enhanced acidic strength of the active sites by the chlorine atom in the matrix of A70 has contributed to its superior activity. Moreover, the less dense property of A70 and hence larger space between polymer chains has allowed higher accessibility of reactants to the acid sites (Siril et al., 2008).

A15 was also employed for 2-ethyl hexyl acrylate synthesis via esterification of AA with 2 ethyl hexanol (Chin et al., 2015). In view of the severity of the operating condition, A15 has shown an inferior performance in relative to A70. The highest yield, 70% was observed after 500 mins in the reaction carried out at 388 K with initial molar ratio AA to 2-ethyl hexanol of 1:3 and catalyst loading of 10 wt%. The lower performance of A15 was due to the activity reduction ascribed to the coverage of catalyst active sites by the co-produced water and polymer. Part of the AA was polymerised because the inhibitor concentration was only 20-200 ppm, a much lower concentration comparing to the study done by Komon et al. (2013) using A70 as catalyst.

Table 2.6 summarizes the significant findings of the studies for the esterification of AA using different types of heterogeneous catalysts and alcohols. Apparently, the studies on heterogeneously catalysed esterification of AA were mostly carried out in a batch system. No report was found in the literature about the heterogeneously catalysed esterification of AA with 2-ethyl hexanol in a tubular packed bed reactor, a system that is mimicking the reactive section in the RDC. The present study with the aim to close this particular research gap, identified the suitable IER catalysts and operating windows for the esterification of AA with 2EH in a batch and tubular packed bed reactors. The fundamental data on reaction kinetics, mass transfer and mixing for the development of the intensified process such as RDC would also be obtained.

Table 2.6 Operating conditions of the heterogeneously catalysed esterification of AA with different alcohol

| Alcohol used | Reaction time (h) | Temperature (K) | Molar Ratio (Acid to alcohol) | Catalyst and the loading | References |
|---------------------|-------------------|-----------------|-------------------------------|---|----------------------------|
| 2 ethyl hexanol | 2-6 | 353-393 | 7:1-1:7 | Amberlyst 39, Amberlyst 46, Amberlyst 70 (1–10 wt%), Amberlyst 131 | Komon et al., 2013 |
| 2 ethyl hexanol | 4-6 | 358-388 | 3:1-1:5 | Amberlyst 15 (1-15 wt%) | Chin et al., 2015 |
| 1-butanol | 5 | N/A | N/A | Various catalyst (Amberlyst, Nafion, Cs _{2.5} H _{0.5} PW ₁₂ O ₄₀); 0-2 g | Chen et al., 1999 |
| 2-ethyl hexanol | 6 | 333-373 | 7:1-1:7 | Amberlyst 70; 5% wt | Komon et al., 2013 |
| Methanol | 1 | 333 | 1:1 | Amberlyst 15 | Ströhlein et al., 2006 |
| 1-butanol | N/A | N/A | N/A | Cs _{2.5} H _{0.5} PW ₁₂ O(Cs _{2.5}) | Okuhara, 2002 |
| Butanol | 4.5 | 353 | 1:1.35-1:3 | H ₃ P ₁₂ W ₄₀ | Dupont et al., 1995 |
| Tripropylene glycol | N/A | N/A | N/A | phosphorous tungstic acid | Shanmugam et al. 2004 |
| Hexanol | 6 | 333-348 | 2:1-1:2 | Amberlyst 131 (4-8 wt%) | Sert and Atalay, 2012 |
| 1-butene | N/A | 473 | - | Amberlite resin | Essayem et al., 2007 |
| Butanol | N/A | 333-364 | 1:1-1:10 | Amberlyst 15 (2-10 g) | Darge & Thyriou, 1993 |
| Butanol | 4 | 338-358 | 1:1-1:3 | Amberlyst 15 (2-20 g/l), Amberlyst 131, Dowex 50W _X -400 | Sert et al., 2013 |
| Isobutanol | 4 | 338-358 | 1:1-1:3 | Amberlyst 15, Amberlyst 131 (10-20 g/L), and Dowex 50w _X -400 | Karakus et al., 2014 |
| 2 ethyl hexanol | 5 | 368 | 1:3 | Amberlyst 15 (15 wt%) | Ahmad et al., 2014 |
| Propylene glycol | 3-7 | 333-358 | 1:1 | Amberlyst 15 (3-8.5 wt%), Amberlyst 36, as well as cs salt of phosphorous tungstic acid | Altioka & Odes, 2009 |
| Hexanol | 4 | 338-358 | 1:1-1:4 | Amberlyst 131 (10-20 g/L), Amberlyst 15, and Dowex 50W _X -400 | Buluklu et al., 2014 |
| Methanol | 8 | 303-333 | 1:1-1:10 | Lewatit K1221, Lewatit K2640, Lewatit K2629 and Amberlyst 15 | Van de Steene et al., 2014 |
| Butanol | 1-5 | 323-363 | 1:3-1:5 | Amberlyst 15 | Constantino et al., 2015 |

2.7 Reaction Kinetics for the Heterogeneously Catalysed Esterification Reaction

The reaction kinetics is important for reactor design. Kinetics is required in analysing the reactive process and controlling the reaction variables. It is used to simulate the process and predict the industrial potential of the catalyst (Johannessen et al., 2000; Sayyed et al., 2009; Shi et al., 2011; Tsai et al., 2011). The reaction mechanism can be elucidated using different type of kinetic model. The model must be fitted with the experimental data which gives positive activation energy (Teo and Saha, 2004).

The pseudohomogeneous (PH) model is widely used in esterification systems (Komon et al., 2013; Pappu et al., 2013; Yu et al., 2004). In the PH model, adsorption and desorption of all components are negligible. The PH model assumes complete swelling of the polymeric catalyst in contact with polar solvents, leading to an easy access of the reactants to the active sites. Equation 2.1 shows the PH model (Fogler, 2008).

$$-r_A = k_f \left(c_A c_{AL} - \frac{1}{K_{eq}} c_{ES} c_W \right) \quad (2.1)$$

Where r_A , k_f , K_{eq} , denote for reaction rate of acid, forward reaction constant, and equilibrium constant respectively and c_A , c_{AL} , c_{ES} , and c_W denote for concentration of acid, alcohol, ester and water respectively.

On the other hand, the Eley–Rideal (ER) model can be applied when reaction between one adsorbed reactant and one non-adsorbed reactant from the bulk liquid phase is assumed to occur. Depending on which of the two reactants is adsorbed, for a single site surface reaction rate-controlling step, the reaction between an adsorbed and a non-adsorbed reactant molecule on the catalyst surface can be represented by the ER model as shown in Equation 2.2 and Equation 2.3 (Fogler, 2008).

$$-r_A = \frac{k_f \left(c_A c_{AL} - \frac{1}{K_{eq}} c_{ES} c_W \right)}{(1 + K_A c_A + K_W c_W)} \quad (2.2)$$

$$-r_A = \frac{k_f \left(c_A c_{AL} - \frac{1}{K_{eq}} c_{ES} c_W \right)}{\left(1 + K_{ES} c_{ES} + K_{AL} c_{AL} \right)} \quad (2.3)$$

Where K_A , K_{AL} , K_{ES} , and K_W represent adsorption constant for acid, alcohol, ester and water respectively.

The Langmuir–Hinshelwood–Hougen–Watson (LHHW) model takes into account the adsorption of all components. Assuming that the process is controlled by the reaction on the catalyst surface, the LHHW model assumes that the reaction takes place between two adsorbed molecules (Sert and Atalay,2012). Equation 2.4 depicts the LHHW model.

$$-r_A = \frac{k_f \left(c_A c_{AL} - \frac{1}{K_{eq}} c_{ES} c_W \right)}{\left(1 + K_A c_A + K_{AL} c_{AL} + K_{ES} c_{ES} + K_W c_W \right)^2} \quad (2.4)$$

2.7.1 Reaction Kinetics for the Esterification of Other Carboxylic Acids

Pseudo-homogeneous model was claimed to be well fitted with the kinetic experimental data of the esterification reaction catalysed by ion exchange resins. This conclusion was drawn by Yu et al. (2004) for the esterification of acetic acid with methanol catalysed by Amberlyst 15 and Pappu et al. (2013) for the esterification of butyric acid and hexanol catalysed by Amberlyst 70. Instead of using the concentration based PH model, Pappu et al., (2013) has taken into account the non-ideality of the liquid phase by using the activity of the components. The activity coefficients were predicted using the UNIFAC group contribution method.

Kinetic studies for the esterification of lactic acid and acetic acid with methanol in batch reactor were carried out by Sanz et al. (2002) and Sert and Atalay (2012) respectively. The corresponding catalysts for these reactions were Amberlyst 15 and Amberlyst 131. Three kinetic models were compared and it was concluded that activity based LHHW model was well agreed with the experimental kinetic data.

Sert and Atalay (2012) and Yu et al. (2004) studied the kinetic of esterification of acetic acid with methanol and both employed ion exchange resin as their catalyst but

using the different kinetic model that is LHHW activity based and PH concentration based. An identical activation energy was found. Adam et al. (2012) reacted acetic acid with ethanol and resulted a higher activation energy which employed the PH ideal kinetic modelling. This is in line with the study of Pappu et al. (2013).

The esterification of oleic acid with methanol and ethanol has been studied by Song et al. (2009) and Sarkar et al. (2010) respectively in a batch reactor system. Activation energy of approximately 40 kJ/mol was determined based on the pseudo homogeneous concentration base kinetic model. The other carboxylic acids such as myristic acid, lactic acid, and naphthenic acid which were studied by Rattanaphra et al. (2011), Sanz et al. (2002), and Wang et al. (2008) in the batch reactor exhibit the similar thermodynamic trend of exothermic also determined using pseudo homogeneous kinetic model.

2.7.2 Reaction Kinetics for the Esterification of AA

The kinetic modelling studies of the esterification of wastewater containing acrylic acid with alcohol are scarce. To date, most of the kinetic studies for the esterification of AA with alcohol were using concentrated or pure acrylic acid.

Komon et al. (2013) has carried out the kinetic study for the esterification of AA with 2EHA. Activity based PH model was claimed to well describe the reaction. The non-ideality of the liquid phase was considered by the activity of the components where the activity coefficients were estimated using the UNIFAC method. The activation energy obtained was 50.1 kJ/mol.

Kinetic behaviour of the esterification of acrylic acid and n-butanol, leading to n-butyl acrylate and water catalysed by Amberlyst 131 was studied by Sert et al. (2013). The experiments were carried out in a batch reactor. The acrylic acid conversion increased with an increase in temperature, which confirmed that the reaction is intrinsically kinetically controlled. The experimental data were correlated by the LHHW model and the activation energy was found to be 57.4 kJ/mol.

LHHW model was also well fitted with the experimental reaction rate generated by Altıokka and Ödeş (2009) for the kinetic study of the esterification of acrylic acid with propylene glycol. The reaction catalysed by Amberlyst 15 was conducted in a

batch reactor. The simultaneous dimerization/polymerization of acrylic acid and products, in addition to the reversible esterification reaction, was proposed as the reaction mechanism. Phenothiazine (0.3 wt%) was also used as an inhibitor to reduce the polymerization of acrylic acid and product. The activation energy was 80.37 kJ/mol. The kinetic studies reported in the preceding section were summarised in Table 2.9. Evidently, all the reaction kinetics for the esterification of AA were only evaluated using pure AA. The reaction kinetics were not investigated using a diluted AA because the present of water in the esterification reaction only affects the chemical equilibrium but not the reaction kinetics.

Table 2.7 Kinetic studies for the esterification reaction of acrylic acid and other carboxylic acids with different type of alcohols

| Esterification | Thermo-dynamic type | Catalyst | Activation Energy | References |
|--|---------------------|---|---|------------------------------|
| Lactic acid + methanol | Endothermic | Amberlyst 15 | 48.67 kJ/mol (PH activity base) | Sanz et al. (2002) |
| Acetic acid + methanol | Exothermic | Amberlyst 15 | 44.2 kJ/mol (PH concentration base) | Yu et al. (2004) |
| Naphthenic acid (diluted) + methanol | N/A | Tin oxide | 104.2 kJ/mol (PH concentration base) | Wang et al. (2008) |
| Oleic acid + methanol | Endothermic | Zinc acetate | 32.46 kJ/mol (PH concentration base) | Song et al. (2010) |
| 4-methoxyphenyl acetic acid + dimethyl carbonate | N/A | mesoporous sulfated zirconia (MSZ) | 75.3 kJ/mol (PH concentration base) | Devulapelli and Weng, (2009) |
| Oleic acid + ethanol | Endothermic | SnO ₂ /WO ₃ | 39.5 kJ/mol (PH concentration base) | Sarkar et al. (2010) |
| Myristic acid + methanol | N/A | sulfated zirconia | 22.51 kJ/mol (PH concentration base) | Rattanaphra et al. (2011) |
| Acetic acid + methanol | Endothermic | Amberlyst 131 | 37.8 kJ/mol (LHHW activity base) | Sert & Atalay (2012) |
| Butyric acid + hexanol | Exothermic | Amberlyst 70 | 41.7±2.3 kJ/mol (PH activity base) | Pappu et al. (2013) |
| Acrylic acid + n-butanol | Exothermic | Amberlyst 131 | 57.4 kJ/mol (LHHW activity base) | Sert et al. (2013) |
| Acetic acid + ethanol | N/A | L-(N-α-acetylphenylalanine)-ruthenium (III) complex (RHAPhe-Ru) immobilized on silica | 343.92 kJ/mol (PH concentration base) | Adam et al. (2012) |
| Acrylic acid + 2-ethylhexanol | Endothermic | Amberlyst 70 | 52.3±1.9kJ/mol (PH conc. based) 50.1±3.1kJ/mol (PH activity based) | Komon et al. (2013) |

2.8 Summary

Recovery of AA in the wastewater through the esterification in a RDC is a potential method to treat the wastewater containing AA. The continuous in situ product removal from RDC could shift the equilibrium of the esterification of AA with 2EH in a dilute system to the forward direction, hence increasing the conversion of AA to acrylate ester, 2EHA. To date, experimental studies for the esterification of AA with 2EH in a tubular packed bed reactor are scarce. The important basic data for the RDC process design and development such as reaction kinetics, mass transfer parameters and residence time distribution data have not been generated for the esterification of AA in the wastewater. The present works are designed to obtain these data through the IER heterogeneously catalysed esterification of the AA in the wastewater in a packed bed reactor, a mode which is identical to the reactive section in the RDC. These data will be bridging the gap between the previous feasibility studies (Ahmad et al., 2014) and the RDC process design and development for the esterification of AA in the wastewater.



UMP

CHAPTER 3

METHODOLOGY

3.1 Introduction

This chapter includes the methodology for all the research activities planned to achieve the objectives. It encompasses the methods used to measure the physico-chemical properties of the ion-exchange resin (IER) and the procedures of carrying out the esterification reaction study in a batch reactor as well as in a packed bed reactor. In addition, the experimental procedures of residence time distribution and adsorption isotherm studies using PBR were also delineated. A flow chart summarizing the research activities is shown in Figure 3.1 which would start with catalyst screening, then move to batch and continuous flow (PBR) studies where the kinetic modelling would be determined before pursuing with simulation with process modelling tools.

UMP

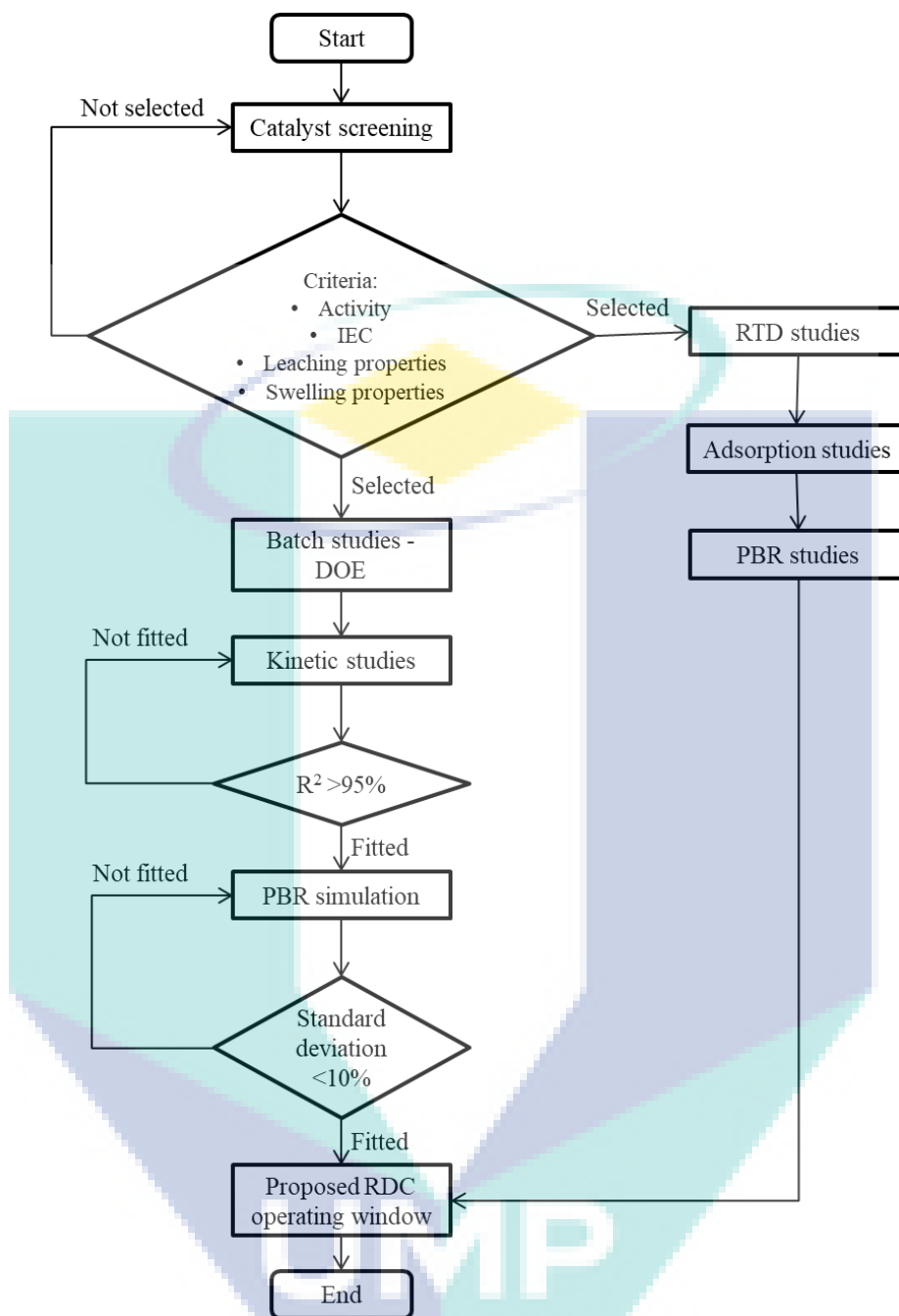


Figure 3.1 Summary of the research activities

3.2 Materials

The chemicals used in the present studies are listed in Table 3.1 with their purity, brand and function. All these chemicals were used without further purification.

Table 3.1 List of chemicals

| Chemical/Reagent | Assay | Brand | Function |
|-------------------------------|--------------|---------------|--|
| 2-ethyl hexanol (2EH) | 99.99% | Fluka | Reactant |
| Acrylic acid (AA) | 99.9% | Sigma Aldrich | Reactant |
| n-Hexane | 99.99% | Sigma Aldrich | Solvent for GC-FID analysis |
| Sodium chloride (NaCl) | 99% | Rohm & Haas | Solvent for ion exchange capacity (IEC) analysis |
| Potassium Hydroxide (KOH) | 99% | Rohm & Haas | Titrant for IEC analysis |
| 2-ethyl hexyl acrylate (2EHA) | 99.99% | Sigma Aldrich | Standard for GC-FID analysis |
| Butyl acrylate (BA) | 99.99% | Sigma Aldrich | Internal standard for GC-FID analysis |
| Phenothiazine | 98% | Sigma Aldrich | Polymerisation inhibitor |
| 4-Methoxyphenol (MEHQ) | 99% | ReagentPlus | Polymerisation inhibitor |
| Dextran solution | 99% | Sigma Aldrich | Tracer for residue time distribution studies |
| Nitrogen | 99.99% | Air Product | Inert gas for GC-FID analysis |
| Compressed air | 99.99% | Air Product | Makeup gas for GC-FID analysis |
| Hydrogen | 99.99% | Air Product | Gas to ignite GC-FID |
| Helium | 99.99% | Air Product | Carrier gas during GC-FID analysis |

The IER obtained from Mitsubishi Chemical Corporation (gelular type; SK104, SK1B; macroporous type; PK208, PK216, PK228 and highly porous; RCP145, and RCP160) was used as catalyst. Prior to using the IER in the experimental studies, it was pre-washed with distilled water/ deionized water until the pH of supernatant liquid become neutral (to eliminate free sulphonic acids). It was then dried at 353 K and atmospheric pressure until the mass remained constant (Delgado et al., 2007; Komon et al., 2013).

Table 3.2 Properties of selected ion exchange resin

| Catalyst | Type | DVB % | Ionic form | Mean particle size (μ m) | Particle Density (g/ml) | T_{max} (K) |
|-----------------|---------------|-----------------|-------------------|---|--------------------------------|----------------------------|
| SK104 | Gelular | 4 | H ⁺ | 730 | 1.13 | 393 |
| SK1B | Gelular | 8 | H ⁺ | 750 | 1.28 | 393 |
| PK208 | Porous | 4 | Na ⁺ | 650 | 1.18 | 393 |
| PK216 | Porous | 8 | Na ⁺ | 730 | 1.26 | 393 |
| PK228 | Porous | 14 | Na ⁺ | 740 | 1.32 | 393 |
| RCP145 | Highly porous | NA ² | H ⁺ | 680 | 1.22 | 423 |
| RCP160 | Highly porous | NA ² | H ⁺ | 530 | 1.19 | 393 |

3.3 Catalyst Characterisation

3.3.1 Particle Size Distribution Analysis

Malvern Mastersizer 2000 was used to determine the particle size distribution of ion-exchange resin. The samples was dispersed though the measurement area of the optical bench where the system of analyser accurately measured the scattered size range of particles. The Mastersizer 2000 software v5.6 was used to process and analyse the scattering data to calculate a particle size distribution.

3.3.2 Structural Analysis

Bruneauer-Emmet-Teller (BET) surface area, pore volume and pore size distribution of catalysts were quantified from the nitrogen adsorption isotherms measured using Thermo Surfer equipment at 77 K. The samples were degassed under vacuum at 373 K for 12 h prior to the adsorption process. Adsorption isotherms were generated by dosing nitrogen (>99.99% purity) onto the catalyst contained in a sample tube dipped in a bath of liquid nitrogen. The surface area was calculated using the BET method (Micropore version 2.46). The pore volume and pore size distribution were calculated using the Barrett-Joyner-Halenda (BJH) method.

3.3.3 Fourier Transform Infrared Spectroscopy (FTIR) analysis

Fourier-transform infrared spectroscopy (FTIR) is an equipment use to obtain an infrared spectrum of absorption or emission of a solid, liquid or gas sample by

simultaneously collecting high-spectral-resolution data over a wide spectral range. FTIR analysis was done prior to observing the chemical structure and bond in catalyst.

FTIR spectra were recorded by Perkin Elmer Series II IR spectrometer at room temperature. The sample was dried first and analysed as it is using a testing probe. The IR spectrum was recorded in the range of 400-4000 cm^{-1} under the atmospheric conditions with a resolution of 1 cm^{-1} .

3.3.4 Ion Exchange Capacity (IEC) Measurement

Ion exchange capacity (IEC) expresses the total number of ion sites available for exchange during reaction. In order to quantify the IEC of resin, the ions need to be chemically removed from a measured quantity of the resin and quantitatively determined in solution by conventional analytical methods.

0.1 g of catalyst was immersed in 100 ml of 0.1 M NaCl solution for 24 hours. NaCl is used to extract prior of acidic compound of the catalyst apparently sulphonic group. The NaCl solution was then titrated with 0.01M KOH with phenolphthalein as an indicator. The ion exchange capacity in milliequivalents/gram (meq/g) was calculated using Equation 3.1:

$$IEC \text{ or TLC} = \frac{V_{KOH} \times M_{KOH}}{m_{cat}} \quad (3.1)$$

where V_{KOH} and M_{KOH} is respectively volume and molarity of potassium hydroxide and m_{cat} is mass of catalyst (Golden, 2000).

3.3.5 Leaching Test

Leaching test was performed to observe to what extent do the resin catalyst would withstand to hold the ion sites from being released to the surrounding solution. The amount of ion site the resin released indicates how much the bond strength between the resin with the ion site itself.

0.5 g of catalyst was immersed in 50 ml of water and 2 ethyl hexanol (2EH) at 368 K for 4 hours (imitating the reaction duration) respectively for each catalyst. The solution was then titrated with 0.01 M KOH with phenolphthalein as an indicator. The

total leaching capacity (TLC) in meq/g was calculated based on Equation 3.1 while the percentage of leaching (L%) is calculated using Equation 3.2 respectively:

$$L = \frac{\text{TLC}}{\text{IEC}} \times 100 \quad (3.2)$$

3.3.6 Swelling Test

A designated amount of dried IER was placed in a graduated cylinder and its volume was recorded. Then, an appropriate amount of solvent such as water or 2EH was then added to submerge the resin. The mixture was swirled for 30 seconds for maximum resin/solvent mixing. The extra solvent was removed after the resin was ceased to swell. The volume of the swollen resins was recorded. The degree of swelling (DOS) was calculated using Equation 3.3:

$$\text{DOS} = \frac{V_{\text{after swelling}} - V_0}{m_{\text{cat}}} \quad (3.3)$$

Where $V_{\text{after swelling}}$ is the total volume after swelling (after no more significant changes observed), V_0 is the initial volume before adding resin and m_{cat} is the mass of catalyst (Golden, 2000).

3.4 Experimental Studies of AA Esterification with 2EH in a Batch Reactor

3.4.1 Catalyst Screening

Seven types of DIAION IER (SK104, SK1B, PK208, PK216, PK228, RCP145, and RCP160) were tested for their performance in a batch system at temperature 368 K, catalyst loading of 10% w/w (catalyst/acrylic acid) and molar ratio of AA:2EH is 1:3. The samples were withdrawn at every 1h for 4h. The catalyst that show the highest yield/conversion was selected in subsequent experimental work.

All the experiments were conducted in a 500ml 3-necked round bottom flask fitted with reflux condenser and thermocouple. Rotamantle is the source of heat and stirring. The temperature was maintained within $\pm 0.1\text{K}$ by PID temperature controller. A known amount of 2EH and AA were preheated separately until achieving the desired

temperature. Then, both the reactants were mixed 0.02 wt.% of MEHQ (weight of MEHQ/weight of AA) and catalysts were loaded into the reactor. Subsequently, the measurement of the reaction time was considered start.

Sample was collected for performance analysis. To avoid any further reaction, the collected samples were cooled rapidly at 277 K prior for gas chromatography (GC) analysis. Figure 3.1 and Table 3.2 show the experimental set up and the function of each part in the set up.

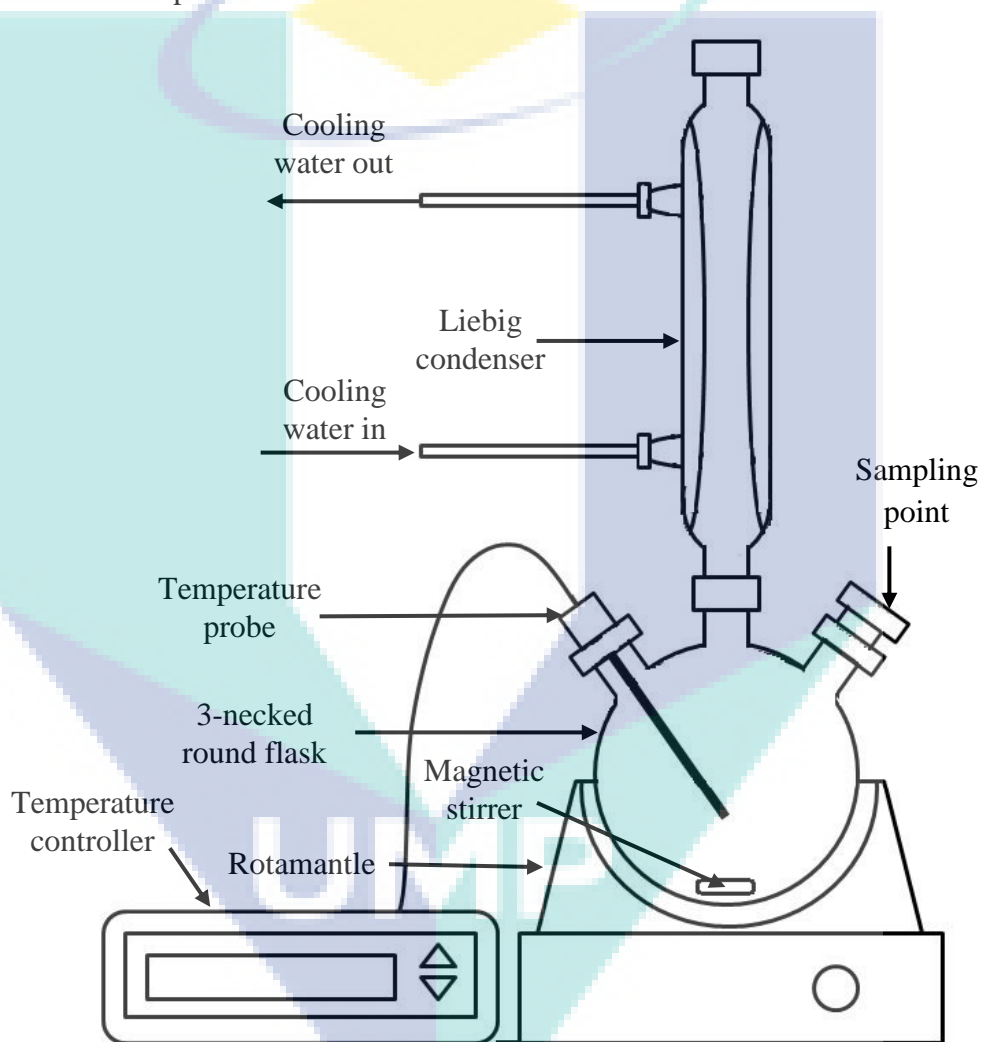


Figure 3.2 The experimental setup for the esterification reaction studies

Table 3.3 List of main components in the experimental setup for the esterification reaction studies

| Component | Description | Function |
|------------------------|---|--|
| Rotamantle | Equipment which holds the 3-necked round flask. Equipped with heating and magnetic stirring system. The heating system was modified and connected to the temperature controller | To supply heat required during the esterification reaction and to provide the magnetic field to stir the reaction mixture. |
| 3-necked round flask | A round bottom flask with capacity of 500 ml. There are three openings on the flask. The condenser was connected to the middle opening. The thermocouple was connected to the first opening. The third opening was used for charging the reactants and catalyst and sampling purposes. The reactor was equipped with digital temperature indicating controller (Cole Parmer). | As the batch reactor. |
| Liebig Condenser | Glass condenser with the length of 50 cm (Fluka) | To condense the reaction mixture vapours during the esterification reaction. |
| Temperature probe | J-type thermocouple with the length of 10 cm. | To measure the process temperature during the reaction. |
| Temperature controller | The heat controller with function of proportional-integral-derivative controller (PID) and on/off system. Compatible with K-type, J-type, I-type, and type of thermocouple. | To control the process temperature during the reaction. |
| Magnetic stirrer | 3 cm magnetic bar | To stir the reaction mixture continuously. |

3.4.2 Mass Transfer Analysis

It is necessary to eliminate both external and internal diffusion limitations before proceed with the study the reaction kinetic. Mass transfer effects causes discrepancy between the experimental behaviour and simulation.

To consider the effect of external mass transfer resistance on the rate of reaction, the Mears criterion for external diffusion was examined and the dimensionless Mears parameter (C_M) was calculated as follows (Fogler, 2008):

$$C_M = \frac{r_{A,obs} \rho_b R_C n}{k_C C_{Ab}} < 0.15 \quad (3.4)$$

Where n is the reaction order, R_C is the catalyst particle radius, ρ_b is the bulk density of catalyst, $r_{A,obs}$ is observed reaction rate, C_{Ab} is the bulk concentration of AA and k_C is the mass transfer coefficient.

To estimate the mass transfer coefficient (k_C), the following equation was employed (Fogler, 2008):

$$k_C = \frac{2D_{AB}}{d_p} + 0.31 N_{Sc}^{-2/3} \left(\frac{\Delta\rho\mu_C g}{\rho_c^2} \right)^{1/3} \quad (3.5)$$

Where D_{AB} is the diffusivity of the AA in solution, d_p is the diameter of the catalyst particle, μ_C is the viscosity of the solution, g is the gravitational acceleration, N_{Sc} is the Schmidt number (defined as $\mu_C/\rho_c D_{AB}$) and $\Delta\rho = |\rho_l - \rho_c|$ where ρ_l and ρ_c are the density of the solution and the density of the catalyst, respectively.

The occurrence of any internal pore diffusion limitation is determined on the basis of the Weisz–Prater criterion, where the dimensionless Weisz–Prater parameter (C_{WP}) was calculated as follows (Fogler, 2008):

$$C_{WP} = \frac{-r_{A,obs} \rho_c R_c^2}{D_{eff} C_A} \quad (3.6)$$

The symbols of R_c , D_{eff} and C_A represent the effective radius of the catalyst, the effective diffusivity and the limiting reactant concentration in the mixture.

3.4.3 Screening of Important Operating Variable

Design Expert DX7, the statistical software is commonly used to design the experimental studies for screening and optimizing the vital factors that affect the esterification process. Two level factorial design (half factorials) was used as the number of factors as shown in Tables 3.3 and 3.4 is more than 3. It is sufficiently and efficiently used to identify the critically significant factors and to estimate the effects of all interactions between factors. Each factor was set to only two levels for the screening

Table 3.4 Value for high and low level

| Parameters | High level | Low level |
|--------------------------|------------|-----------|
| Initial AA concentration | 100% w/w | 10% w/w |
| Temperature | 373 K | 353 K |
| Molar ratio | 1:5 | 1:1 |
| Catalyst loading | 10% w/w | 3% w/w |
| Inhibitor loading | 0.5% w/v | 0% w/v |

Table 3.5 Experimental design for 2 factorial analysis (half factorial)

| Experiment | AA Conc. (% w/w) | Temperature (K) | Molar Ratio (AA:2EH) | Cat. Loading (% w/w) | Inhibitor Loading (% w/v) |
|------------|---------------------|--------------------|----------------------------|----------------------------|---------------------------------|
| 1 | 10 | 353 | 1:1 | 3 | 0.5 |
| 2 | 100 | 353 | 1:1 | 3 | 0 |
| 3 | 10 | 373 | 1:1 | 3 | 0 |
| 4 | 100 | 373 | 1:1 | 3 | 0.5 |
| 5 | 10 | 353 | 1:5 | 3 | 0 |
| 6 | 100 | 353 | 1:5 | 3 | 0.5 |
| 7 | 10 | 373 | 1:5 | 3 | 0.5 |
| 8 | 100 | 373 | 1:5 | 3 | 0 |
| 9 | 10 | 353 | 1:1 | 10 | 0 |
| 10 | 100 | 353 | 1:1 | 10 | 0.5 |
| 11 | 10 | 373 | 1:1 | 10 | 0.5 |
| 12 | 100 | 373 | 1:1 | 10 | 0 |
| 13 | 10 | 353 | 1:5 | 10 | 0.5 |
| 14 | 100 | 353 | 1:5 | 10 | 0 |
| 15 | 10 | 373 | 1:5 | 10 | 0 |
| 16 | 100 | 373 | 1:5 | 10 | 0.5 |
| 17 | 55 | 363 | 1:3 | 6.5 | 0.25 |
| 18 | 55 | 363 | 1:3 | 6.5 | 0.25 |
| 19 | 55 | 363 | 1:3 | 6.5 | 0.25 |

3.4.4 Recyclability

The catalyst was reused after the first catalytic test for 4 h. Before the resin was reused for each cycle, it was dried at 388 K for 12 h without prior washing. The spent resins were subsequently used to catalyse the reaction with the same operating condition as the first catalytic test. The spent resins were reused for 4 cycles.

3.4.5 Kinetic Studies

The best DIAION resin was chosen for kinetics study to obtain kinetic data at various temperatures (358, 368, 378, and 388 K). The other operating parameters were

remained. The samples were withdrawn subsequently until no more increment in yield/conversion equilibrium conversion had reached.

The conversion and yield profile generated from the study of the effect of temperature was used to develop the kinetic model of the esterification of AA with 2EH. Pseudohomogeneous (PH), Eley Rideal (ER) and Langmuir Hinshelwood Hougen-Watson (LHHW) reaction models were used to fit with the experimental kinetic data. The activity based model was used to account for the non-ideal mixing of the bulk liquid phase. PH model is widely used in the esterification systems (Pappu et al., 2013; Komoń et al., 2013; Yu et al., 2004). In the PH model, adsorption and desorption of all components are negligible. The PH model assumes complete swelling of the polymeric catalyst in contact with polar solvents, leading to an easy access of the reactants to the active sites. LHHW and ER models are appropriate for heterogeneously catalysed reactions. Both models are applicable whenever the rate of reaction is limited by surface reaction. LHHW model well describes the surface reaction between adsorbed molecules while ER model well represents the surface reaction takes place between one adsorbed species and one non-adsorbed reactant from the bulk liquid phase (Fogler, 2008). In the present study, the activity based kinetic model was preferred due to the non-ideal mixing of the bulk liquid phase. The activity of component i , α_i can be related to its mole fraction, x_i using Equation 3.7:

$$\alpha_i = \gamma_i x_i \quad (3.7)$$

where γ_i is the liquid activity coefficient for component i and it can be calculated using UNIFAC group contribution method (Komoń et al., 2013; Peykova et al., 2012). The UNIFAC model splits up the activity coefficient for each species in the system into two components; a combinatorial, γ_{ci} and a residual component, γ_{ri} as shown in Equation 3.8 and it was calculated using a UNIFAC program written in Microsoft Excel:

$$\ln \gamma_i = \ln \gamma_{ci} + \ln \gamma_{ri} \quad (3.8)$$

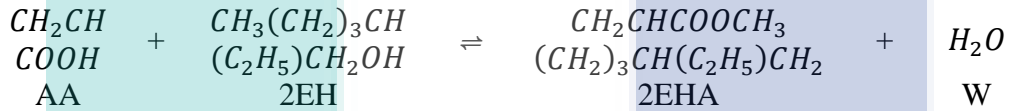
The PH, ER and LHHW models are as in Equation 3.9 – 3.11:

$$r_{2EHA} = k_f \left(\alpha_{AA} \alpha_{2EH} - \frac{1}{K_A} \alpha_{2EHA} \alpha_W \right) \quad (3.9)$$

$$r_{2EHA} = \frac{k_f (\alpha_{AA} \alpha_{2EH} - (1/K_A) \alpha_{2EHA} \alpha_W)}{(1 + K_{AA} \alpha_{AA} + K_W \alpha_W)} \quad (3.10)$$

$$r_{2EHA} = \frac{k_f (\alpha_{AA} \alpha_{2EH} - (1/K_A) \alpha_{2EHA} \alpha_W)}{(1 + K_{AA} \alpha_{AA} + K_{2EH} \alpha_{2EH} + K_{2EHA} \alpha_{2EHA} + K_W \alpha_W)^2} \quad (3.11)$$

where K_a is the activity based equilibrium constant, K_i is the adsorption equilibrium constant for species i and k_f is the rate constant. The esterification of AA with 2EH occurs based on the chemical reaction as in following equation:



This reaction is an acid-catalysed equilibrium limited esterification. The thermodynamic equilibrium constant of the reaction, K_a is shown in Equation 3.12.

$$K_a = \exp\left(-\frac{\Delta G^0}{RT}\right) = \prod a_i^{v_i} = \prod_i (x_i \gamma_i)^{v_i} = \frac{x_{2EHA} x_W \gamma_{2EHA} \gamma_W}{x_{AA} x_{2EH} \gamma_{AA} \gamma_{2EH}} \quad (3.12)$$

k_f can be related to the temperature with Arrhenius equation as in Equation 3.13:

$$k_f = k_{f0} \exp\left(-\frac{E_f}{RT}\right) \quad (3.13)$$

where k_{f0} is the pre-exponential factors for the reactions, E_f denotes the activation energy of reaction, R is the gas constant and T is the temperature of the reaction. In the case of batch-wise heterogeneously catalysed reaction, r_{2EHA} was determined using Equation 3.14 (Teo and Saha, 2004). The derivative (dC_{2EHA}/dt) was obtained by differentiating the concentration-time data,

$$r_{2EHA} = \frac{dC_{2EHA}}{dt} \quad (3.14)$$

where C_{2EHA} is the concentration of 2EHA and t is the reaction time. k_f and K_i were obtained simultaneously by fitting r_{2EHA} profile at different temperatures to the

proposed kinetic models using L–M (Levenberg–Marquardt) method for non-linear regression analysis in POLYMATH6.10. k_{f0} and E_f were obtained by plotting the Arrhenius plot.

3.4.6 Sample Analysis Using GC

The Agilent gas chromatography equipped with flame ionize detector was used to analyse the composition of 2-ethyl hexyl acrylate in the collected samples. DB200 GC column was use for the analysis. Helium was use as carrier gas. N-hexane is used as solvent. The injector and detector block temperatures were maintained at 523 K and 573 K respectively. The oven temperature was maintained isothermal at 418 K.

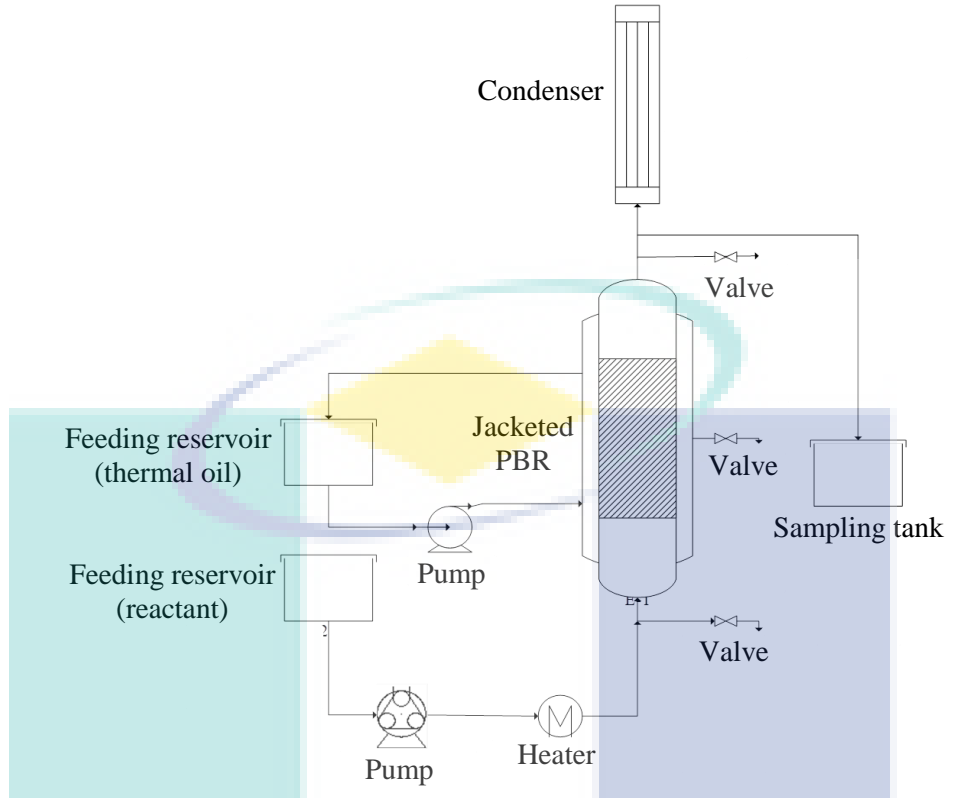
The standard calibration curve of 2-ethyl hexyl acrylate and acrylic acid from GC-FID analysis was performed to obtain the concentration of the components in the samples. The analytical/GC standard for each component was use to perform the calibration curve.

The range of concentration to be used for 2-ethyl hexyl acrylate calibration curve was between 200 ppm to 2000 ppm with 200 ppm interval for each point and the range of concentration to be used for acrylic acid calibration curve was 400 ppm to 4000 ppm with 400 ppm interval for each point.

3.5 Experimental Studies in a Packed Bed Reactor Studies

Laboratory-scale packed bed reactor (PBR) was designed and fabricated for experimental studies. The design has considered the residence time, mass transfer resistance, and heat transfer resistance during the reaction. Figure 3.3 shows the reactor system process flow diagram and real photo.

i)



ii)



Figure 3.3 i) Packed bed reactor process flow diagram; ii) Packed bed reactor real photo

3.5.1 Residence Time Distribution (RTD) Studies

The packed bed reactor (PBR) cross sectional diagram has been shown in Figure 3.4. The portable catalyst cage was design due to the improper RTD profile which will be discuss in section 4.3.1 later. The design and photo of the catalyst cage was shown in Figure 3.5. Due to the installation of portable catalyst cage, only sampling port 1 was used. The steady state temperature was assumed when all temperature probe show the similar temperature.

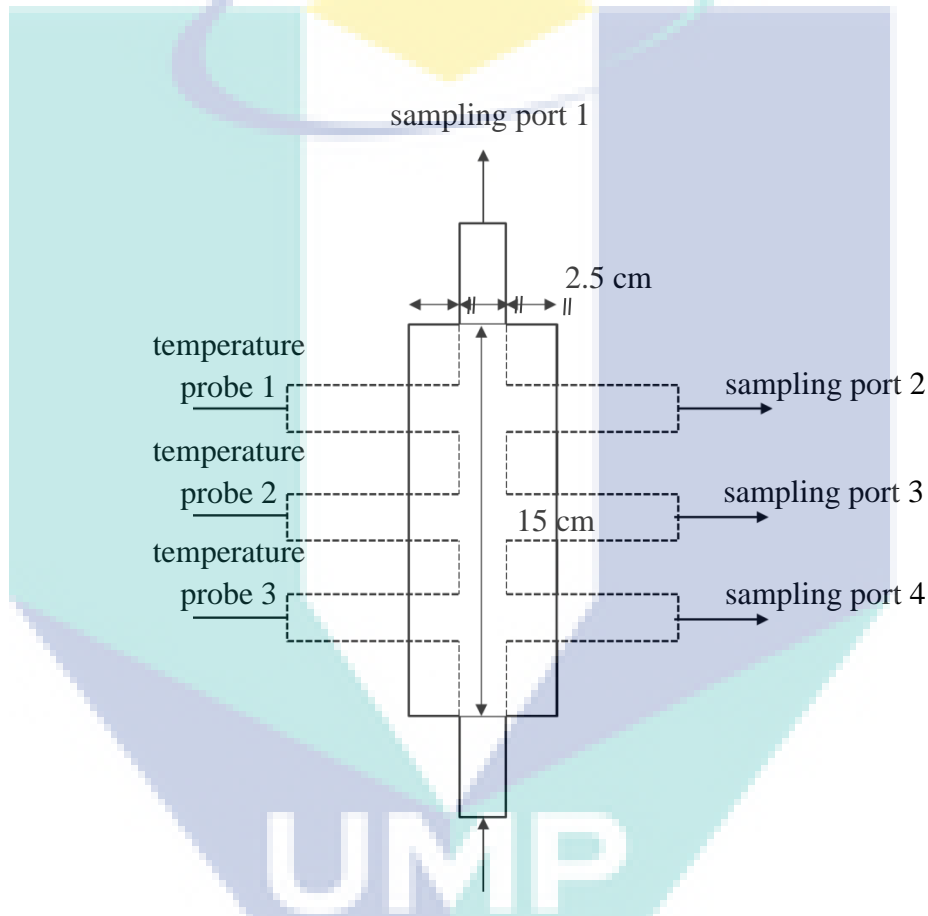


Figure 3.4 Jacketed PBR cross sectional diagram

The residence time distribution in PBR was gauged by carrying out the tracer experiments using pulse injections of a Dextran solution (15 kg/m^3) in water. Samples with the volume of 0.2 ml were injected at different flow rates (1, 3, and 5 mL/min) using water as an eluent and the reactor outlet concentration was monitored using a UV-VIS spectrophotometer at 300 nm. At least three runs were performed for each flow rate to check the reproducibility of experimental data.

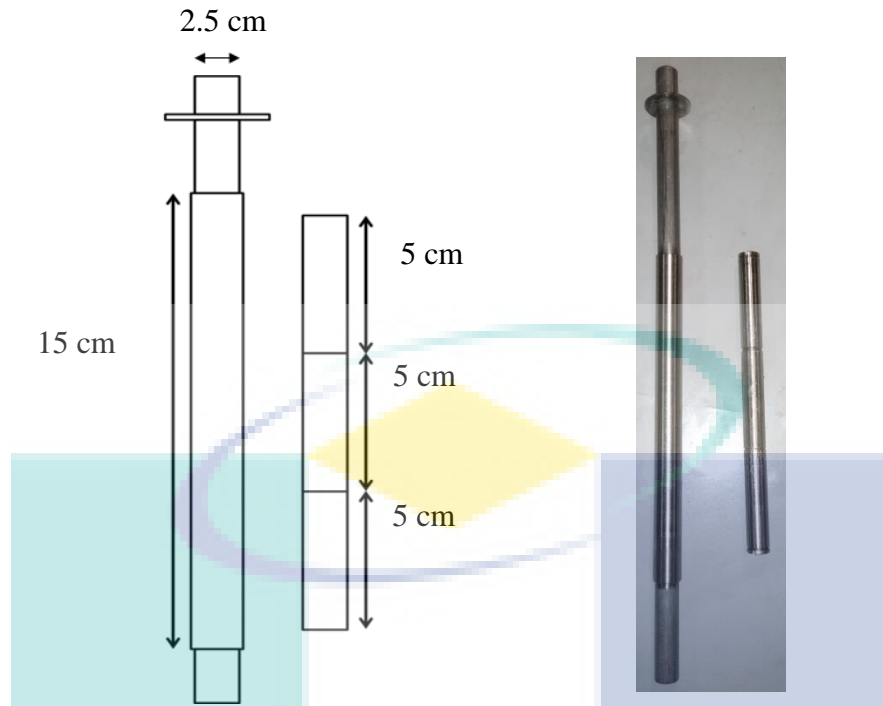


Figure 3.5 Catalyst cage of tubular PBR

The bed porosity and the Peclet number (Pe) were calculated according to Equation 3.15 - 3.18;

$$E(t) = \frac{C_{out}(t)}{\int_0^{\infty} C_{out}(t) dt} \quad (3.15)$$

$$\varepsilon = \frac{\bar{t}}{V_b/Q} = \frac{\int_0^{\infty} tE(t) dt}{V_b/Q} \quad (3.16)$$

$$Pe = \frac{2\bar{t}^2}{\sigma^2} = \frac{2\bar{t}^2}{\int_0^{\infty} (t - \bar{t})^2 E(t) dt} \quad (3.17)$$

$$\sigma^2 = \bar{t} - \left[\int_0^{\infty} tE(t) dt \right]^2 \quad (3.18)$$

where \bar{t} is the mean residence time and σ^2 is the variance of the residence time distribution curve. The results obtained are presented in Table 4.9.

The following assumptions were take account into consideration:

1. Isothermal operation;
2. Constant bed and packing porosities;
3. Plug flow model with axial dispersion but negligible radial dispersion;

4. Velocity variations due to changes in the bulk composition;
5. Mass transfer described by the linear driving force model;
6. Multicomponent adsorption equilibrium described by extended Langmuir isotherm model

3.5.2 Adsorption Isotherm Studies

The adsorption experiments were performed by feeding to different binary mixtures of known composition of a reactant and a product of the esterification reaction to the PBR, at constant temperature and feed flow rate. To obtain the breakthrough curves, 1 ml samples were collected at the reactor outlet, at certain time intervals, and analysed by gas chromatography (GC) equipped with flame ionize detector (FID) and Agilent DB-200 column. The experiments proceeded until no changes were observed in the outlet stream composition

3.5.3 Experimental Study of the Effect of Important Operating Parameters in the PBR

The effect of the important operating parameters such as temperature (328-368 K), feed flow rate (1-5 ml/min), aspect L/D ratio of tubular packed bed reactor (5:1-15:1), reactants feed molar ratio of AA:2EH (1:1 to 1:5), and amount of catalyst (1-15 g) were investigated. For the real wastewater, the variation concentration (5-90% of AA w/w) was manipulated by adding AA (99.9%) accordingly in the real wastewater. The required amount of prepared reactants was charged to the PBR using a peristaltic pump. The volumetric flow rate of feed was calibrated periodically with pure water. Ion exchange resins and stainless steel spring were packed in the PBR. The desired catalyst amount was loaded. The reaction temperature was regulated to within ± 1 K by circulating thermostatic silicon oil through the jacket of the reactor. The thermocouples were placed at the inlet and outlet of the reactor to monitor the reaction temperature. Samples were withdrawn from the sampling ports at a regular interval until the steady state was attained. The samples were analysed with the gas chromatography (GC) equipped with flame ionize detector (FID) and Agilent DB-200 column for 2EHA, AA and 2EH composition analysis.

3.5.4 Mass Transfer Parameter Calculations

In overall mass transfer coefficient model, a global mass-transfer coefficient, K_L was considered that combines external and internal mass-transfer coefficients, k_e and k_i , respectively, according to the resistances-in-series model given by the following equation:

$$\frac{1}{K_L} = \frac{1}{k_e} + \frac{1}{\varepsilon_p k_i} \quad (3.19)$$

The internal mass-transfer coefficient was estimated by Glueckauf (1955) Equation 3.20 while the external mass-transfer coefficient was estimated by the Wilson and Geankopolis correlation (Ruthven, 1984), expressed by Equation 3.21:

$$k_i = \frac{5D_m/\tau}{r_p} \quad (3.20)$$

$$S_p = \frac{1.09}{\varepsilon} (Re_p Sc)^{0.33} \quad 0.0015 < Re_p < 55 \quad (3.21)$$

Where Sh_p and Re_p are the Sherwood and Reynolds numbers relative to the particle, respectively, described by Equation 3.22 and 3.23. The Schmidt number, Sc , was determined according to Equation 3.24

$$S_p = \frac{k_e d_p}{D_m} \quad (3.22)$$

$$Re_p = \frac{\rho d_p u}{\eta} \quad (3.23)$$

$$S_c = \frac{\eta}{\rho D_m} \quad (3.24)$$

The infinite dilution diffusivities were estimated by the Scheibel correlation (Scheibel, 1954)

$$D_{A,B}^0 = \frac{8.2 \times 10^{-8} T}{\eta_B V_{M,A}^{1/3}} \left[1 + \left(\frac{3V_{M,B}}{V_{M,A}} \right)^{2/3} \right] \quad (3.25)$$

where $D_{A,B}^0$ is the diffusion coefficient for a dilute solute A into a solvent B and η_B is the viscosity of pure solvent B. Vignes equation (Vignes, 1966), based on coefficients at infinite dilution, was used to predict the diffusion coefficient in concentrated solutions

for binary systems

$$D_{B,A} = D_{A,B} = (D_{A,B}^0)^{x_2} (D_{B,A}^0)^{x_1} \quad (3.26)$$

The diffusion coefficient for multicomponent concentrated solutions was determined by the Perkins and Geankoplis mixing rule (Perkins and Geankoplis, 1969)

$$D_{A,m} \eta_m^{0.8} = \sum_{\substack{i=1 \\ i \neq 1}}^n x_i D_{A,i}^0 \eta_i^{0.8} \quad (3.27)$$

where η_m is the viscosity of the mixture and η_i is the viscosity of the component i .

3.6 Simulation Studies

3.6.1 Simulation of The Esterification Of AA With 2EH In A Tubular Reactor Using Aspen Plus V8

The simulation study was performed using Aspen Plus V8 to predict the concentration profile of PBR applied in the esterification of 2EH with AA adopting DIAION PK208 resin as catalyst. The assumptions made are as follow:

1. Ideal packed bed reactor
2. There is no mixing in axial direction (direction of flow)
3. Complete mixing in radial direction.
4. Uniform velocity profile across the radius

The conversion profile generated from the parametric study was then used to obtain the rate data. The rate data was then fit to the Pseudohomogeneous (PH) and Eley Rideal (ER) kinetic models. In the PH model, adsorption and desorption of all components are negligible. The PH model assumes complete swelling of the polymeric catalyst in contact with polar solvents, leading to an easy access of the reactants to the active sites. ER models are appropriate for heterogeneously catalyzed reactions. These models are applicable whenever the rate of reaction is limited by surface reaction. ER model well represents the surface reaction takes place between one adsorbed species and one non-adsorbed reactant from the bulk liquid phase (Fogler, 2008). The mass balance equation for PBR is expressed in Equation 3.28 (Fogler, 2008).

$$W / F_{AA0} = \int \frac{dX_{AA}}{-r_{AA}} \quad (3.28)$$

Where F_{AA0} is the initial molar flow rate of the AA in the feed stream, X_{AA} is the conversion of AA and r_{AA} is the rate of consumption of AA.

r_{AA} can be determined from the slope of tangent in the plot of X_{AA} vs W/F_{AA0} , weight hourly liquid velocity (WHLV). PH and ER models as shown in Equation 3.29 - 3.30 were used to correlate r_{AA} :

$$r_{AA} = k_f \left(C_{AA} C_{2EH} - \frac{C_{2EHA} C_W}{K_x} \right) \quad (3.29)$$

$$r_{AA} = \frac{k_f \left(C_{AA} C_{2EH} - \frac{C_{2EHA} C_W}{K_x} \right)}{(1 + K_{AA} C_{AA} + K_W C_W)} \quad (3.30)$$

where k_f is forward rate constant, K_x is thermodynamic equilibrium constant, C_{AA} , C_{2EH} , C_W and C_{2EHA} are the mole concentration of component AA, 2EHA, W and 2EHA respectively, K_{AA} and K_W are the adsorption equilibrium constant for AA and W respectively.

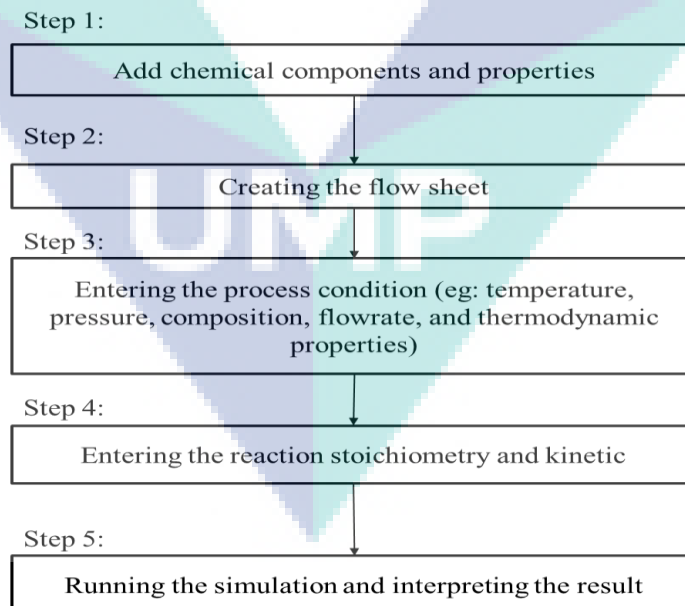


Figure 3.6 Procedure of simulating the esterification of AA with 2EH in a tubular PBR using Aspen Plus software

Figure 3.6 shows the step of running the Aspen Plus software for the esterification of AA with 2EH to produce 2EHA in tubular PBR system.

3.6.2 Simulation of The Esterification of AA With 2EH In A Tubular Packed Bed Reactor With Dispersion

In order to consider the mass transport of the reacting species in the reactor which accounts for diffusion, convection, and reaction in diluted solutions is modelled with the Transport of Diluted Species interface in COMSOL software to simulate the reaction. This model will consider the following transport phenomena:

1. Free channel flow: Navier-Stokes equation
2. Porous media flow: Brinkman equation
3. Mass transfer transport: Diffusion and convection with chemical reaction kinetics
4. Heat transfer: Assumption at isothermal condition.

The reaction inside the pellets is added to the mass balances in the Transport of Diluted Species interface with the Reactive Pellet Bed feature. This feature has a predefined extra dimension (1D) on the normalized radius ($r = r_{\text{dim}}/r_{\text{pe}}$) of the pellet particle. The mesh on the extra dimension has a default of 10 elements with a cubic root sequence distribution. If spherical pellets are selected, the following spherical diffusion/reaction equation is set up and solved along the pellet radius for each species i :

$$4\pi N \left\{ r^2 r_{\text{pe}}^2 \varepsilon_{\text{pe}} \frac{\partial c_{\text{pe},i}}{\partial t} + \frac{\partial}{\partial r} \left(-r^2 D_{\text{pe},i} \frac{\partial c_{\text{pe},i}}{\partial r} \right) = r^2 r_{\text{pe}}^2 R_{\text{pe},i} \right\} \quad (3.31)$$

Where, r is a dimensionless radial coordinate that goes from 0 (center) to 1 (pellet surface), r_{pe} is the pellet radius, and N the number of pellets per unit volume of bed. The advantage of formulating Equation 3.31 on a dimensionless 1D geometry is that the pellet radius can be changed without changing the geometry limits.

D_{pe} is an effective diffusion coefficient (SI unit: m^2/s) and $R_{\text{pe},i}$ is the reaction source term (SI unit: $\text{mol}/(\text{m}^3 \cdot \text{s})$). Note that the latter term is taken per unit volume of porous pellet material.

At the pellet-fluid interface, a film condition assumption is made. The flux of mass across the pellet-fluid interface into the pellet is possibly rate determined by the resistance to mass transfer on the bulk fluid side. The resistance is expressed in terms of a film mass transfer coefficient, h_{Di} , such that:

$$N_{i,\text{inward}} = h_{D,i}(c_i - c_{pe,i}) \quad (3.32)$$

where $N_{i,\text{inward}}$ is the molar flux from the free fluid into a pellet and has the unit moles/(m².s). The mass transfer coefficient to calculate automatically as described in the section Theory for the Reactive Pellet Bed in the Chemical Reaction Engineering Module User's Guide.

The pressure drop in the reactor is also accounted for and is modeled with the Darcy's Law Interface.

The Navier-Stokes equation was arise from applying Isaac Newton's second law to fluid motion, together with the assumption that the stress in the fluid is the sum of a diffusing viscous term (proportional to the gradient of velocity) and a pressure term—hence describing viscous flow. This equation is given as below:

$$\rho(u \cdot \nabla) u = \nabla \cdot [-pl + \mu(\nabla u + (\nabla u)^T)] + F \quad (3.33)$$

$$\rho \nabla \cdot u = 0 \quad (3.34)$$

The left side of the equation describes acceleration, and may be composed of time-dependent and convective components (also the effects of non-inertial coordinates if present). The right side of the equation is in effect a summation of hydrostatic effects, the divergence of deviatoric stress and body forces (such as gravity). In this equation, ρ is the density, u is the flow velocity, $\nabla \cdot$ is the divergence, p is the pressure, and F is the gravitation force.

Equation 3.35 shows the Brickman equation calculation for the diffusion and convection considering the porous media flow in the reactor.

$$\nabla \cdot (-D_i \nabla_i) + u_i \cdot \nabla_{ci} = R_i \quad (3.35)$$

$$N_i = -D_i \nabla c_i + u c_i \quad (3.36)$$

Heat transfer phenomenon was calculate using the following equation:

$$\rho (p u \cdot \nabla T + \nabla \cdot q = Q + Q_p + Q_v) \quad (3.37)$$

$$q = -k \nabla T \quad (3.38)$$

It is known that, for thermodynamic consistency, the maximum molar capacity of an adsorbent should be the same for the all species to follow the ER equilibrium model assumption. However this assumption is not verified for molecules of very different sizes. (Siva & Rodrigues, 2002). Therefore, in some scientific works, it is assumed a constant monolayer capacity in terms of mass (Popken et al., 2000) or in terms of volumes (Periera et al., 2009). In this simulation studies, it was considered a contant volumetric monolayer capacity for all species, Q_v , which is given by $Q_v = Q_i \times V_{M,j}$. This assumption allowed reducing the adjustable adsorption parameters from 9 (one molar monolayer capacity and one equilibrium constant for each species) to 5 (one volumetric monolayer capacity for all species and one equilibrium constant for each species), at each temperature.

The rate of chemical reaction is given by the ER equation as follow:

$$r = k_c \frac{\alpha_{2EH} \alpha_{AA} - \frac{\alpha_{2EHA} \alpha_W}{K_a}}{(1 + K_{AA} \alpha_{AA} + K_W \alpha_W)} \quad (3.39)$$

where K_a is the activity based equilibrium constant, K_i is the adsorption equilibrium constant for species i and k_f is the rate constant.

The steps involved in the simulation of PBR with dispersion using COMSOL Multiphysics software is shown in Figure 3.7.

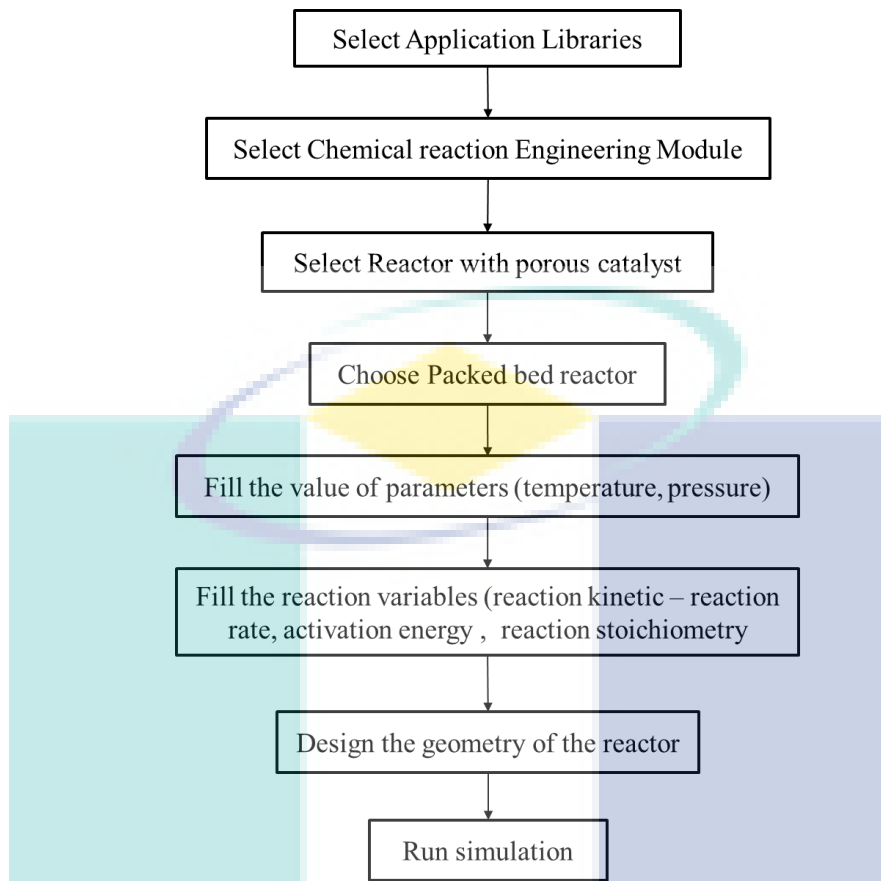


Figure 3.7 Summary of procedure of simulating packed bed reactor with dispersion using COMSOL Multiphysics software

CHAPTER 4

RESULTS AND DISCUSSION

4.1 Catalyst Characterisation

Prior to the esterification reaction study, the ion exchange resin (IER) was characterised for its physicochemical properties through particle size analysis, nitrogen physisorption measurement, Fourier Transform Infrared Spectroscopy (FTIR) analysis, ion exchange capacity (IEC) measurement, leaching analysis, and swelling analysis.

4.1.1 Measurement of Particle Size Distribution

The particle size distribution of the fresh DIAION's IER catalysts was measured using Malvern Mastersizer 2000 and shown in Figure 4.1. Most of the catalysts have narrow distribution range with the particles size in between 400-600 μm except IER SK104 and PK228 that possess the mean particle size of 600 μm and 800 μm respectively. It is known a smaller catalyst particle size would reduce the internal diffusion resistances. The catalyst particle size was then used to verify the presence of mass transfer resistances in the experimental studies for the esterification of AA with 2EH and the findings are reported in section 4.2.3

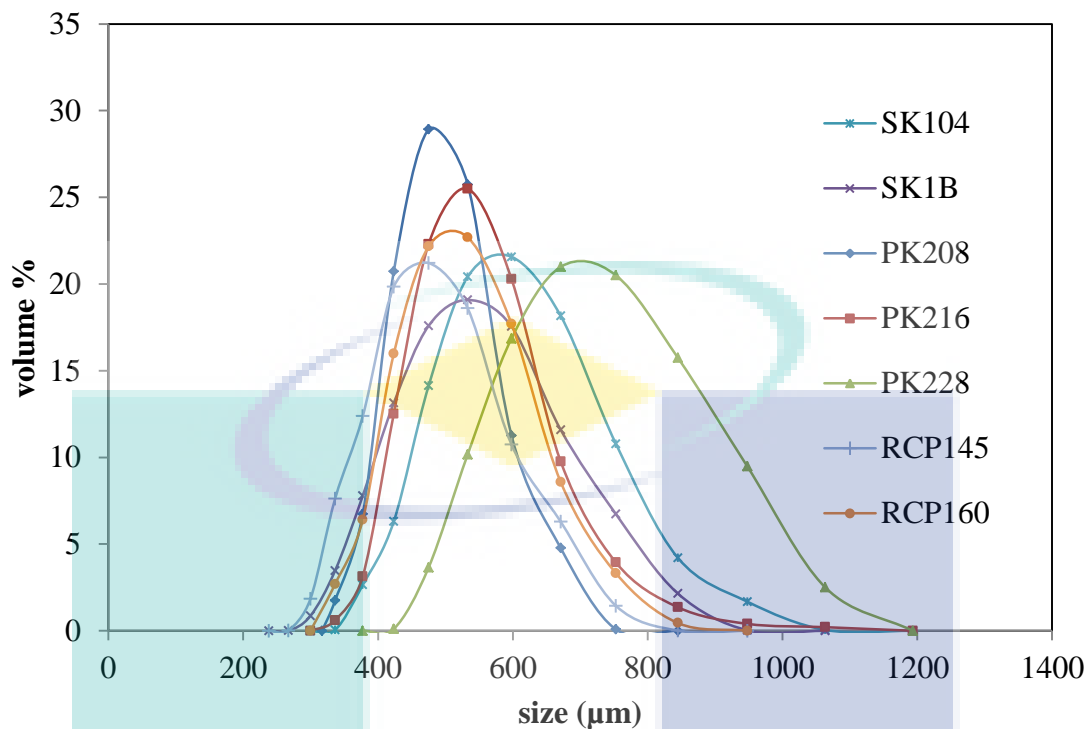


Figure 4.2 Particle size distribution for DIAION IER catalyst

4.1.2 Nitrogen Physisorption Analysis

The porous structure (surface area, pore volume and average pore diameter) of each type of IER that was adopted in the present studies are summarized in Table 4.1. The IER catalysts are grouped into gel type resins and macroporous type resins on the basis of its pore structure. As known, the surface area and pore volume measurement are not applicable for the un-swollen gel type IER as it is non-porous. The highly macroporous IER, RCP145 and RCP160 possessed the highest surface area (39-51 m^2/g) and average pore diameter (206-283 Å). Relatively, macroporous IER, PK208, PK216 and PK228 had lower surface area (13-16 m^2/g) and average pore diameter (112-261 Å). The variation of surface area among similar types of catalyst is commonly contributed by the DVB% of crosslinking in each catalyst. This was discussed in depth in section 4.1.5.

Table 4.2 Surface area and porosity of the tested acidic ion exchange resins

| Catalyst | Type | BET surface area (m ² /g) | Pore volume (cm ³ /g) | Average pore diameter (Å) |
|----------|---------------|--------------------------------------|----------------------------------|---------------------------|
| SK104 | Gelular | 0.40 | *NA | NA |
| SK1B | Gelular | 0.52 | NA | NA |
| PK208 | Macroporous | 13.28 | 0.087 | 261.00 |
| PK216 | Macroporous | 14.21 | 0.029 | 112.13 |
| PK228 | Macroporous | 15.94 | 0.033 | 139.43 |
| RCP145 | Highly porous | 39.25 | 0.298 | 206.68 |
| RCP160 | Highly porous | 50.25 | 0.355 | 282.49 |

* NA: Not applicable

4.1.3 Fourier Transform Infrared Spectroscopy (FTIR) analysis

Figure 4.2 illustrates the spectra of FTIR analysis for the fresh DIAION IER catalysts. The peaks at 580 cm⁻¹, 1600 cm⁻¹, and 2920 cm⁻¹ belong to the aromatic ring stretching of the polystyrene support. The peaks at wavenumber of 1250 cm⁻¹, 1030 cm⁻¹, and 709 cm⁻¹ represent the sulfur-oxygen double bonds of the catalyst. The intensity of these peaks was closely related to the ion exchange resin capacity of the resin. RCP type resins, the highly porous resins were expected to have lowest ion exchange capacity IEC, whereas the macroporous (PK type) and SK (gel type) possessed comparable IEC. The IEC of these resins was analysed and reported in the subsequent section. The peak at wavenumbers of 1600 cm⁻¹ indicates the deformation and skeletal vibrations of C-H in divinylbenzene which contribute toward the Lewis acid features (Salem, 2001). The peak at 1645 cm⁻¹ meanwhile indicates aromatic C=C bond Bronsted acid which associate with sulfonic group sites respectively (Naushad et al., 2014). The wide peak at 3426 cm⁻¹ in Figure 4.2 is ascribed to the O-H stretching vibrations in the SO-H groups grafted to the poly(styrene-co-divinylbenzene) backbone as well as to the absorbed moisture. In summary, the FTIR analysis affirmed the presence of sulfonic acid, the Bronsted acid sites on the polystyrene support.

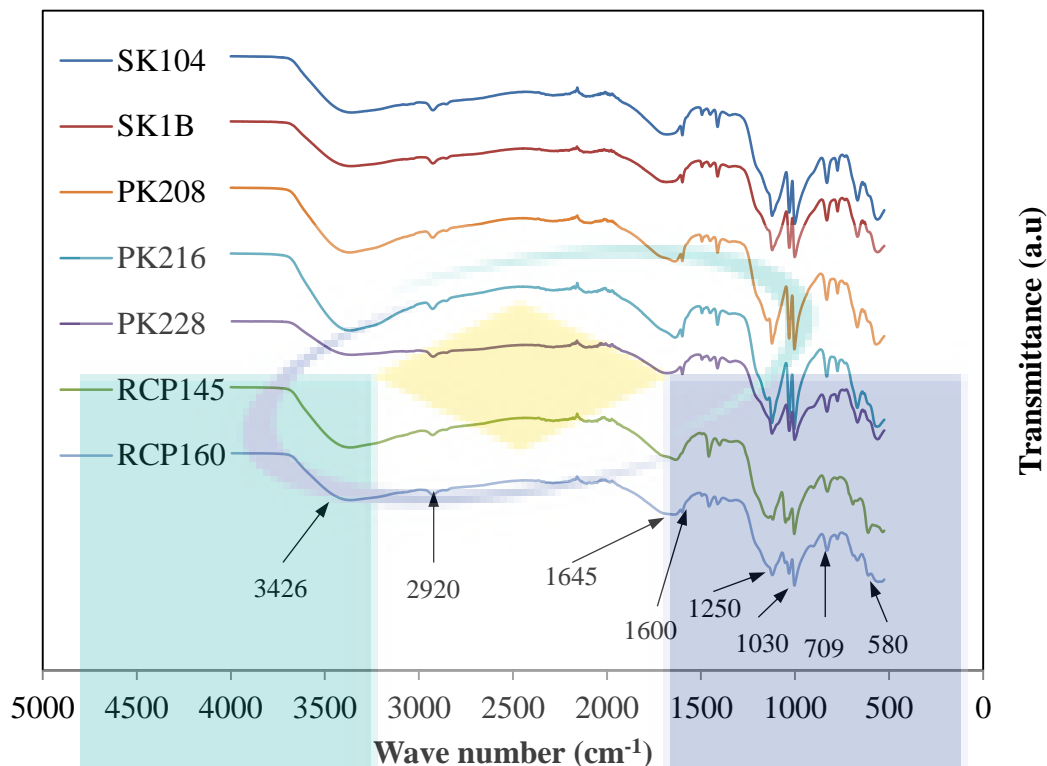


Figure 4.3 FTIR spectra for DIAION IERs catalyst (SK104, SK1B, PK208, PK216, PK228, RCP145, and RCP160)

4.1.4 Ion Exchange Capacity, Swelling, and Leachability Analysis

The IER catalysts can be categorised into gel type resins (SK type) and macroporous type resins (PK type and RCP type) on the basis of its pore structure to minimize the pore diffusion resistances. The microporosity (< 2 nm) and high surface area of the gel type resins can only be exhibited when it swells. It usually possesses very low crosslinking agent, di-vinyl benzene (DVB) content since swelling is a very important effect to the gel type resins (Van de Steene et al., 2014). Commonly, the capacity of active site increases with the increase of catalyst surface. The advantages of having higher catalyst surface area is offset by the enhanced leaching phenomenon due to the increase of catalyst surface area that leads to the catalyst recyclability issues (Gruber et al., 2012).

Figure 4.3 summarizes the ion exchange capacity (IEC), divinylbenzene crosslinkage percent (DVB CL%) and sulfonic acid (SO_3^-) leaching properties of each IER used in these studies. SK1B exhibited the highest IEC, followed by PK228 and

PK216 whereas RCP type IER possessed lowest IEC. It was observed that, within the same category of IER, the raise of %CL in the IER could improve the IEC because of a more stable and constrict structure to uphold the sulfonic acid group (Ma et al., 2018). IEC represents the amount of sulfonic acid on the surface of IER. A higher IEC indicates more active sites are available for catalysing esterification of AA with 2EH. Nevertheless, IEC is not the sole indicator to reflect the availability of active sites. Exposure of active sites to the reactants during the esterification reaction also rely on DVB CL% and surface area of the IER. In addition, the DVB CL% and structural properties of IER would also significantly influence the deactivation through sulfonic acid leaching particularly in a liquid phase esterification reaction.

Table 4.3 shows that the decline of crosslinking degree in the all type of IER has increased its degree of swelling. The pore of gel type IER in dry form cannot stand out and be assessed by the reactants. These resins require a swelling agent like solvent to expand the polymeric matrix by generation of spaces between polystyrene chains. These micro-porous spaces enable the access of reactant molecules to the sulfonic acid active sites. Typically, the amount of cross-linking is kept less than 12% in gel type IER. Higher cross-linking would cause lower catalytic property due to increasing resistance of diffusion (Rohm and Haas, 1980). The increase of the diffusion resistances restricted the access of solvent to the sulfonic acid and hence causing less sulfonic acid or sulfuric acid leach out from the IER catalysts with higher DVB CL%. Apparently, more sulfonic acid or sulfuric acid was leached in water comparing to 2EH because of the lower stability of hydrophilic ion SO_3^- in the highly polar water. It was believed that the majority of the leached species from these IER are trapped in the catalyst pores or weakly bonded sulfuric acid rather than chemically bonded sulfonic acid groups (Zhu, 2013).

The same findings were observed for the macroporous IER catalysts. In comparison to the gel type IER catalysts, the polymer matrix of the macroporous (2-50 nm) type IER beads is a conglomerate of permanent macropores and micropore gel particles. The macropore structure with higher surface area in the dry state does not significantly vary with the solvent, allowing the easy access to their interior without swelling. On the other hand, the micropore gel particles swell to certain extent when the macroporous IER is contacted with a solvent. Therefore, as indicated in Table 4.3, the

increase of degree of swelling also accelerated the leaching of ion SO_3^- in water and 2EH for the macroporous type IER. Exceptional findings were found for IER PK228 with low degree of swelling but remarkable leaching. The outlier may be due to the larger surface area and pore diameter of IER PK228.

Table 4.3 Degree of swelling for the tested acidic ion exchange resins

| Catalyst | %CL | Degree of swelling (ml/g dry resin) in different solvents | | Leaching in water (%) | Leaching in 2EH (%) |
|----------|-----------------|---|-----|-----------------------|---------------------|
| | | Water | 2EH | | |
| SK104 | 4 | 4.1 | 3.2 | 3.47 | 2.00 |
| SK1B | 8 | 2.8 | 2.4 | 3.25 | 1.45 |
| PK208 | 4 | 4.6 | 3.7 | 6.00 | 2.67 |
| PK216 | 8 | 2.8 | 2.4 | 2.56 | 2.69 |
| PK228 | 14 | 2.2 | 1.6 | 4.38 | 4.00 |
| RCP145 | NA ² | 2.1 | 1.5 | 2.17 | 4.17 |
| RCP160 | NA ² | 1.9 | 1.3 | 1.86 | 1.57 |

4.2 Esterification of Acrylic Acid with 2-Ethyl Hexanol in a Batch System

In this section, the findings from the reaction study of esterification of AA with 2EH in a batch system are reported and discussed. The activities of different types of IER catalysts were compared in the catalyst screening study. The significance of the important operating parameters, catalyst reusability, kinetic and chemical equilibrium analysis were reported based on the studies employing the best IER catalyst.

4.2.1 IER Catalyst Screening Study

Three types of ion exchange resins were tested. It included highly macroporous resins (RCP145 and RCP160), macroporous resins (PK208, PK216, and PK228) and gelular resins (SK104 and SK1B). All IER were tested for their catalytic performance in the synthesis of 2EHA via esterification of AA with 2EH at the operating condition that would not deactivate the IER. Ion exchange resins can be deactivated through the functional groups hydrolysis and/or the active sites blockage. This phenomena may be caused by the polymerization of reactant/product, depolymerisation, and the release of oligomeric sulfonic group (Neier, 1991, Chin et al., 2015). It was reported that partial desulfonation occurred and the three dimensional network shrinkage took place in IERs when the temperature was increased up to 413 K (Teo and Saha, 2004). In the present

study, all the IER was anticipated to remain its activity despite a slight leaching of non-covalently bonded sulfonic acid in 2EH. A reaction temperature of ≤ 95 °C could prevent the polymerisation of AA and depolymerisation of IER polystyrene back bone that would deactivate the catalyst.

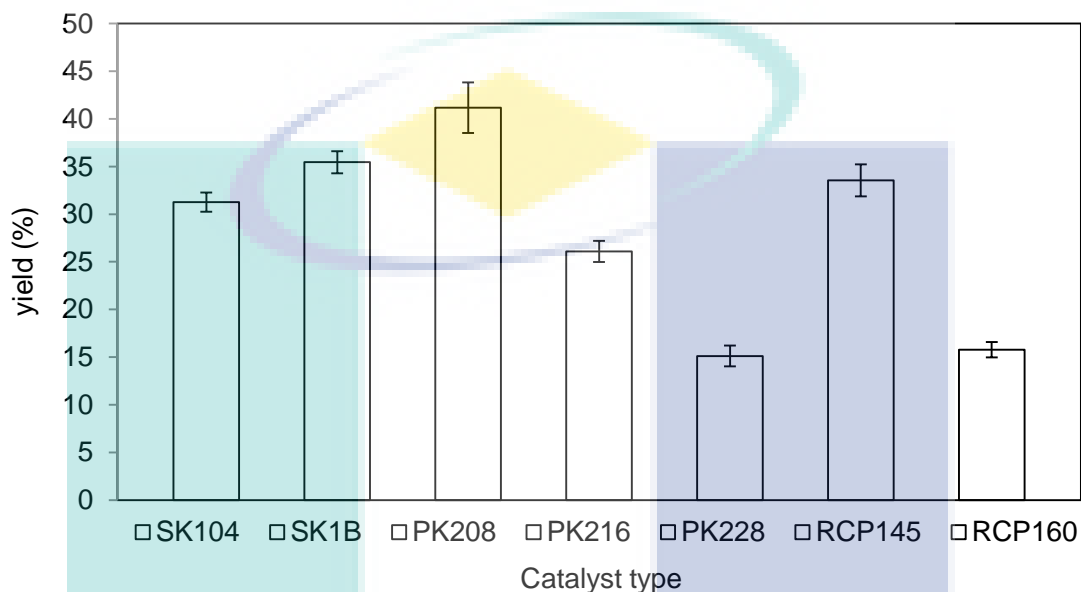


Figure 4.4 Yield of 2EHA for the reaction catalysed by different types resin catalysts for 4 h. Operating condition: Initial conc. AA: 100%; Temperature: 95°C; Catalyst loading of 10% w/w (catalyst/AA); molar ratio of AA:2EH is 1:3

The yields of 2EHA obtained through the esterification reaction catalysed by different types of resin are shown in Figure 4.4. It is noteworthy that, the highest 2EHA yield of 41% was achieved in the reaction catalysed by PK208 after 4 h, followed by the reactions catalysed by SK1B (35%), RCP145 (34%), SK104 (31%), PK216 (26%), RCP160 (16%) and PK228 (15%).

The catalytic activity of these IER catalysts was attributed to its characteristics. The correlation was done and it was found that other than IEC, other factors like the structural properties, DVB CL% and leaching were not the limiting factors to the activity of gel type IER. The gel type IER, SK1B with DVB CL% as high as 8 could also sufficiently swell the resin and expose its microporosity that enabling the access of reactants to the active sites. Therefore, the activity of the gel type IER was correlated to its IEC. The gel type resins like SK1B and SK104 performed better when its IEC increased. .

For the porous resins like PK208, PK216, PK228, RCP145 and RCP160, their catalytic performances profoundly depended on %CL. The resins with lower %CL showed higher yield of 2EHA attributing to its higher degree of swelling. The resin swelling capacity that controls the reactant accessibility to the acid sites strongly affects overall reactivity of the resin catalysts. Thus, a higher rate can be obtained for the reaction catalysed by resins with a lower %CL (Lotero et al., 2005).

SK1B exhibited the highest IEC followed by PK228 and PK216. This indicated that the catalyst activity did not depend solely on IEC but other factors like the resin active sites accessibility. PK208, SK1B, and RCP145 showed the best catalyst activity in the esterification of AA with 2EH. Similar to most of the cases, the macroporous type resin, PK208 outperformed SK1B, the gel type resin due to its higher surface area and porosity that facilitates to access of reactant to the active sites. The gel type resin is a hard glassy transparent resin bead which consists of a homogeneous matrix on a microscopic scale without discontinuities (Chakrabarti & Sharma, 1993). It does not have permanent pore and hence possessing a very low surface area when it is dry (Ali, 2009). These resins swell when brought into contact with a solvent and swelling creates space or 'solvent porosity' inside the resin to enable the access of reactant molecules to the polymer network (Martinec et. al, 1978). Meanwhile, the activity of RCP145 fell behind PK208 due to its lower degree of swelling.

4.2.2 Parametric Studies Using 2 Factorial Design as Design of Experimental in Batch System

The effect of some factors to the reaction can sometimes be less significant. These insignificant factors would lead to wrong results on the importance of the most significant variables (Jalbani et al., 2006). The purpose of using screening design is to be economical, by saving time and money on chemicals, and to identify the significant factors (Prasad et al., 2012).

Table 4.4 Two factorial result for experimental studies

| Experiment | Response (Yield (%)) |
|------------|----------------------|
| 1 | 9.55 |
| 2 | 2.12 |
| 3 | 21.56 |
| 4 | 5.10 |
| 5 | 12.21 |
| 6 | 4.98 |
| 7 | 1.42 |
| 8 | 1.54 |
| 9 | 0.23 |
| 10 | 0.82 |
| 11 | 36.02 |
| 12 | 11.33 |
| 13 | 1.14 |
| 14 | 2.31 |
| 15 | 0.26 |
| 16 | 18.90 |
| 17 | 2.29 |
| 18 | 17.06 |
| 19 | 1.68 |

Table 4.5 shows that the initial AA concentration and temperature significantly affected the 2EHA yield in the esterification of AA with 2EH (p-value < 0.0001). However, other factors such as 2EH to AA molar ratio, catalyst loading and inhibitor loading were insignificant (p-value > 0.0001). The initial AA concentration was the major contributing factor (66.52%), followed by the temperature (11.9%) as shown in Table 4.5. The interaction of initial AA concentration with temperature was also prominent (9.13%). The yield of 2EHA increased from 1.3 to 14.7 % with the increase of initial AA concentration from 10 to 100 % w/w (Figure 4.5(A)). In addition, the yield of 2EHA also increased from 5.2 to 10.8 % when the reaction temperature was increased from 80 to 100 °C (Figure 4.5(B)).

Table 4.5 P-values of responses against factors

| Factor | p-value for response |
|----------------------------------|----------------------|
| Initial AA concentration | <0.0001 |
| Temperature | <0.0001 |
| Molar ratio | 0.0344 |
| Catalyst loading | 0.0003 |
| Polymerisation inhibitor loading | 0.0381 |

Table 4.6 The percentage contribution of factors on response variables

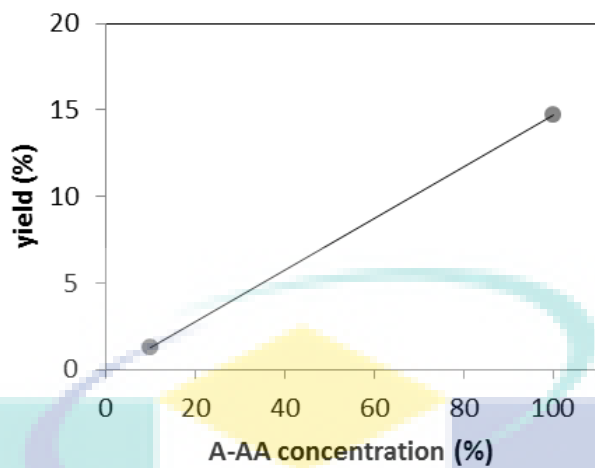
| Factor | Percentage contribution |
|---------------------|-------------------------|
| A-AA concentration | 66.52 |
| B-Temperature | 11.90 |
| C-Molar ratio | 0.50 |
| D-Catalyst loading | 2.58 |
| E-Inhibitor loading | 0.47 |
| AB | 9.13 |
| AC | 4.02×10^{-3} |
| AD | 1.31 |
| AE | 0.21 |
| BC | 0.36 |
| BD | 1.04×10^{-3} |
| BE | 0.016 |
| CD | - |
| CE | 0.02 |
| DE | 0.08 |

The significance of the initial AA concentration and reaction temperature was implied by the steeper slope of the line plots for these factors as shown in Figure 4.5(A). A higher initial AA concentration is preferred in esterification reaction of AA with 2EH to produce 2EHA due to its reversibility. The surplus of water in the reactant could shift the reaction to reactant side. In addition, the presence of huge amount of water would also interrupt the adsorption of the reactant to the active site of catalyst (Hans et al., 2005; Ratz et al., 2008; Ahmad et al., 2014). The affinity of IER to the polar solvent, water, is stronger than the affinity to the organic solvent, 2EH.

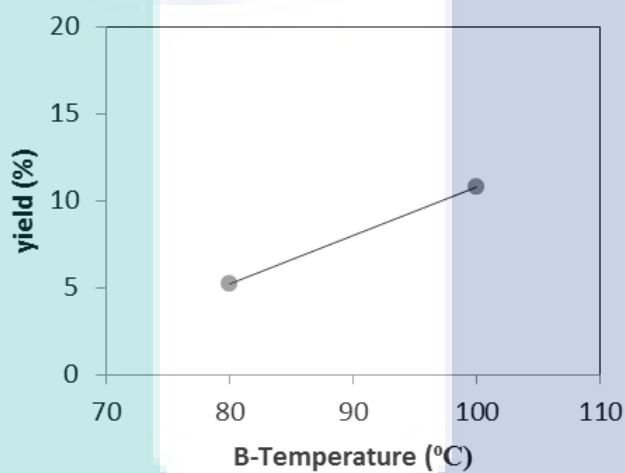
The increase of temperature also gave a better yield. This was attributed to the increasing kinetic energy of the reactant molecules that enhances the effective collision between AA and 2EH molecules and subsequently reduces the minimum energy required to form products (Chin et al., 2015).

The other factors like molar ratio of AA:2EHA, catalyst loading and polymerisation inhibitor loading were insignificant ($p > 0.0001$). The effect of molar ratio of AA:2EHA to the yield of 2EHA was negligible in the present study due to the presence of water in the reactant. The water in the reactant has traded off the positive effect of using excess amount of 2EH in driving the reaction equilibrium to 2EHA side.

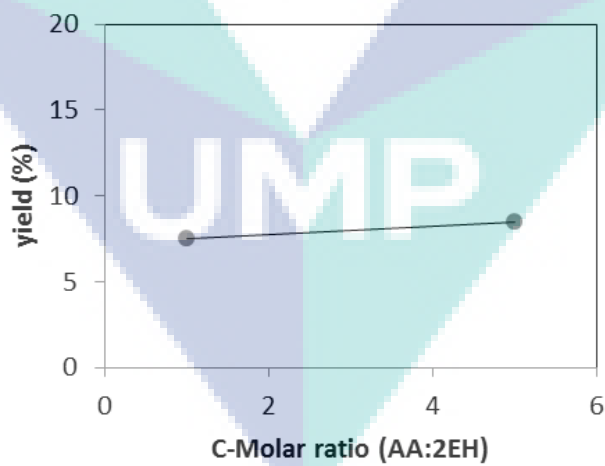
a)



b)



c)



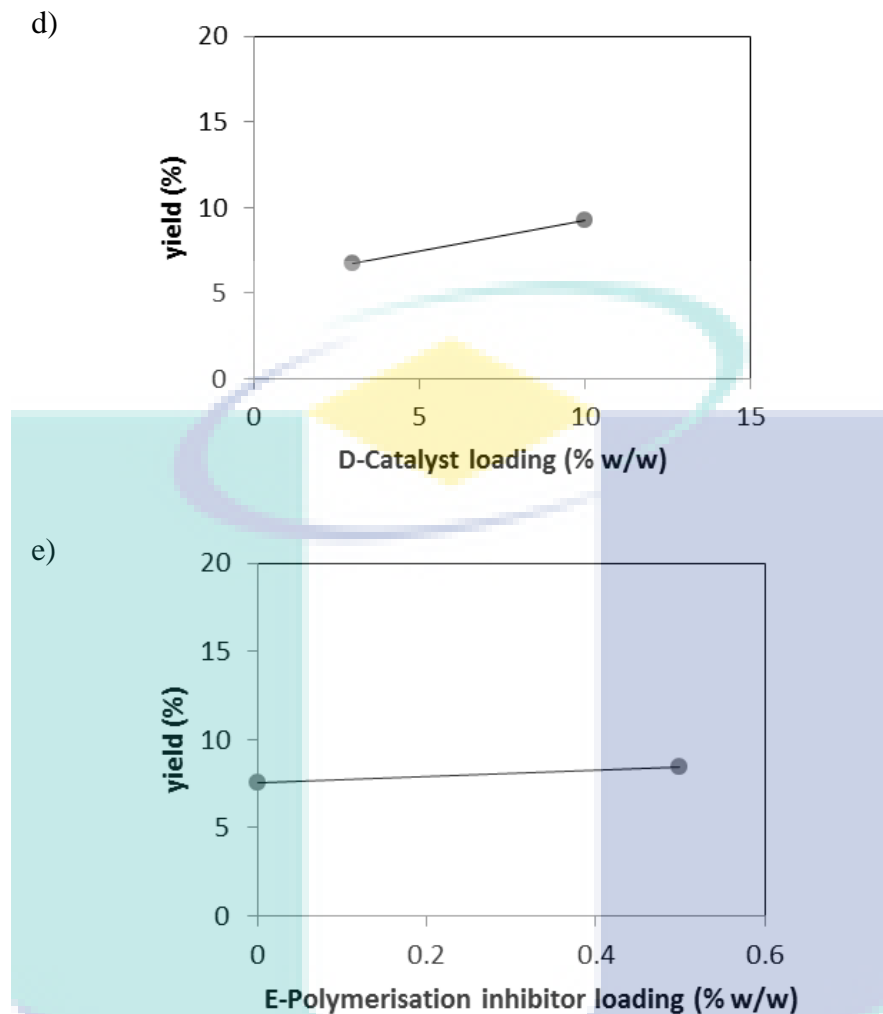


Figure 4.5 Effect of the initial AA concentration (A), temperature (B), molar ratio of AA:2EH (C), catalyst loading (D) and polymerisation inhibitor loading (E) on the performance in term of yield of esterification AA with 2EH

The catalyst amount used has provided a sufficient number of active site. Similarly, the amount of the polymerisation inhibitor used was adequate to diminish the AA polymerisation reaction since this side reaction is minimal at the reaction temperature below 100°C.

Statistically, the model F-value of 133.31 in Table 4.7 implies that the model is significant. The model equation is shown in Equation 4.1. There was only a 0.01% chance that a "Model F-Value" could occur due to noise. The "Curvature F-value" of 122.71 inferred there is significant curvature (as measured by difference between the average of the center points and the average of the factorial points) in the design space. The "Lack of Fit F-value" of 5.82 indicated the Lack of Fit was not significant relative

to the pure error. This model equation can be used to predict the yield of 2EHA accurately at different reaction operating conditions. There was a 15.44% chance that a "Lack of Fit F-value" could occur due to noise. Non-significant lack of fit shows the positive diagnose on how well each of the full models fit the data.

$$\text{Yield} = 0.17480 + 0.39279*A - 0.020243*B + 0.29406*C + 0.049829* D + 2.29400*E + 5.60806E-003*A*B + 6.07063E-003*A*D \quad (4.1)$$

Table 4.7 Analysis of variance (ANOVA) table for 2 factorial studies

| Source | Sum of Squares | df | Mean Square | F-Value | |
|----------------------------|----------------|----|-------------|---------|-----------------|
| Model | 740.35 | 7 | 105.764 | 133.310 | significant |
| A-AA Concentration | 660.13 | 1 | 660.128 | 832.056 | |
| B-Temperature | 118.13 | 1 | 118.129 | 148.895 | |
| C-Molar Ratio | 4.92 | 1 | 4.919 | 6.201 | |
| D-Catalyst Loading | 25.65 | 1 | 25.652 | 32.333 | |
| E-Inhibitor Loading | 4.68 | 1 | 4.678 | 5.896 | |
| AB | 90.58 | 1 | 90.577 | 114.167 | |
| AD | 13.00 | 1 | 13.002 | 16.388 | |
| Curvature | 97.36 | 1 | 97.356 | 122.712 | significant |
| Residual | 7.14 | 9 | 0.793 | | |
| Lack of Fit | 6.81 | 7 | 0.972 | 5.822 | not significant |
| Pure Error | 0.33 | 2 | 0.167 | | |
| Cor Total | 844.84 | 17 | | | |

4.2.3 Mass Transfer Analysis

The effect of external and internal mass transfer should be minimised or eliminated in order to develop an accurate intrinsic kinetic model for the reactions catalysed by heterogeneous catalysts. The significant effect of external and internal mass transfer could be identified by calculating the Mears criterion and Weisz–Prater criterion respectively.

To consider the effect of external mass transfer resistance on the rate of reaction, the Mears criterion for external diffusion was examined and the dimensionless Mears parameter (C_M) was calculated using the following equation:

$$C_M = \frac{r_{A,obs} \rho_b R_C n}{k_C C_{Ab}} < 0.15 \quad (4.2)$$

Where n is the reaction order, R_C is the catalyst particle radius, ρ_b is the bulk density of catalyst, $r_{A,obs}$ is observed reaction rate, C_{Ab} is the bulk concentration of AA and k_C is the mass transfer coefficient.

The occurrence of any internal pore diffusion limitation was determined on the basis of the Weisz–Prater criterion, where the dimensionless Weisz–Prater parameter (C_{WP}) can be calculated using Equation 4.3:

$$C_{WP} = \frac{-r_{A,obs} \rho_c R_C^2}{D_{eff} C_A} < 1 \quad (4.3)$$

Where R_c , D_{eff} and C_A represent the effective radius of the catalyst, the effective diffusivity and the limiting reactant concentration in the mixture respectively.

The corresponding Mears parameters (C_M) and Weisz–Prater parameters (C_{WP}) as shown in

Table 4.8 Mears and Weisz-Prater parameter for experimental studies

| Experiment | Mears parameter (C_M) | Weisz - Prater parameters (C_{WP}) |
|------------|---------------------------|--|
| 1 | 0.077 | 0.55 |
| 2 | 0.092 | 0.59 |
| 3 | 0.091 | 0.52 |
| 4 | 0.103 | 0.60 |
| 5 | 0.099 | 0.53 |
| 6 | 0.087 | 0.55 |
| 7 | 0.099 | 0.61 |
| 8 | 0.079 | 0.59 |
| 9 | 0.075 | 0.54 |
| 10 | 0.089 | 0.62 |
| 11 | 0.094 | 0.63 |
| 12 | 0.089 | 0.55 |
| 13 | 0.077 | 0.57 |
| 14 | 0.079 | 0.58 |
| 15 | 0.082 | 0.59 |
| 16 | 0.101 | 0.60 |
| 17 | 0.080 | 0.55 |
| 18 | 0.083 | 0.53 |
| 19 | 0.079 | 0.55 |

Table 4.8 are less than 0.15 and 1 respectively, implying that the external and internal mass transfer resistances were sufficiently small and can be ignored in all the reaction studies in batch system . A sample of calculation for all these parameters is given in Appendix D

4.2.4 Reusability Studies

All these resins were reused up to four times for 4 h at 368 K in order to validate occurrence of the catalyst fouling due the polymerised AA. The blank test result proved that the autocatalysed reaction occurred at a very slow rate and this further justified the needs of catalyst in the esterification reaction of AA with 2EH . Based on the results depicted in **Figure 4.6**, the yield of 2EHA obtained in the reaction catalysed by PK208 was higher as compared to RCP145 attributing to the lesser leached sulfonic acid from PK208 as stated previously. Despite the better leaching resist property and higher ion exchange capacity of SK1B as compared to PK208, the reaction catalysed by SK1B gave lower yield of 2EHA possibly due to limited access to active site per surface area. Approximately 20% reduction in the yield of 2EHA was observed in both resins after reusing these catalysts for the first cycle, owing to the active site blockage by the components like water. The attachment of water molecule to sulfonic group has resulted a reduction in the number of available active sites to the reactants and thus a decrease in the reaction rate (Dixit and Yadav, 1996; Zundel, 1969). A gradually and uniformly distributed yield reduction of $\leq 10\%$ over the subsequent reusability runs implied that the catalysts were fouled. The catalysts may be fouled by poly acrylic acid, due to the insufficient of MEHQ inhibitor. Despite the loss of activity, the yield of 2EHA obtained in the reaction catalysed by the spent resins was significantly higher than the blank test without catalyst. The recyclability tests of these resins demonstrate their immense potential in the industrial application for the production of 2EHA through the esterification of AA with 2EH.

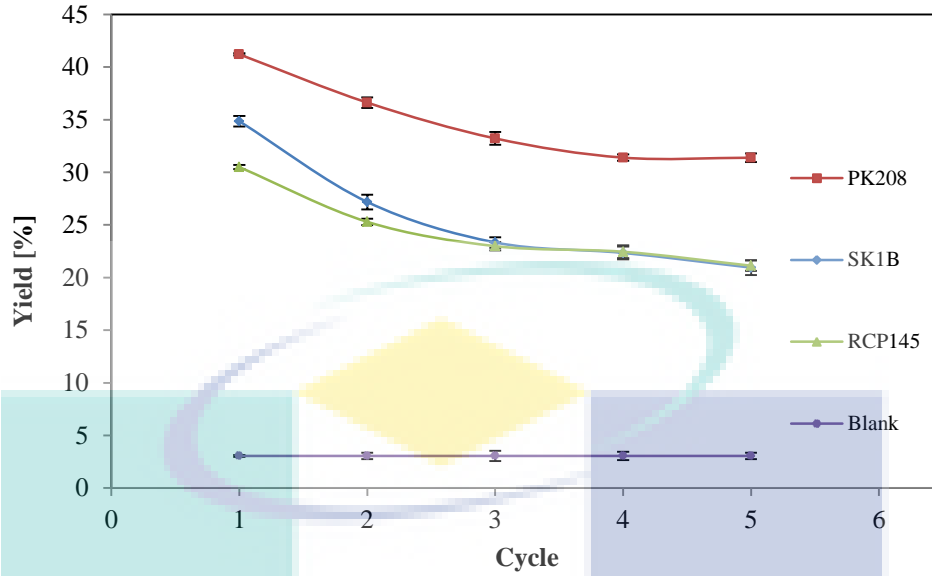


Figure 4.6 The 2EHA yield (%) after 4 h of reaction for 5 cycles of reaction (purity AA 99.9%; temperature of 368 K; catalyst loading of 10 wt% ; initial molar ratio acid to alcohol of 1:3)

4.2.5 Chemical Equilibrium Studies

The apparent equilibrium constant of the reaction, K_x , expressed in terms of mole fractions can be written as Equation 4.4:

$$K_x = \sum x_i^{v_i} = \frac{x_{2EHA}x_W}{x_{AA}x_{2EH}} = \frac{x_{2EHA}^2}{(x_{AA}^0 - x_{2EHA})(x_{2EH}^0 - x_{2EHA})} \quad (4.4)$$

where x_i is the mole fraction of component i at steady state.

The concentration based equilibrium constant, K_x as shown in Table 4.9 was adopted from our previous batch kinetic studies.

Table 4.9 The equilibrium conversion of AA (X_e) and the corresponding equilibrium constants (K_x)

| T (K) | X_e | K_x |
|-------|-------|-------|
| 338 | 0.515 | 1.33 |
| 368 | 0.555 | 1.83 |
| 378 | 0.577 | 2.11 |
| 388 | 0.723 | 7.73 |

Prior the kinetic study, the chemical equilibrium of the esterification of AA with 2EH was measured at different reaction temperature and represented as concentration

based equilibrium constants, K_x . The activity-based thermodynamic equilibrium constant, K_A was then calculated by relating the concentration based equilibrium constants, K_x with activity coefficient. K_A can be expressed as a function of temperature in Equation 4.5 (Chin et al., 2015).

$$K_A = K_{A0} \exp\left(-\frac{\Delta H_r^\circ}{RT}\right) \quad (4.5)$$

Where K_{A0} is pre-exponential factor for thermodynamic equilibrium constant and H_r is the standard enthalpy of reaction.

K_{A0} and H_r can be obtained from the graph in Figure 4.7 plotting logarithm of thermodynamic equilibrium constants against inverse temperature. It shows the increase of the equilibrium constant and equilibrium conversion with the temperature, indicating that the esterification of AA with 2EH is an endothermic reaction with the standard enthalpy of reaction of 44,753 J/mol. The results are slightly differ from the study of Komoń et al. (2013), in which the estimated enthalpies of reaction are 43,864 J/mol.

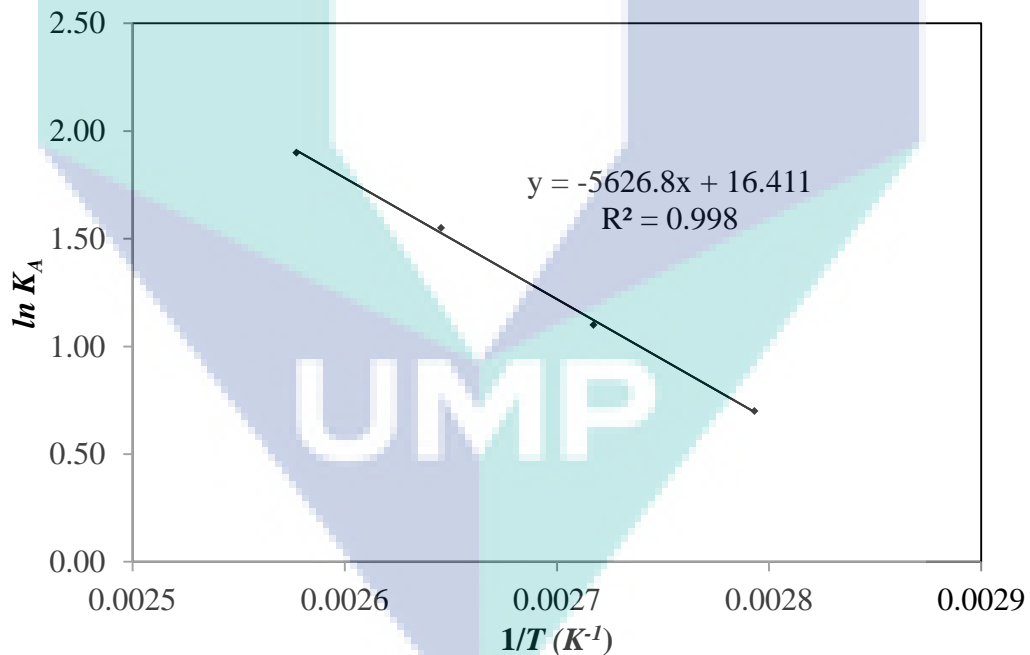


Figure 4.7 $\ln K_A$ vs $1/T$ plot.

The temperature dependence of the K_x and K_a can be described by Equation 4.6 (Komon et al., 2013):

$$K = \exp(b_1 + b_2 T^2) \quad (4.6)$$

where b_i , the adjustable variable of i^{th} can be fitted to the experimental data using the least squares method. The sum of squared deviations between experimental and calculated values were evaluated for all experimental points as the objective function., The standard deviation as shown in Equation 4.7 can be used as a measure of the quality of the fit:

$$\sigma(K) = \sqrt{\frac{\sum_{i=1}^N (K_i^{\text{exptl}} - K_i^{\text{calc}})^2}{(N - m)}} \quad (4.7)$$

where N is the number of experimental points and m is the number of adjusted variables. The fitted variables of Equation 4.6 and their standard errors are tabulated in Table 4.6. The corresponding standard deviations for K_x, σ_{K_x} and standard deviations for K_a, σ_{K_a} are 1.21 and 8.45 respectively.

Table 4.10 The b_i variables and their standard errors, $\sigma(b_i)$

| I | 1 | 2 |
|---------------|----------|---------------------|
| b_i | -7.532 | 3.403×10^5 |
| $\sigma(b_i)$ | 0.112 | 2.232×10^6 |

Based on the Van't Hoff equation as shown in Equation 4.8, the thermodynamic equilibrium constant is related to the standard enthalpy of reaction, ΔH_r^0 :

$$\left(\frac{d \ln K_a}{dT}\right) = \frac{\Delta H_r^0}{RT^2} \quad (4.8)$$

Equation 4.9 was obtained by combining Equation 4.6 and 4.8.

$$\Delta H_r^0 = 2b_2T^3 \quad (4.9)$$

The enthalpy of the reaction estimated based on the appropriate combinations of standard enthalpies of formation $\Delta_f H_i^0$ as shown in Equation 4.10 was done for the comparison purposes.

$$\Delta H_r^0 = \sum_{\text{product}} v_i \Delta_f H_i^0 - \sum_{\text{reactant}} v_i \Delta_f H_i^0 \quad (4.10)$$

The enthalpies of formation of each component in the liquid state at 298 K are given in Table 4.7. Considering that the temperature dependence of the enthalpy of reaction at 298 K, the calculated enthalpy based on Eq. 4.8 is 14.976 kJ/mol. It is just slightly differ with the theoretical enthalpy of reaction calculated by Eq 4.9 which was found to be 14.8 kJ/mol at 298 K.

Table 4.11 Enthalpy of formation of the selected components

| Compound | Enthalpy of formation (kJ/mol) |
|------------------|--------------------------------|
| Acrylic acid | -383.8 |
| 2 ethyl hexanol | -432.8 |
| 2 ethyl acrylate | -516.0 |
| Water | -285.8 |

Source: Daubert and Danner, 1998

4.2.6 Kinetic Studies in a Batch System

Adopting the heterogeneous catalyst mechanism behaviour, PH, ER, and LHHW models were selected in order to correlate the kinetic data for the esterification between 2EH and AA catalysed by PK208. Taking the natural log of Equation 4.11, the Arrhenius plots for each models are displayed in Figure 4.8.

$$k_f = k_{f0} \exp\left(\frac{-E_f}{RT}\right) \quad (4.11)$$

The kinetic parameters (k_{f0} and E_f denote the pre-exponential factor for rate of reaction and activation energy respectively) obtained with its corresponding standard deviation, σ are shown in Table 4.12 and Table 4.13. ER model gave the best fit among other models as validated by the coefficient of determination (R^2) which was closest to one, in addition to its randomly distributed residuals around the line of error=0. Table 4.10 also demonstrates that the adsorption affinity for both AA and water are comparable.

Figure 4.10 is the parity plot of the experimental reaction rate with the calculated reaction rate for all temperatures. This figure concluded that ER was best fitting with least error as corresponded by a reasonably good agreement between the predicted and experimental value of 2EHA concentration in Figure 4.10. The predicted value deviated marginally from the experimental data at higher temperature. It was ascribed to the

presence of the side reaction, the AA polymerisation at higher temperature due to the deactivation/denaturation of MEHQ.

A good correlation of the experimental data with ER model indicates that the reaction is controlled by surface reaction but not mass transfer (Sert and Atalay, 2012). It is suggested that AA molecule first adsorbs on the catalyst active site to form oxonium ion. This intermediate is then attacked by 2EH in the bulk liquid. Subsequently, water molecule at the adsorbed state is formed whereas 2EHA molecule is formed and instantly desorbed to the bulk liquid. All the adsorbed molecules finally desorb and release the vacant catalyst active sites. Figure 4.8 displays the graphical representation of the esterification of AA with 2EH through the ER mechanism.

The apparent activation energy for the esterification reaction was 70.27 kJ/mol. The activation energy of the esterification of AA with 2EH catalysed by DIAION PK208 is comparable than the activation energy for the resins catalysed esterification of AA with the various types of alcohols as reported by Chin et al., (2015) (71.3 kJ/mol), Fomin et al. (1991) (72.8 kJ/mol), and Komoń et al. (2013) (50.1 kJ/mol). This shows that PK208 is a better catalyst in reducing the energy barrier that must be surmounted by the AA and 2EH for an esterification reaction to occur.



UMP

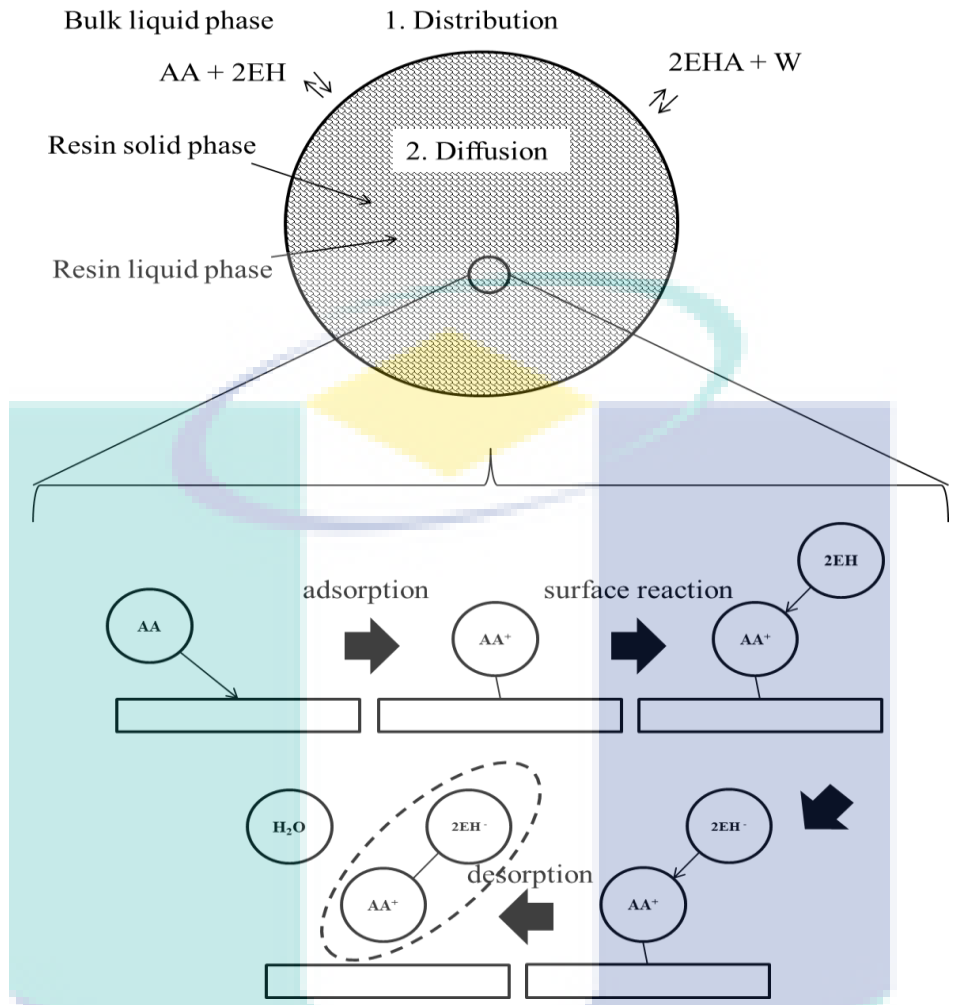


Figure 4.8 Schematic diagram of reaction of esterification of AA with 2EH followed ER

Table 4.12 Parameters of the kinetic models used

| Model | Kinetic Parameter | | R ² |
|-------|---|--------------------------------|----------------|
| | k_{f0} (σk_{f0}) (mol/L/min) | E_f (σE_f) (J/mol) | |
| PH | 2.09×10^7 (9.85×10^5) | 61,990 (9166.28) | 0.87 |
| ER | 8.05×10^9 (2.03×10^8) | 70,270 (90.07) | 0.96 |
| LHHW | 2.00×10^7 (4.35×10^2) | 43,760 (13.49) | 0.92 |

Table 4.13 Adsorption parameters of the kinetic models used

| Model | Adsorption parameter | | | | R ² |
|-------|------------------------------|--------------------------------|----------------------------------|------------------------|----------------|
| | K_{AA} (σK_{AA}) | K_{2EH} (σK_{2EH}) | K_{2EHA} (σK_{2EHA}) | K_w (σK_w) | |
| PH | - | - | - | - | 0.87 |
| ER | 102 (3.68) | - | - | 93.77 (7.20) | 0.96 |
| LHHW | 35.13 (0.01) | 11.52 (0.01) | 0.16 (0.05) | 30.92 (0.02) | 0.92 |

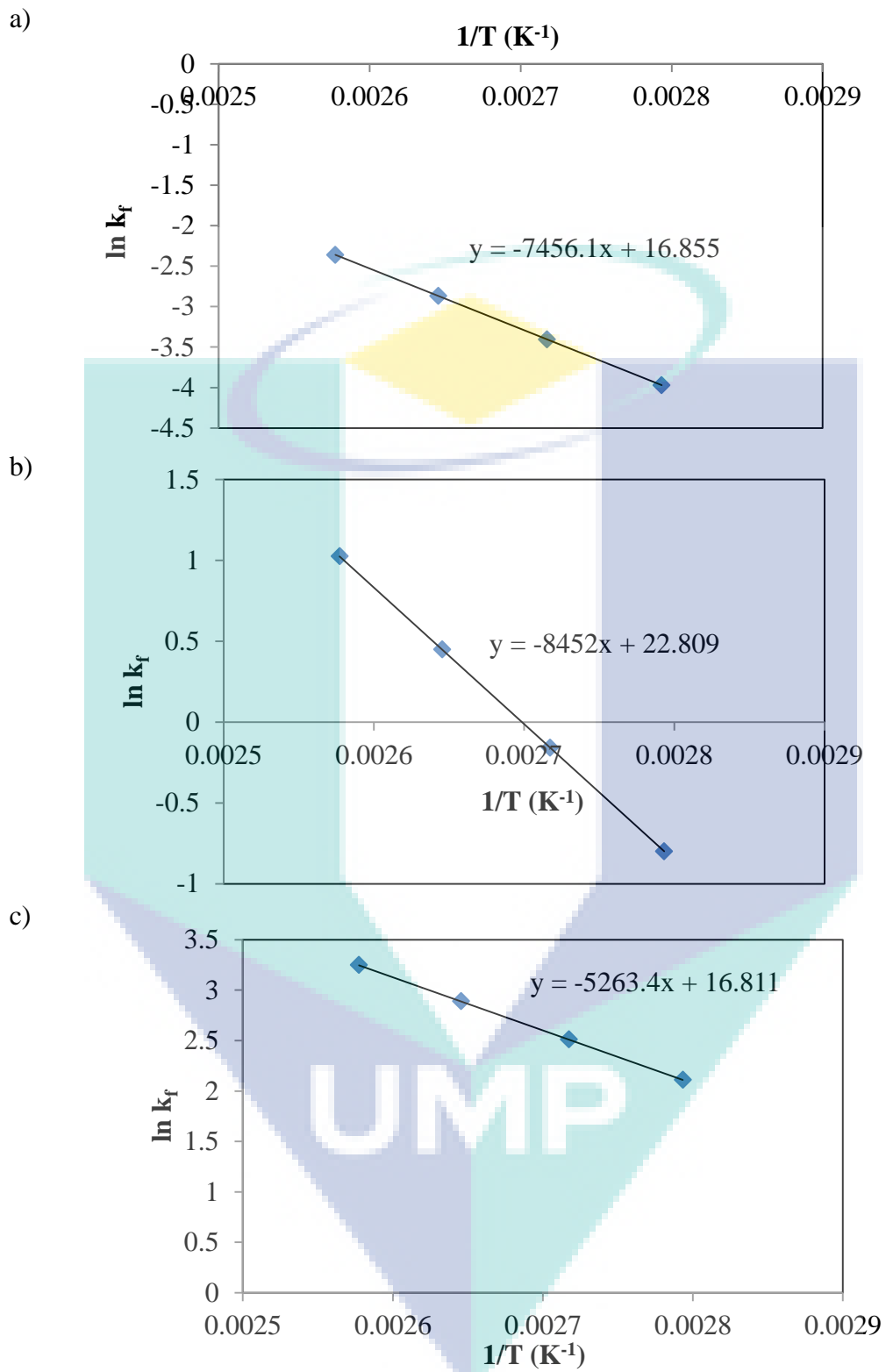


Figure 4.9 Arrhenius plot for a) PH model; b) ER model; c) LHHW model

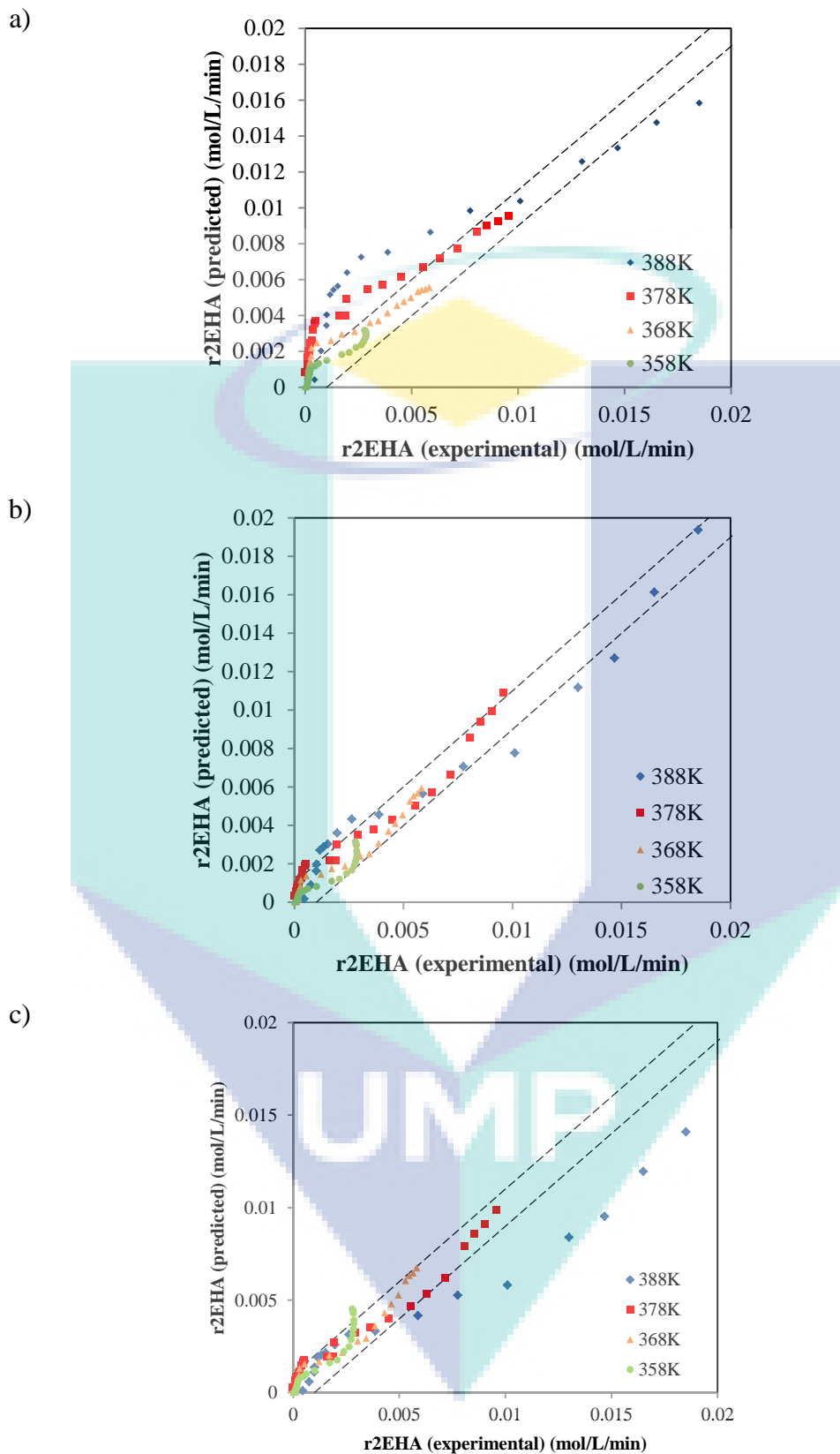


Figure 4.10 Parity plot for the experimental and predicted rate of reaction of (a) PH; (b) ER and (c) LHHW (dotted linear line = $\pm 5\%$ deviation)

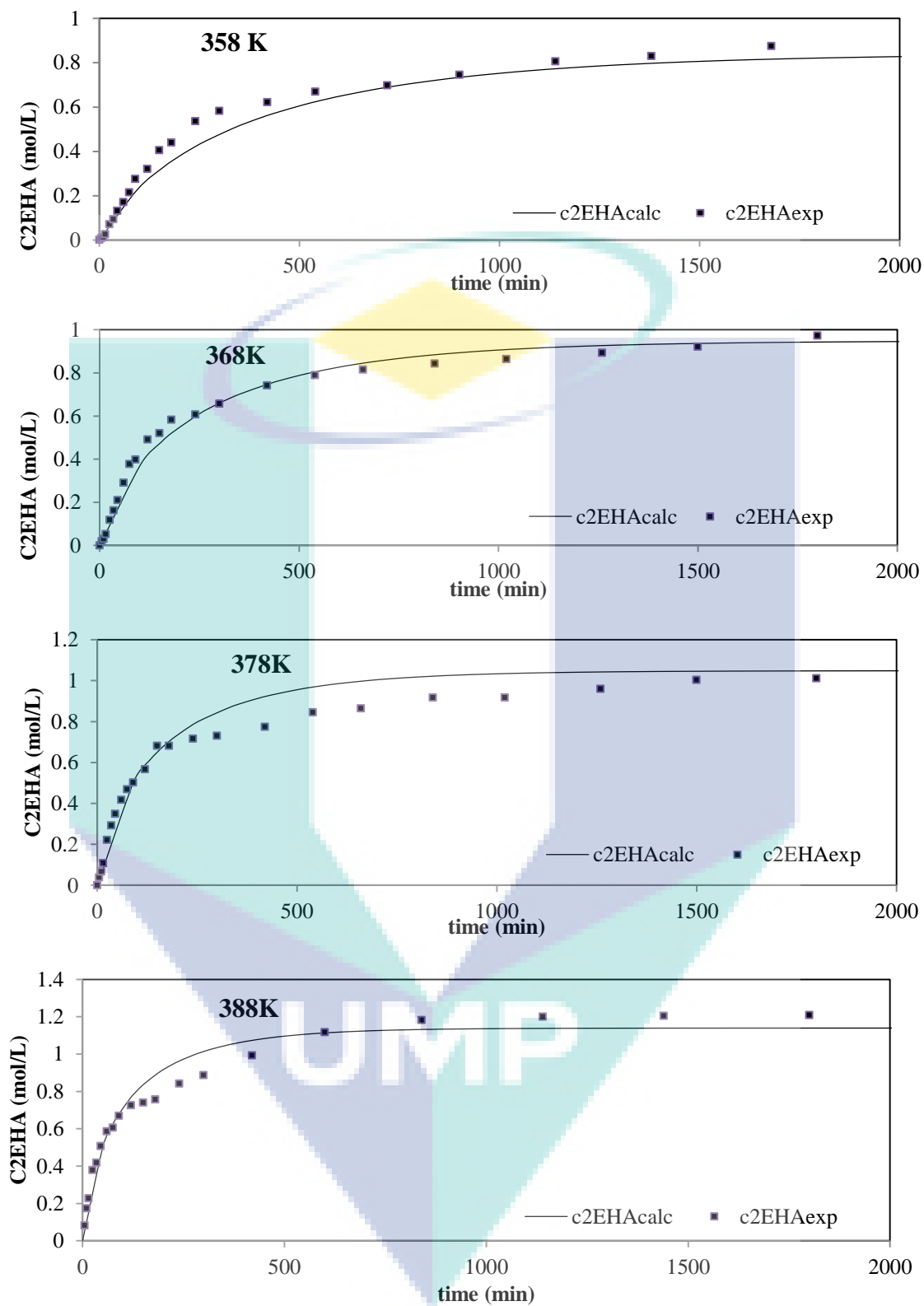


Figure 4.11 Comparison between experimental and calculated (with ER model) of 2EHA concentration profiles. Molar ratio of AA to 2EH is 1:3, catalyst loading is 10 wt% and stirring speed at 500 rpm

4.3 Esterification of AA with 2EH in a Packed Bed Reactor (PBR)

The studies of esterification of AA with 2EH in a batch system affirmed that PK 208 was the best catalyst among the IER tested. The best operating window and the reaction kinetics of the esterification of AA with 2EH were also identified. In order to validate the operating window in the intensified system like reactive distillation column (RDC), the esterification reaction of AA with 2EH was studied in a tubular packed bed reactor (PBR), imitating the reactive section of RDC. The following section discusses comprehensively the PBR studies that include the residence time distribution (RTD) phenomenon, adsorption phenomenon between catalyst and reactant/product, mass transfer coefficient studies, and parametric studies of important parameter contributed toward esterification of AA and 2EH.

4.3.1 Residence Time Distribution (RTD) Studies

Axial dispersion is significant in a tubular packed bed reactor (PBR) when the reactors have insufficiently high flow rates and reactor lengths. The occurrence of flow dispersion and flow channelling phenomena in PBR could cause deviations from the uniform residence time distribution (Mark and Robert, 2003). In the present study, tracer experiments were performed to investigate the residence time distribution of the PBR. These experiments were carried out using pulse injections of a Blue Dextran solution. Blue Dextran was chosen because its sufficiently large molecule could be prevented from diffusing to the internal surface of IER PK208

The trends in Figure 4.11-4.13 imply that the existing PBR system is a non-ideal continuous reactor as it matches neither the exit distribution trend of CSTR nor PBR. The dispersion and channelling were observed in the RTD profile generated at different flow rates. The noticeable asymmetry trend profiles indicate the dispersion phenomenon while the long end tailing indicates the occurrence of channelling. This phenomenon was worsen when the catalyst cage was not installed. Severe channelling occurred in the PBR without catalyst cage at lower flow rate due to its flow direction as shown in Figure 4.13. It was also found that the peak concentration was observed at shorter period after the injection of tracer corresponding to a higher flow rate, owing to the shorter residence time as tabulated in Table 4.11.

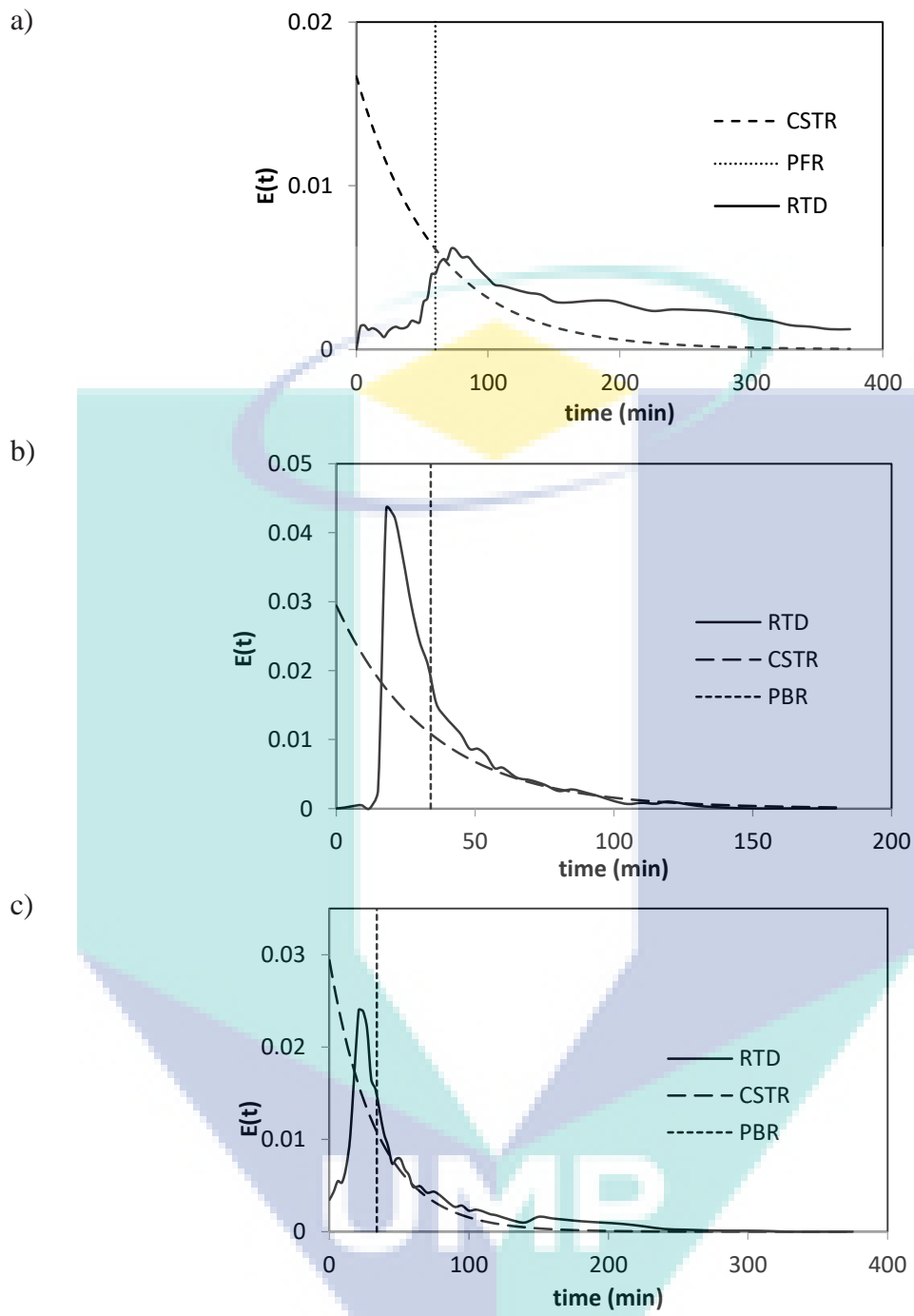


Figure 4.12 Exit distribution age for PBR [a) without cage; b) with cage; and c) with cage and catalyst at a flow rate of 5 ml/min]

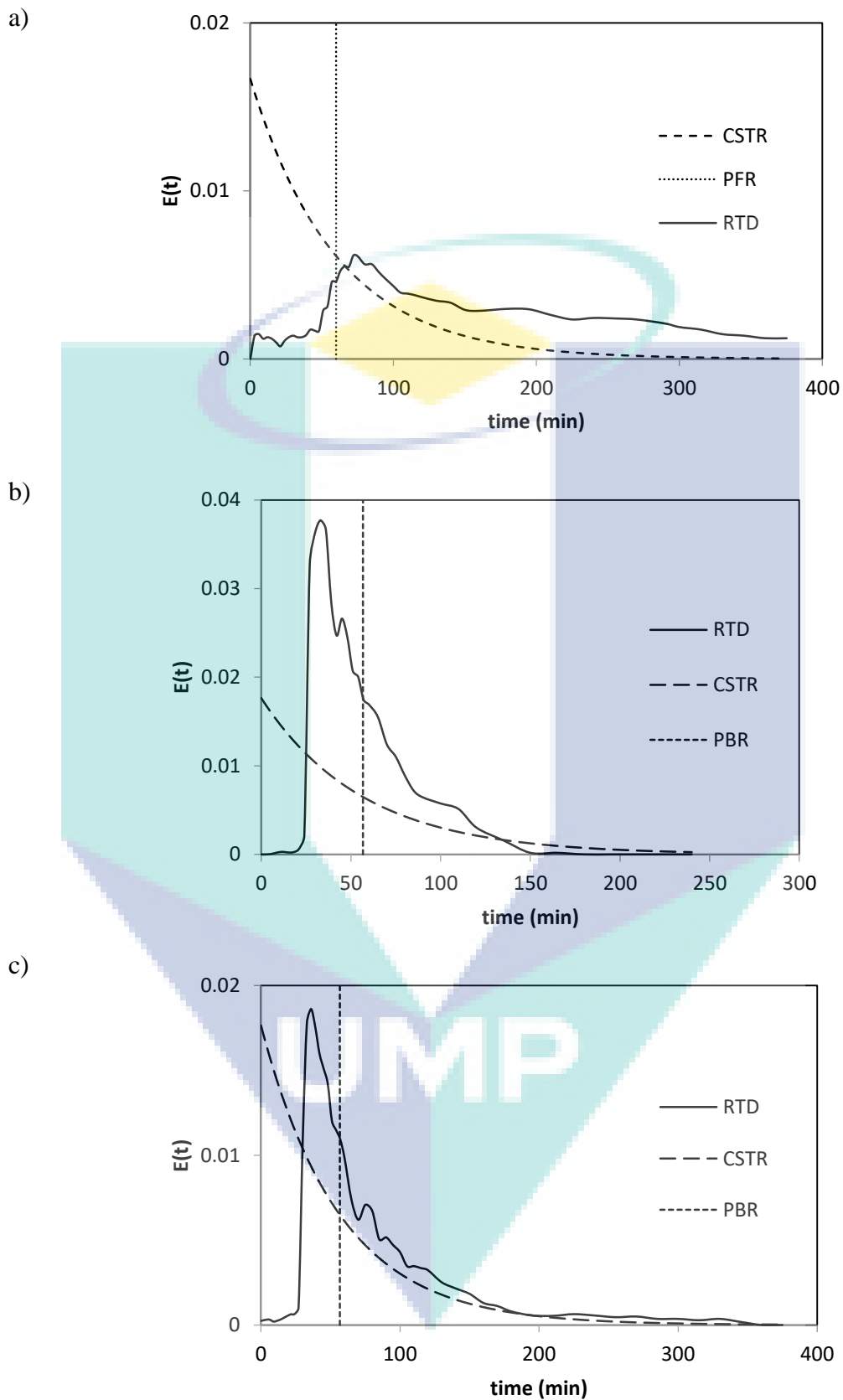


Figure 4.13 Exit distribution age for PBR [a) without cage; b) with cage; and c) with cage and catalyst at flow rate 3 ml/min]

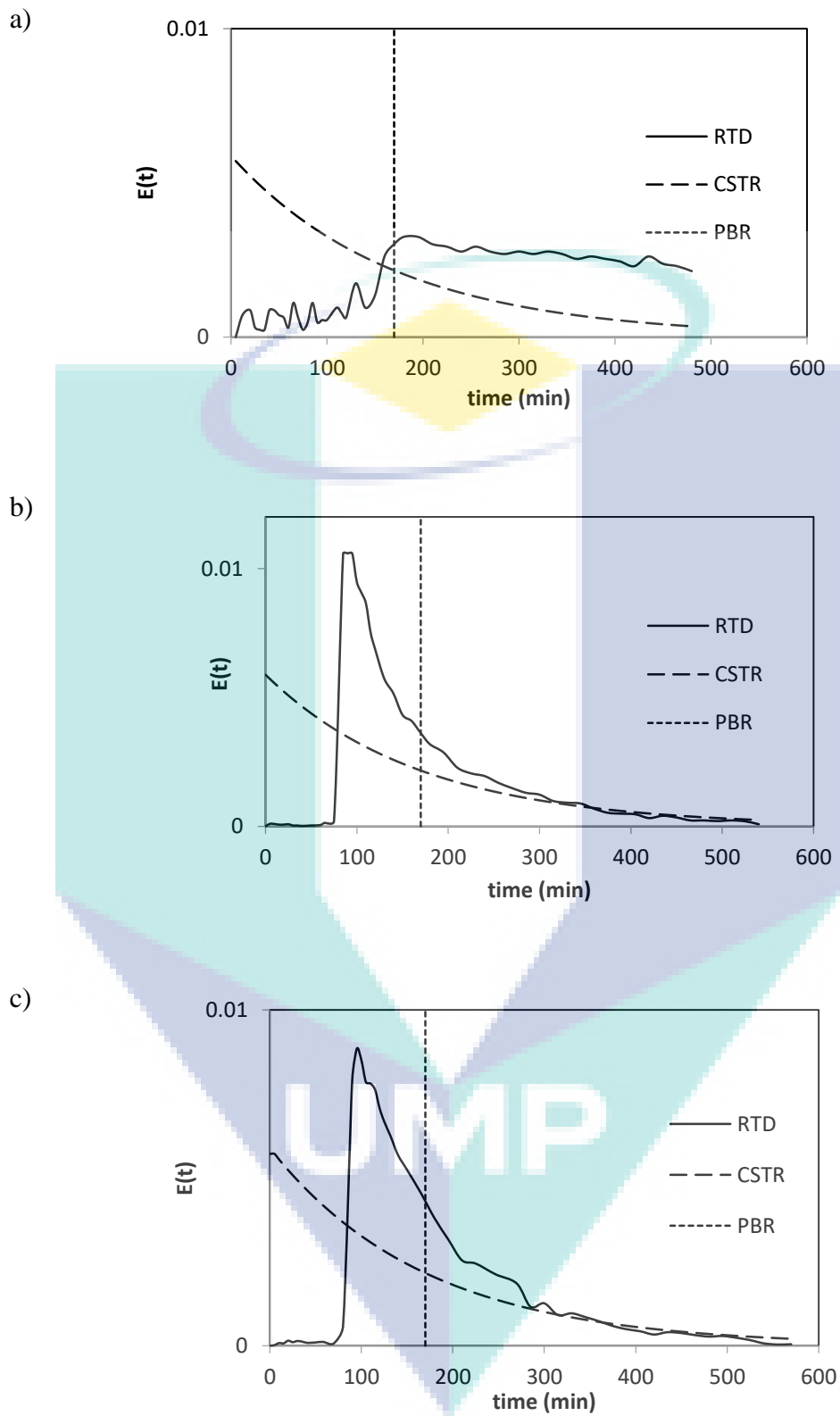


Figure 4.14 Exit distribution age for PBR [a) without cage; b) with cage; and c) with cage and catalyst at flow rate 1 ml/min]

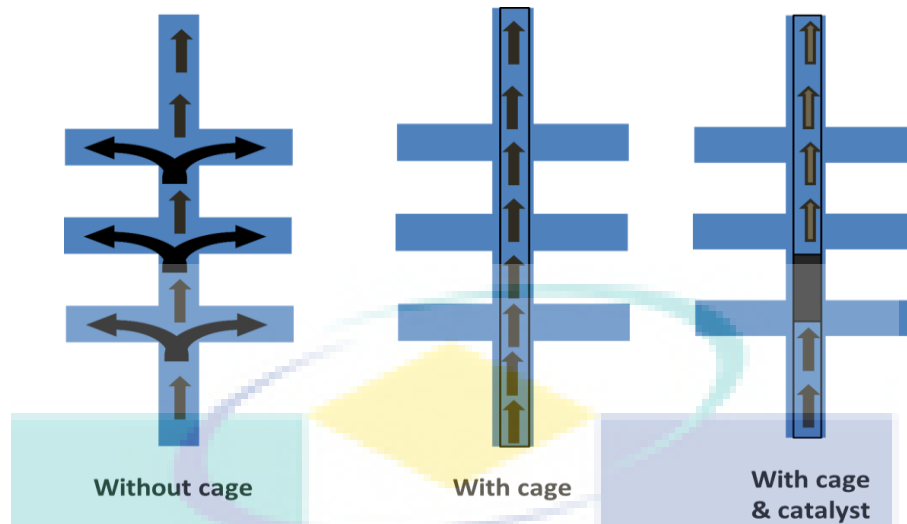


Figure 4.15 Flow direction in PBR for design without cage, with cage and with cage and catalyst

Table 4.14 The results of tracer study at 30°C

| Q (mL/min) | Re | Configuration | \bar{t} (min) | ϵ | Pe | $\sigma^2 \text{ min}^2$ |
|----------------------|-----------|------------------------|-----------------|------------|-----------|--------------------------|
| 1 | 0.0949 | Without cage | 283.25 | 0.2878 | 7.61 | 8946.06 |
| | | With cage | 175.86 | | | |
| | | With cage and catalyst | 184.51 | | | |
| 3 | 0.2847 | Without cage | 164.87 | 0.2950 | 4.08 | 3488.33 |
| | | With cage | 81.96 | | | |
| | | With cage and catalyst | 84.39 | | | |
| 5 | 0.4745 | Without cage | 82.48 | 0.2703 | 2.32 | 3140.12 |
| | | With cage | 38.15 | | | |
| | | With cage and catalyst | 60.29 | | | |

Dimensionless Peclet number (Pe) is normally applied to describe the flow behavior in a PBR. Pe can be used to quantitatively define the ratio of plug-flow to mixed-flow in an actual reactor. There is no mixing and the flow pattern is ideal plug-flow when Pe approaches infinity while the flow pattern is completely mixed-flow when Pe approaches 0. Practically, Pe of the actual reactor lies between these limit states. The flow pattern in the reactor can be assumed well-mixed if the Pe is less than one (Ding et al., 2013). Table 4.9 shows that the Pe of PBR with cage and catalyst is less than 10, indicating the occurrence of dispersion in these reactors. A declined Pe shown in the PBR with high liquid flow rate signified a higher degree of dispersion.

The bed porosity (ϵ), showing the fraction level of volume of voids over the total volume of packed catalyst was within the range of 0.3-0.5.

4.3.2 Adsorption Studies

Figure 4.15 (a), (b), and (c) show the breakthrough curves for AA/water binary mixtures at the vol% of 60/40, 30/70 and 70/30 respectively. The figure clearly shows that the affinity of PK208 to water is stronger than its affinity to AA. In the case of water composition in the binary mixture was more than 40 vol%, approximately 20 vol% of the water was adsorbed. PK208 resin was saturated with the adsorbates after 20-25 min at a feed flowrate of 1ml/min. After 20-25 min, the outlet composition of each compound was remained the same as its inlet concentration. Figure 4.15(c) indicates that both water and AA are equally adsorbed on PK208 when the water concentration is ≤ 30 vol%. The concentration of the outlet was remained at $\pm 5\%$ from the inlet concentration. These findings were well supported by the adsorption equilibrium constants for both AA and water for Eley Rideal model as reported in Table 4.10 and discussed in section 4.2.6.

Figure 4.16 (a), (b), and (c) shows the breakthrough curve for AA/2EHA binary mixtures at the vol% of 60/40, 30/70 and 70/30 respectively. The figure indicates that the affinity of PK208 resin to AA is stronger than to 2EHA. Approximately 20 vol% of AA was adsorbed on PK208 when the composition of AA in the mixture was higher than 60 vol%, whereas only 5-10 vol% of AA was adsorbed if the AA composition in the mixture is lower than 60 vol%. The adsorption equilibrium was attained within 20 mins when the AA concentration was lower than or equal to 60 vol% while the equilibrium was achieved only after 45 mins when the AA concentration was 70 vol%. At equilibrium, the composition of each compound was remained almost the same as the inlet concentration with error of $\pm 5\%$.

Figure 4.17 (a), (b), and (c) shows the breakthrough curve for 2EH/2EHA binary mixtures at the vol% of 60/40, 70/30 and 30/70 respectively. The figure indicates that both compounds are equally adsorbed on PK208. The concentration of the outlet is remained at $\pm 5\%$ from the inlet concentration. The adsorption studies concluded that the preferable compound to be adsorbed on the PK208 is according to sequence of water>AA>2EH/2EHA.

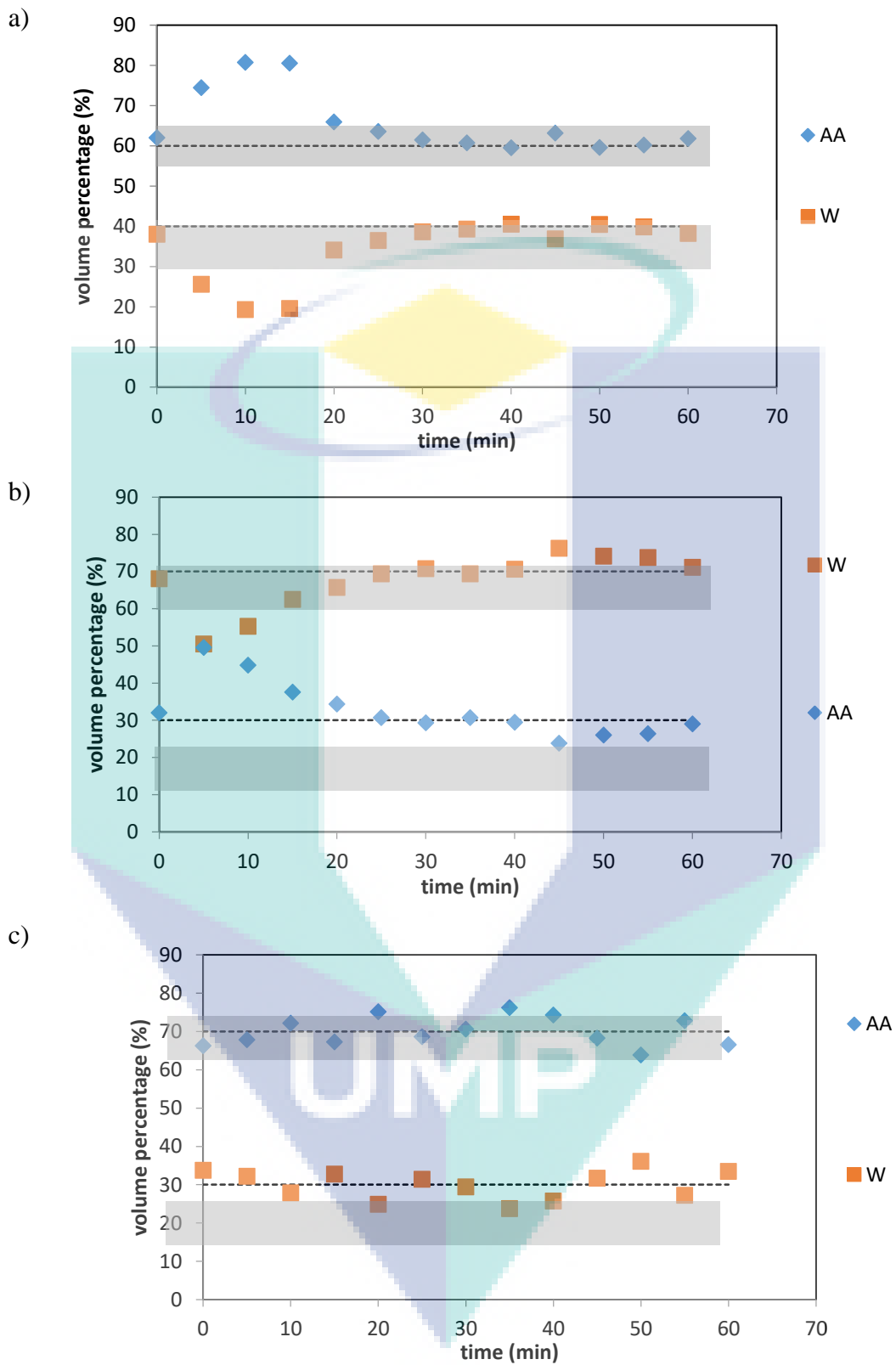


Figure 4.16 Breakthrough curves for AA/water binary mixtures [(a) 60/40, (b) 30/70 and (c) 70/30 % v/v] at 3 mL/min and 30 °C

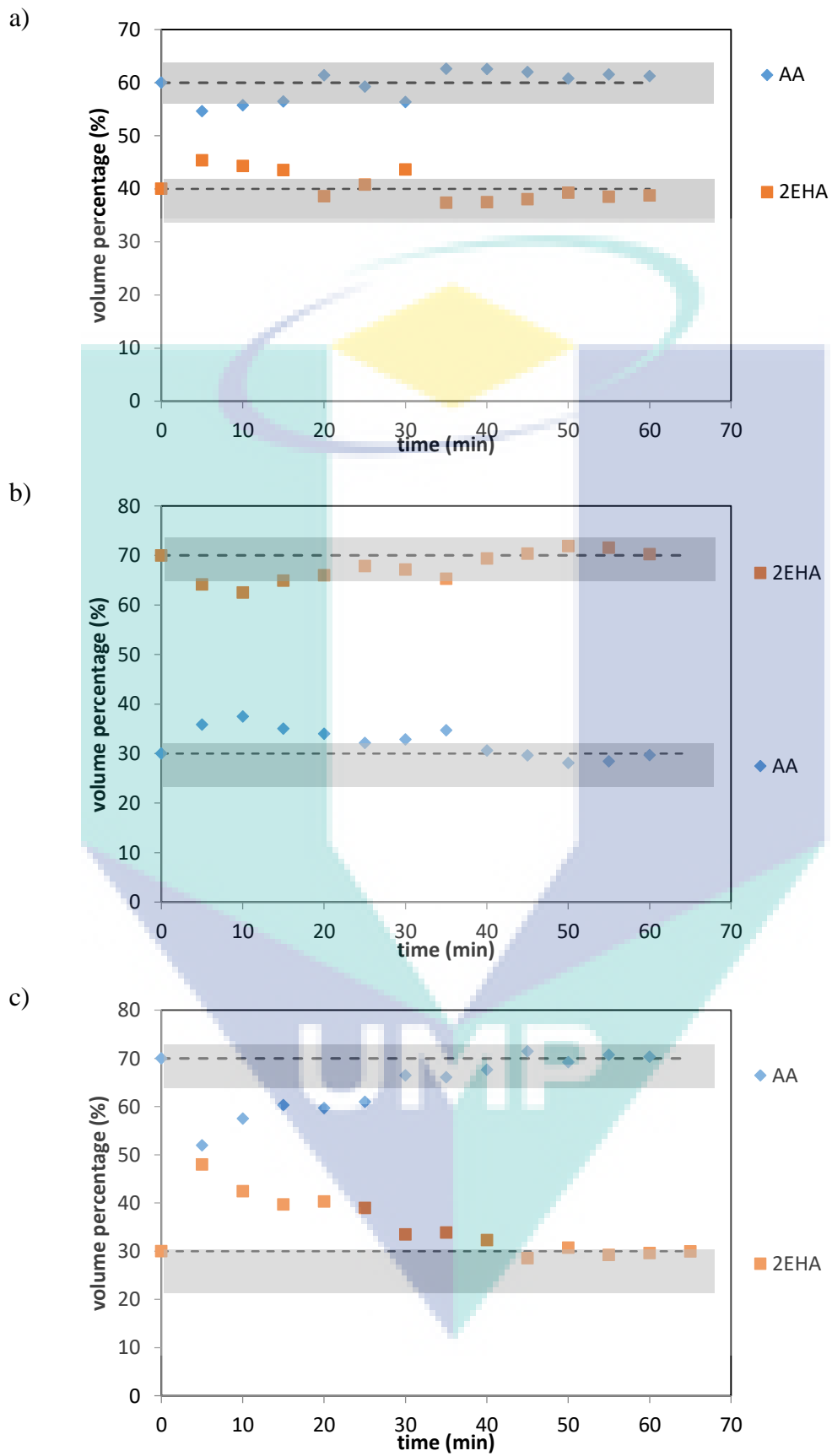


Figure 4.17 Breakthrough curves for AA/2EHA binary mixtures [(a) 60/40, (b) 30/70 and (c) 70/30 % v/v] at 3 mL/min and 30 °C

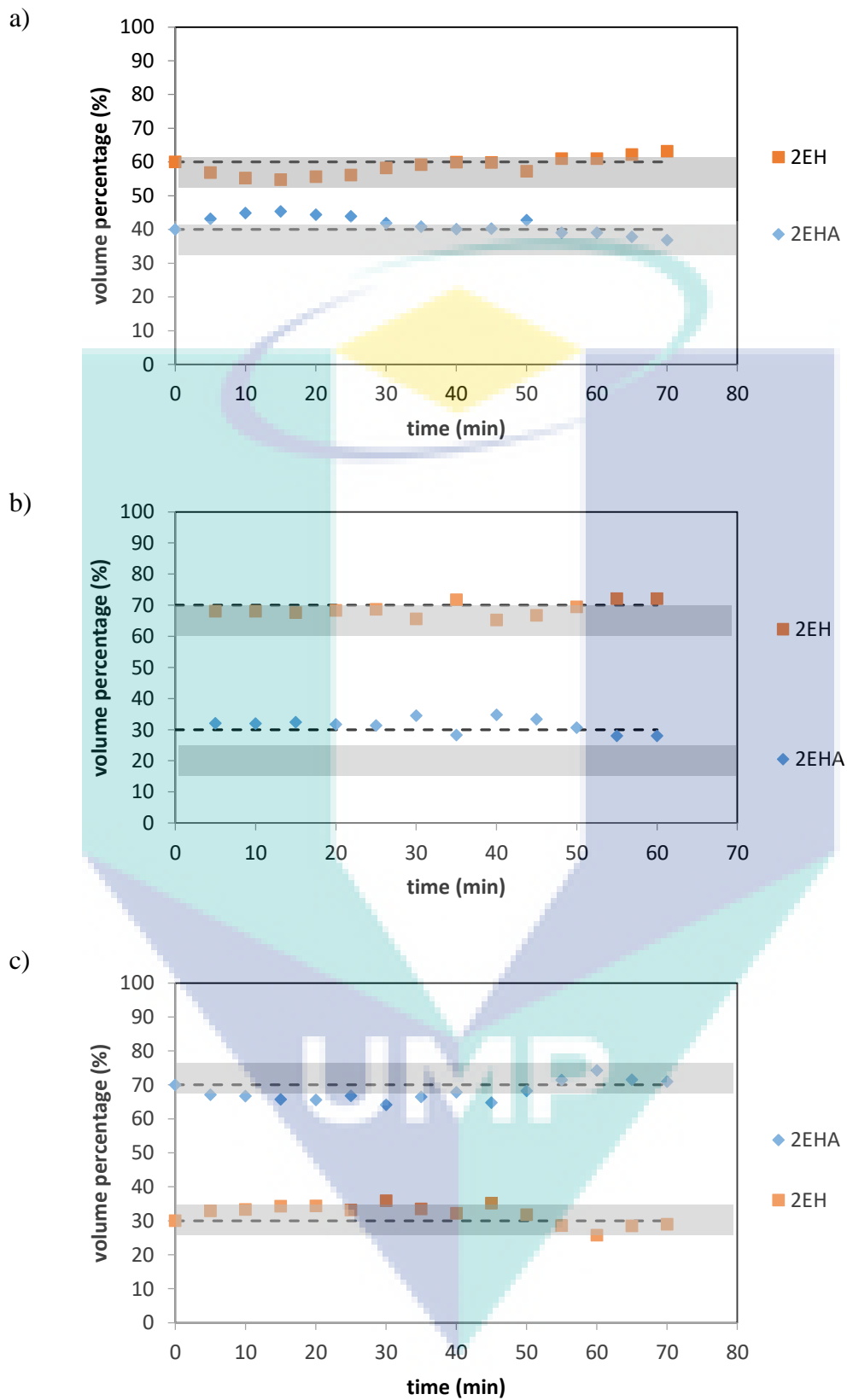


Figure 4.18 Breakthrough curves for 2EH/2EHA binary mixtures [(a) 60/40, (b) 70/30 and (c) 30/70 % v/v] at 3 mL/min and 30 °C

4.3.3 Mass Transfer Parameter Studies (PBR System)

To study the kinetics of the esterification reaction, the effect of external and internal mass transfer limitations must be eliminated. The external mass transfer resistance is determined by increasing the inlet reactant flow rate but remain weight hourly space velocity (WHSV) at constant. Consequently, 5 experiments were operated at different flow rates (1, 2, 3, 4, and 5 ml/min) in PBR, (see Table 4.14) at constant temperature (95°C) and molar ratio of AA:2EH (1:3). It was found in Table 4.14 that the 2EHA yield % were approximately deviate less than 10% in no runs 1–5. It indicates that the yield of 2EHA was independent of flow rate. That is to say, the contact time between the catalyst and reactant could keep constant under the same retention time (reaction time). Principally, the product yield should be consistent at the same contact time.

Table 4.15 Liquid-solid external/internal mass transfer limitation effects in PBR

| Operation conditions | | | Catalyst Loading (g) | Flow rate (mL/min) | WHSV (mL/g.min) | Yield (%) |
|--|--------------------|--|----------------------|--------------------|-----------------|-----------|
| External mass transfer limitation | Run 1 | | 1 | 1 | 1 | 36.09 |
| | Run 2 | | 2 | 2 | 1 | 34.43 |
| | Run 3 | | 3 | 3 | 1 | 33.73 |
| | Run 4 | | 4 | 4 | 1 | 35.77 |
| | Run 5 | | 5 | 5 | 1 | 31.64 |
| Internal mass transfer limitation | <500 μm | | 5 | 1 | 5 | 65.21 |
| | >500 μm | | 5 | 1 | 5 | 63.35 |

By comparisons with different particle sizes of PK208 resins from range <500 μm and >500 μm which was exiled via sieving method it also can be seen in Table 4.14 that the yield almost kept constant at around 64% approximately. It suggests that the particle sizes did not lead to the catalytic performance significantly. These conclude that, the internal mass transfer limitations can be ignored when PK208 resins are chosen to be the catalyst in this study.

4.3.4 Study on the Effect of Important Operating Parameters of The Esterification of AA with 2EH in a Packed Bed Reactor System

4.3.4.1 Effect of temperature

The performance of esterification of AA with 2EH in terms of its yield (%) of 2EHA at various reaction temperatures is displayed in Figure 4.18. A higher temperature has improved the yield. Yield increases from 10.34 mol% to 23.26 mol% when the reaction temperature rises from 55°C to 95°C. The limitation was decided at 95°C is due to the future experimental is using the waste water where it is imposible for the reaction to achieve beyond this temperature consistently. This is coincided with the theory of reaction, in which the rise in heat increases the kinetic energy of molecular and hence increasing the total and effective collisions between the reactant molecules (Fogler, 2008). The reaction temperature of 95°C was then adopted in the subsequent studies for the parameters of catalyst loading, AA to 2EH feed molar ratio and feed flowrate

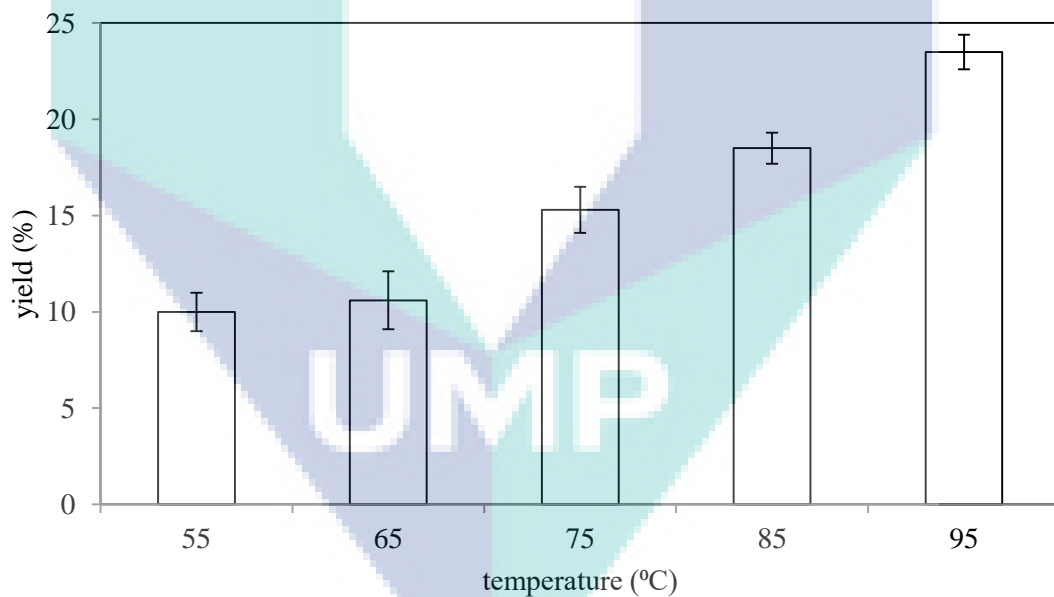


Figure 4.19 Yield (%) of 2EHA for the esterification of AA with 2EH at different reaction temperature with AA to 2EH feed molar ratio: 1:3; catalyst loading: 5 g; total feed flow rate: 3 ml/min

4.3.4.2 Effect of catalyst loading

The yield for the esterification reaction of AA with 2EH carried out at different catalyst loadings are reported in Figure 4.19. Despite the substantial amount of catalyst active sites with higher catalyst loading, there is no increment in yield anymore when the catalyst loading was increase from 5 g to 10 g. It shown that 5 g of catalyst provide enough active sites for the flowed reactant to perform at optimum point. Further increase the catalyst loading thus would not assist anymore the catalytic performance. Moreover, at certain point, the increase in the catalyst amount would create more flow resistances that causing mass transfer issues (Green & Perry, 2008). In view of its best performance in terms of AA conversion, the catalyst loading of 5 g was chosen in the subsequent parametric study.

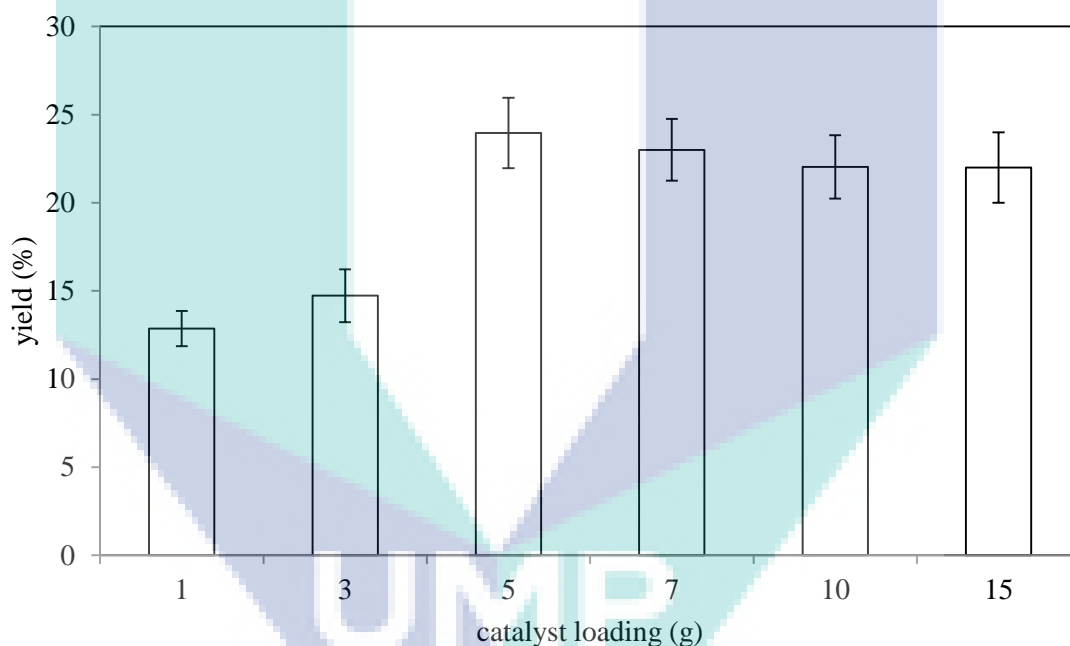


Figure 4.20 Yield (%) of 2EHA for the esterification of AA with 2EH at different catalyst loading with temperature: 95°C; AA to 2EH feed molar ratio: 1:3; total feed flow rate: 3 ml/min

4.3.4.3 Effect of molar ratio

Figure 4.20 shows a significant increment in yield when AA to 2EH feed molar ratio increases from 1:1 to 1:3. The excess amount of 2EH could drive the reaction equilibrium to product side and hence shortens the time needed to achieve equilibrium conversion. However, a further increase of AA to 2EH feed molar ratio from 1:3 to 1:5

has decreased the yield. At the AA to 2EH feed molar ratio of 1:5, the surplus amount of 2EH molecules may block the AA molecules from accessing the active sites. Therefore, AA to 2EH feed molar ratio of 1:3 was selected for the subsequent studies.

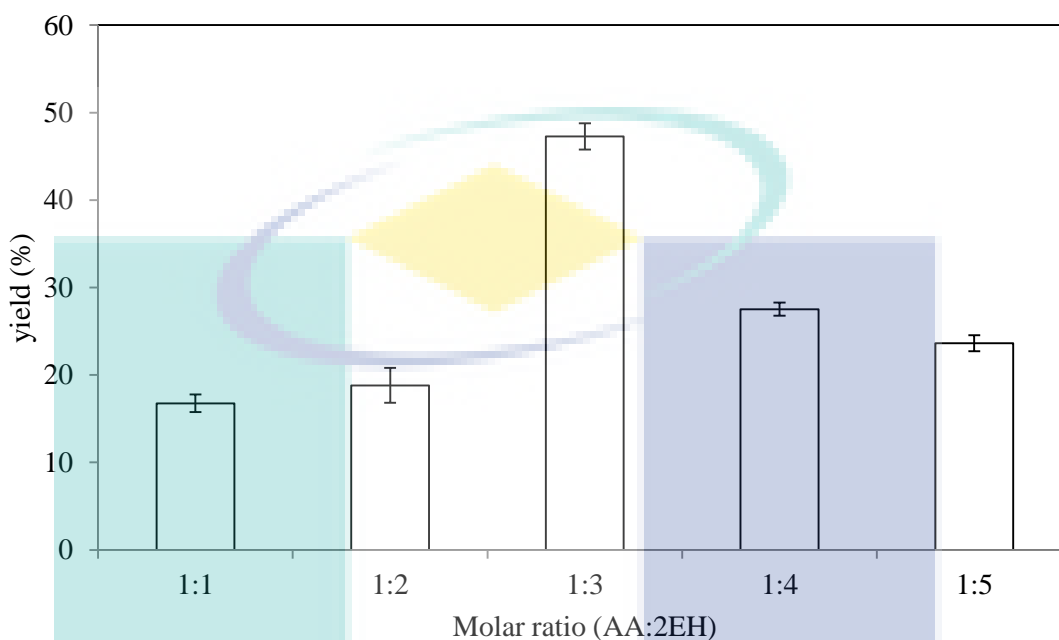


Figure 4.21 Yield (%) of 2EHA for the esterification of AA with 2EH at different AA to 2EH feed molar ratio with temperature: 95°C; catalyst loading: 5 g; total feed flow rate: 3 ml/min

4.3.4.4 Effect of feed flow rate

Total feed flow rate is among the prominent factors that would contribute towards the performance of reaction in PBR system. As the flow rate increases, the residence time of reactant would decrease, thus decrease the yield (%) of 2EHA. This could be seen in Figure 4.21, which shows significant decrement of yield as the flowrate increases. Even though the tailing effect shown by 1 ml/min quite significant, which imply it has channelling issues and imply the flow in laminar or low turbulent region, but the residence time factor is enough to counter this weakness thus exhibit the highest yield.

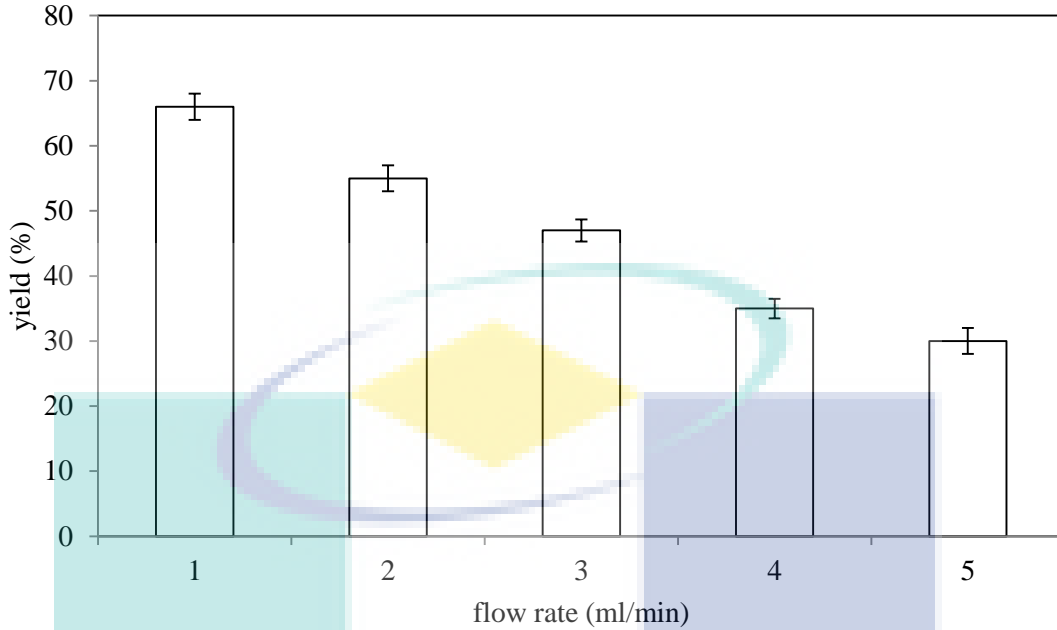


Figure 4.22 Yield (%) of 2EHA for the esterification of AA with 2EH at different total feed flow rate with temperature: 95°C; catalyst loading: 5 g; AA to 2EH feed molar ratio 1:3

4.3.5 Kinetic Studies in Continuous System (PBR Reactor)

The calculated enthalpies of the reaction and K_{X0} for mole fraction based thermodynamic equilibrium constant is 62.07 kJ/mol and $1.29 \times 10^9 \text{ L}^2/(\text{mol.g.min})$ respectively.

The rate constants, k_f can be related to the temperature with Arrhenius equations as below:

$$k_f = k_{f0} \exp\left(\frac{-E_f}{RT}\right) \quad (4.12)$$

Where k_{f0} is the pre-exponential factors for the reactions, E_f denote the activation energy of reactions, R is the gas constant and T is the temperature of the reaction.

The kinetic parameters (k_{f0} and E_f , denoting the pre-exponential factor for rate of reaction and activation energy of reaction respectively) and adsorption parameters for AA and water are shown in Table 4.15. Since the residuals obtained from all the models were randomly distributed around the line of error=0 with zero means, it is to be noted

that the ER model gave the best correlation between the two models adopted because the coefficient of determination (R^2) is closest to one.

Table 4.16 Kinetic and adsorption parameters for the models used to fit the experimental data

| Model | Kinetic Parameter | | Adsorption parameter | | R^2 |
|-------|--|---------------|----------------------|-------|-------|
| | k_{fo} (L ² /(mol.g.min)) | E_f (J/mol) | K_{AA} | K_W | |
| PH | 0.012 | 9543.98 | - | - | 0.91 |
| ER | 0.931 | 9126.05 | 6.15 | 4.41 | 0.93 |

Figure 4.22 shows the parity plot of experimental reaction rate with calculated reaction rate for all temperatures. This figure concludes that ER is best fitting with less error compared with another model fitting.

The good agreement between the experimental data with ER model has shown that the reaction is controlled by surface reaction. Based on the ER model as shown in Eq. (3.3), it is proposed that the AA molecule adsorbs on the catalyst site and forms an oxonium ion intermediate, which is simultaneously attacked by the 2EH in the bulk liquid. During this exchange reaction, and the water molecule is formed in adsorbed state while 2EHA molecule is formed and desorbed immediately to the bulk liquid. All the adsorbed molecules then desorb and give rise to a vacant catalyst site in all cases.

Nevertheless, the kinetic parameters determined using this PBR system mismatched with the one obtained in a batch mode system during the previous study. It implies that the PBR system is restricted by the mass transfer and mixing distribution and it further validates the occurrence of dispersion in the PBR.

4.3.6 Esterification with Real Wastewater

The yield (%) of 2EHA was affected significantly by the changes in the AA concentration as depicted in Figure 4.23. This phenomenon was believed to happen due to the ratio of the active site in the catalyst being more than enough for AA even in lower initial AA concentration (%). Due to the fixed catalyst weight on each run, the ratio of catalyst (or in other hand active site) to mole AA is higher in the lower concentration compared to higher one. This is offset against the reversible effect of water toward the reaction which tends to shift the reaction toward the reactant side and favourable of water to be adsorbed on catalyst.

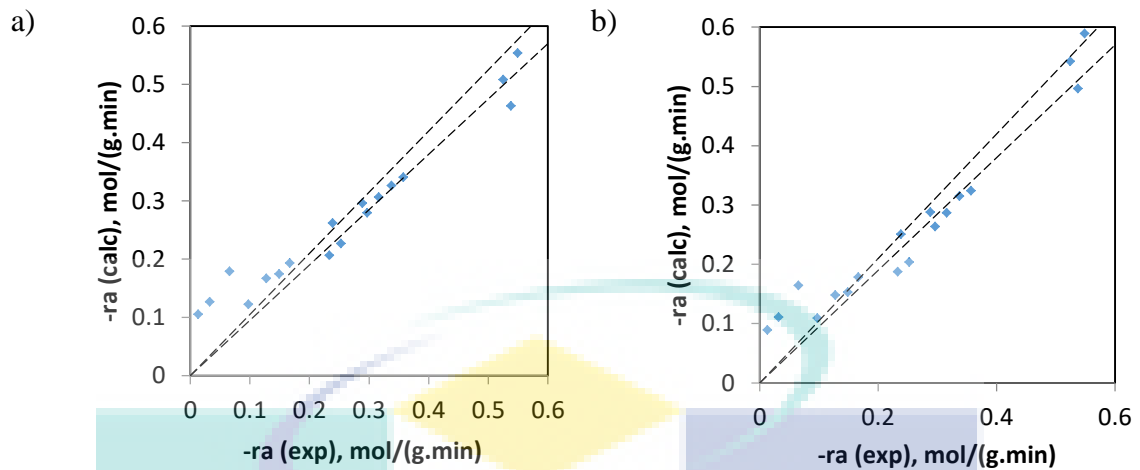


Figure 4.23 Parity plot for the experimental and predicted rate of reaction of (a) PH and (b) ER (dotted line stand for $\pm 5\%$ error)

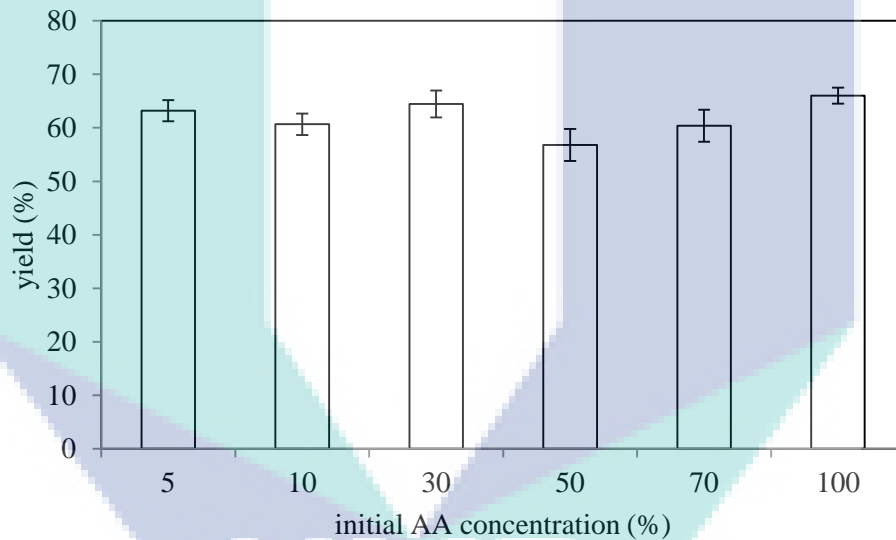


Figure 4.24 Yield (%) of 2EHA for the esterification of AA with 2EH at different AA concentration with temperature: 95°C ; catalyst loading: 5g; AA to 2EH feed molar ratio 1:3; flow rate: 1 ml/min

Slightly changes was identify from the range 5-30% of AA concentration. But when AA concentration was 50% , the changes is quite significant to be compared with 5-30%. This was predicted due to the competition between AA and water to be adsorbed to the active site as AA is more compared to lower concentration previously. The trend show in 5% w/w of AA, the performance is little higher might contributed by the bilayer form in the mixture when water content is too high because of 2EH properties which partially miscible with water.

4.3.7 Simulation Studies

Simulation studies were performed using a plug flow reactor model, RPlug in Aspen Plus V9 and Transport of Diluted Species Interface in COMSOL. The simulation results generated using RPlug deviated remarkably from the experimental data when the feed flow rate was increased at all reaction temperatures. This was well supported by the finding shown in Table 4.9 in which a higher feed flow rate has resulted a reduced Pe , signifying a more severe dispersion in the reactor. On the other hand, the results produced from the simulation using Transport of Diluted Species Interface in COMSOL differed less than 10% from the experimental data obtained at all feed flow rates as shown in Figure 4.25. The accuracy of this model was attributed to the accounts of diffusion, dispersion, and reaction in the diluted solutions. Figure 4.24 indicates that at lower flow rate, the wide deviation errors occurred. However, the similar trend was obtained throughout these simulation studies where shows increment of flowrate and temperature implies positive feedback toward reaction performance. The deviation was believed to be occurred due to the dispersion phenomenon. This is because in Aspen Plus package, the ideal condition of tubular reactor was assumed. These somehow affect the reaction performance itself.

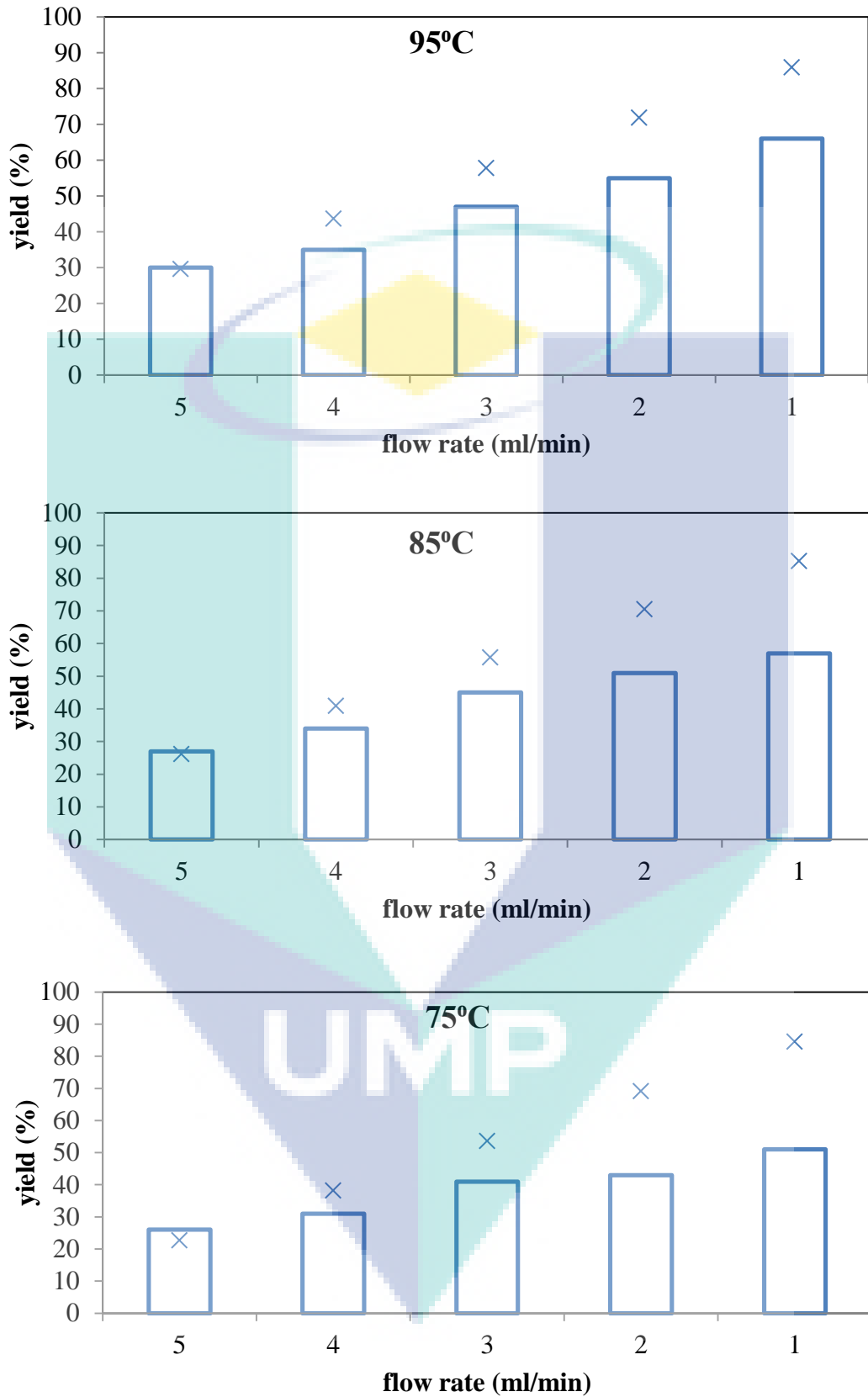


Figure 4.25 Simulation result with Aspen PLUS V8 software (x dotted) and experimental result (bar chart)

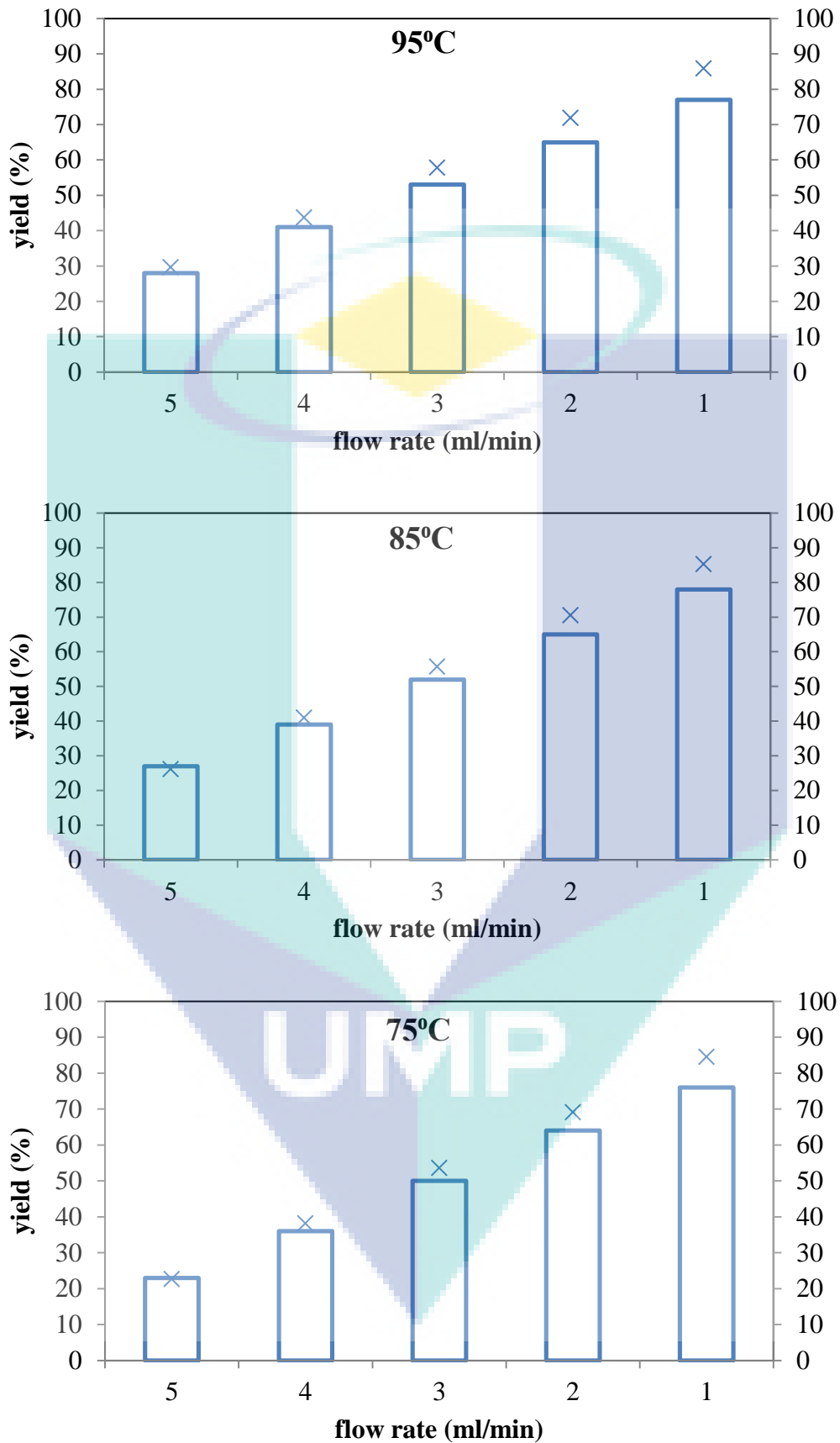


Figure 4.26 Simulation result with COMSOL software (x dotted) and experimental result (bar chart)

CHAPTER 5

CONCLUSION

5.1 Conclusions

The best catalyst was PK208 in comparison to the other DIAION IER such as SK104, SK2B, PK216, PK228, RCP140, and RCP 160. PK208 outperformed the others due to the complement effect of its IEC, DVB CL%, and leaching properties and degree of swelling. Fractional two level factorial design was successfully employed to screen the significant factors that affected the reaction of AA with 2EH catalysed by PK208 . The initial AA concentration and temperature were found to significantly ($p < 0.0001$) influence the yield of 2EHA in the esterification of AA with 2EH. The highest yield of 41% was obtained after 4 hours reaction at a temperature of 388K, an initial reactant molar ratio of AA to 2EH of 1:3 and a catalyst loading of 10 wt%.

It was found that the equilibrium constant and equilibrium conversion increased with the temperature, implying the endothermic behaviour of the esterification of AA with 2EH. The best kinetic model, ER was also proven to predict the yield of 2-EHA more accurately comparing to the LHHW and PH model.

Prior to using the tubular PBR for reaction studies, the RTD and adsorption phenomena in the reactor were investigated. The RTD studies showed that severe channelling issues in the tubular PBR could be overcome by the installation of catalyst cage. The RTD analysis also implied the existence of dispersion in the tubular PBR at all the flow rates investigated. Meanwhile, the adsorption studies concluded that the preferable compound to be adsorbed on the PK208 was according to sequence of water>AA>2EH/2EHA. The adsorption equilibrium of all these compounds could be reached within 20 mins. In a tubular PBR consisted of catalyst bed with the L/D ratio

of 1:5, the highest yield, 66.44% was obtained in the esterification of AA with 2EH carried out at the temperature of 368 K, catalyst loading of 5 g, feed molar ratio of 1:3, and total feed flow rate of 1 ml/min. The relevancy of this study would still be beneficial to be further with more complex system such as RDC or CR due to the restriction issues of temperature window due to the usage of IER catalyst.

The simulation results generated using the Transport of Diluted Species Interface in COMSOL deviated less than 10% from the experimental data obtained at all feed flow rates. The accuracy of this model was attributed to the accounts of diffusion, dispersion, and reaction in the diluted solutions. This further implied the occurrence of dispersion in the tubular PBR. This model is a very important tool to implement and develop the intensified process such as RDC and CR for the recovery of AA from the wastewater through the esterification reaction with 2EH.

5.2 Recommendation

The hybrid process such as laboratory scale RDC and CR could be designed using the validated simulation tool in the present study. Additional experimental data should be obtained by esterifying the AA in the wastewater with 2EH in these equipment. The effectiveness of the AA recovery through these processes could then be verified before the equipment up-scaling. The process optimisation could also be carried out to maximize the AA recovery from the wastewater. In addition, the techno-economic feasibility of these processes could be analysed through simulation studies before commercialising the technology.

The stability and the longevity studies also could be further studies to suit with the hybrid condition further on. Based on the recyclability studies in the batch system, this catalyst would possess the good stability and longevity properties in RDC or CR system.

REFERENCES

- Abdul Rahman, M.B., Jumbri, K., Mohd Ali Hanafiah, N.A., Abdulmalek, E., Tejo, B.A., Basri, M., and Salleh, A.B. 2012. Enzymatic esterification of fatty acid esters by tetraethylammonium amino acid ionic liquids-coated *Candida rugosa* lipase. *Journal of Molecular Catalysis B: Enzymatic*. **79**: 61–65.
- Adam, F., Hello, K.M., and Chai, S.J. 2012. The heterogenization of l-phenylalanine–Ru(III) complex and its application as catalyst in esterification of ethyl alcohol with acetic acid. *Chemical Engineering Research and Design*. **90**(5): 633-642.
- Agilent Technologies, 2011, The Essential Chromatography & Spectroscopy Catalog 2011/2012 Edition.
- Agreda V.H., Partin L.R., and Heise W.H. 1990 High-Purity Methyl Acetate via Reactive Distillation, *Chemical Engineering Progress*. **86**: 40-46.
- Agreda, V.H. and Lilly, R.D. 1990. *Preparation of ultra high purity methyl acetate*. US4939294.
- Ahmad M A A, Kamaruzzaman M R, Chin S Y 2014 New method for acrylic acid recovery from industrial wastewater via esterification with 2-ethyl hexanol. *J. Process Safety and Environmental Protection*. **92** 522–531
- Akbay, E.Ö. and Altıokka, M.R. 2011. Kinetics of esterification of acetic acid with n-amyl alcohol in the presence of Amberlyst-36. *Applied Catalysis A: General*. **396**(1-2): 14–19.
- Ali, S.H., 2009. Kinetics of catalytic esterification of propionic acid with different alcohols over Amberlyst 15. *International Journal of Chemical Kinetics*. **41**: 432–448
- Allen, S.J., Koumanova, B., Kircheva, Z., and Nenkova, S. 2005. Adsorption of 2-nitrophenol by technical hydrolysis lignin: kinetics, mass transfer, and equilibrium studies. *Industrial & Engineering Chemistry. Res.*. **44**: 2281–2287.
- Allison, M., Singh, K., Webb, J., and Grant, S. 2011. Treatment of Acrylic Acid Production Wastewater Using a Submerged Anaerobic Membrane Bioreactor. *Proceedings of the Water Environment Federation, WEFTEC 2011: Session 101 through Session*. **110**: pp. 6554-6564(11).
- Alsalmeh, A., Kozhevnikova, E.F., Kozhevnikov, I.V. 2008 Heteropoly acids as catalysts for liquid-phase esterification and transesterification. *Applied Catalysis A: General*. **349**: 170-176
- Altıokka, M.R. and Ödeş, E. 2009. Reaction kinetics of the catalytic esterification of acrylic acid with propylene glycol. *Applied Catalysis A: General*. **362**(1-2): 115–120.

- Arpornwichanop, A., Koomsup, K., and Kiatkittipong, W. 2009. Production of n-butyl acetate from dilute acetic acid and n-butanol using different reactive distillation systems : Economic analysis, *J. of the Taiwan Institute of Chem Eng.* **40**, 21–28.
- Ayranci, E. and Duman, O. 2006. Adsorption of aromatic organic acids onto high area activated carbon cloth in relation to wastewater purification. *Journal Hazard Material.* **136**(3): 542-52.
- BASF, AG 1988. *Analytisches Labor; unveröffentlichte Untersuchung* (J.Nr. 129304/01 vom 02.09.88).
- BASF, AG 1994. *Sicherheitsdatenblatt Acrylsäure rein* (22.08.1994). BASF
- Bai, Y., Yan, R., Huo, F., Qian, J., Zhang, X., and Zhang, S. 2017. Recovery of methacrylic acid from dilute aqueous solutions by ionic liquids through hydrogen bonding interaction. *J. Separation and Purification Technology*, **184**: 354–364.
- Bauer Jr., W., Kroschwitz, J.I., Howe-Grant, M., and Kirk-Othmer, 1991. *Encyclopedia of Chemical Technology*. vol. 1. fourth ed., Wiley-Interscience, New York: 287–314.
- Berg, L. 1992. *Dehydration of acetic acid by extractive distillation*, US 5167774.
- Bhandari, V.M., Sorokhaibam, L.G., Ranade, V.V. “Ion Exchange Resin Catalyzed Reactions—An Overview” Ed. Joshi, S.S., Ranade, V.V. *Industrial Catalytic Processes for Fine and Specialty Chemicals*. (2016) 393-426.
- Bhattacharyya, D., Allison, M.J., Webb, J.R., Zanatta, G.M., Singh, K.S., and Grant, S.R. 2013. Treatment of an Industrial Wastewater Containing Acrylic Acid and Formaldehyde in an Anaerobic Membrane Bioreactor. *Journal of Hazardous Toxic and Radioactive Waste.* **17** (2): 74-79.
- Bianchi, C.L., Ragaini, V., Pirola, C., and Carvoli, G.A. 2003. New Method to Clean Industrial Water from Acetic Acid Via Esterification, *Journal Applied Catalysis B: Environmental.* **40**: 93–99.
- Bock, H., Wozny, G., and Gutsche, B. 1997. Design and control of a reaction distillation column including the recovery system. *Journal Chemical Engineering Process.* **36**: 101–109
- Bringué, R., Tejero, J., Iborra, M., Izquierdo, J. F., Fité, C., and Cunill, F. 2007. Water effect on the kinetics of 1-pentanol dehydration to di-n-pentyl ether (DNPE) on amberlyst 70. *Topics in Catalysis.* **45**(1-4): 181–186.
- Buluklu, A.D., Sert E., Karakus, S., Atalay, F.S. 2014 Development of kinetic mechanism for the esterification of acrylic acid with hexanol catalyzed by ion-exchange resin. *Int J Chem Kinetic.* **46**(4):197–205
- Calvar, N., Gonzalez, B., and Dominquez, A. 2007. Esterification of Acetic Acid with Ethanol: Reaction Kinetics and Operation in a Packed Bed Distillation Column, *Chemical Engineering Process.* **46**: 1317.

- Chakrabarti, A., and Sharma, M.M., 1993. Cationic ion exchange resins as catalyst. *Reactive Polymers*, 20:1-45
- Chandrasekhar, S., Narsihmulu, C., and Sultana S.S. 2002. Poly(ethylene glycol) (PEG) as a reusable solvent medium for organic synthesis. *Application in the Heck reaction. Organic Letters*. **4**(25): 4399-4401.
- CHEMSAFE. *National database for safety data of the Physikalisch-technische Bundesanstalt Braunschweig*, established by expert judgement.
- Chen, X., Xu, Z., and Okuhara, T. 1999. Liquid phase esterification of acrylic acid with 1-butanol catalyzed by solid acid catalysts. *Applied Catalysis A: General*. **180**: 261-269
- Chiang, W. and Huang, C. 1993, Separation of liquid mixtures by using polymer membranes. IV. water-alcohol separation by pervaporation through modified acrylonitrile grafted polyvinyl alcohol copolymer (PVA-G-AN) membranes. *Journal of Applied Polymer Science* **48**: 199-203.
- Chiang, W.Y. and Hu, C.M. 1991. Separation of liquid mixtures by using polymer membranes. I. Water/alcohol separation by pervaporation through PVA-G-MMA:MA membrane. *Journal of Applied Polymer Science*. **43**: 2005-2012.
- Chin S Y, Ahmad M A A, Kamaruzaman M R , and Cheng C K 2015 Kinetic studies of the esterification of pure and dilute acrylic acid with 2-ethyl hexanol catalysed by Amberlyst 15. *Chemical Engineering Science* **129** 116–125
- Choi, J., and Hong, W.H. 1999. Recovery of lactic acid by batch distillation with chemical reactions using ion exchange resin. *Journal of Chemical Engineering of Japan*. **32**: 184-189.
- Chubarov, G.A., Danov, S.M., Logutov, V.I., and Obmelyukhina, T.N. 1984. Esterification of acrylic acid with methanol. *Journal of Applied Chemistry of the USSR*. **57**: 192–193.
- Constantino, D.S., Pereira, C.S., Faria R.P., Ferreira A.F., Loureiro J.M., Rodrigues A.E. (2015) Synthesis of butyl acrylate in a fixed-bed adsorptive reactor over Amberlyst 15. *AIChE J* **61**:1263–1274
- Cordeiro, C.S., Arizaga, G.G.C., Ramos, L.P., and Wypych, F. 2008. A new zinc hydroxide nitrate heterogeneous catalyst for the esterification of free fatty acids and the transesterification of vegetable oils. *Catalysis Communications*. **9**: 2140–2143
- Cunill, F., Ibbora, M., Fite, C., Tejero, J., and Izquierdo, J.F. 2000. Conversion, selectivity and kinetics of the addition of isopropanol to isobutene catalyzed by a macroporous ion-exchange resin. *Industrial & Engineering Chemistry. Res.* **39**: 1235-1241.
- Darge O, and Thyron F.C. (1993) Kinetics of the liquid phase esterification of acrylic acid with butanol catalysed by cation exchange resin. *J Chem Technol Biotechnology*. **58**(4):351–355

- David, M.O., Nguyen, Q.T., and Neel, J. 1992. Pervaporation membranes endowed with catalytic properties based on polymer blends, *Journal of Membrane Science*. **73**: 129-141.
- Delgado, P., Sanz, M. T., and Beltrán, S. 2007. Kinetic study for esterification of lactic acid with ethanol and hydrolysis of ethyl lactate using an ion-exchange resin catalyst. *Journal Chemical Engineering Journal*. **126**(2-3): 111–118.
- Demirbas, A. 2008. Biofuels sources, biofuel policy, biofuel economy and global biofuel projections. *Journal Energy Conversion and Management*. **49**: 2106–2116.
- Devulapelli, V. G. and Weng, H.-S. 2009. Esterification of 4-methoxyphenylacetic acid with dimethyl carbonate over mesoporous sulfated zirconia. *Catalysis Communications*. **10**(13): 1711–1717.
- Dirk-Faitakis, C.B., An, W., Lin, T.B., and Chuang, K.T. 2009. Catalytic distillation for simultaneous hydrolysis of methyl acetate and etherification of methanol. *Journal Chem. Eng. Process*. **48**: 1080–1087.
- Disteldorf, W., Peters, J., Morsbach, B., Kummer, M., and Rühl, T. 2002. *Method for the production of phthalic anhydride to a specification*. BASF, WO/2002/064539
- Dixit, A. B., & Yadav, G. D. (1996). Deactivation of ion-exchange resin catalysts. Part II: Simulation by network models. *Reactive and Functional Polymers*, 31(3), 251-263.
- DOW Chemical Company, 23 December 2014. Product Safety Assessment: Acrylic Acid.
- Dupont, P. Vcdrine, J. C. Paumard, E. Hecquet, and G. 1995. Heteropolyacids supported on activated carbon as catalysts for the esterification of acrylic acid by butanol, *Journal Applied Catalysis A: General*. **129**(2): 17-227
- ECETOC, 1995. *European Centre for Ecotoxicology and Toxicology of Chemicals. Acrylic Acid*. CAS No. 79-10-7. Joint Assessment of Commodity Chemicals No. 34. ECETOC, Brussels.
- Essayem, N., Martin, V., Riodel, A., and Védrine, J.C. 2007. Esterification of acrylic acid with but-1-ene over sulfated Fe- and Mn-promoted zirconia. *J. Applied Catalysis A: General*. **326**(1): 74–81.
- Faber, K. 1997. *Biotransformations*. In *Organic Chemistry: A Textbook*, 3rd Ed.; Springer-Verlag: Berlin, Germany,
- Falbe, J., Rebitz, M., and Römpf, H. 1995. *Römpf Chemie Lexikon*. Thieme, Stuttgart
- Farnetti, E., Monte, R.D., and Kaspar, J. 2004. Homogeneous and Heterogeneous Catalyst. *J. Inorganic and Bio-inorganic Chemistry*, **2**(2)

- Fernandes, S.A., Cardoso, A.L., and José da Silva, M. 2012. A novel kinetic study of $H_3PW_{12}O_{40}$ -catalyzed oleic acid esterification with methanol via 1H NMR spectroscopy. *J. Fuel Processing Technology*. **96**: 98–103
- Fogler, H.S. 2008. *Elements of Chemical Reaction Engineering* Fourth Edition, United State of America, Pearson Education.
- Fomin, V.A., Etlis, I.V., and Kulemin, V.I. 1991. Some aspects of esterification of acrylic acid with 2-ethylhexyl alcohol on sulfonic cation-exchangers. *Journal Applied Chemistry. USSR*. **64**: 1811–1815.
- Fox, M., Gibson, T., Mulach, R., and Sasano, T. 1990. *CEH Marketing research report*. SRI International.
- Gangadwala, J., Mankar, S., Mahajani, S., Kienle, A., and Stein, E. 2003. Esterification of Acetic Acid with Butanol in the Presence of Ion-Exchange Resins as Catalysts, *J. Ind. Eng. Chem. Res.* **42**: 2146–2155.
- Garcia, T., Coteron, A., Martinez, M., and Aracil, J. 2000. Kinetic model for the esterification of oleic acid and cetyl alcohol using an immobilized lipase as catalyst. *J. Chemical Engineering Science*. **55**: 1411-1423.
- Gerpen, J.V. 2005. Biodiesel processing and production. *Journal Fuel Processing Technology*. **86**: 1097–1107.
- Gómez-Castro, F.I., Rico-Ramírez, V., Segovia-Hernández, J.G., and Hernández-Castro, S. 2011. Esterification of fatty acids in a thermally coupled reactive distillation column by the two-step supercritical methanol method. *Journal Chemical Engineering Research and Design*. **89**(4): 480–490.
- Gonçalves, C.E., Laier, L.O., Cardoso, A.L., and Silva, M.J. 2012. Bioadditive synthesis from $H_3PW_{12}O_{40}$ -catalyzed glycerol esterification with HOAc under mild reaction conditions. *Journal Fuel Processing Technology*. **102**: 46–52.
- Gorak, A., Hoffmann, A., and Kreis, P. 2007. Prozessintensivierung: Reaktive und Membran- unterstützte Rektifikation. *Journal Chemical Engineering & Technology*. **79**: 1581-1600.
- Gref, R., Nguyen, Q.T., Schaetzel, P., and Neel, J. 1993. Transport properties of poly (vinyl alcohol) membranes of different degrees of crystallinity. I. Pervaporation results. *Journal Appl. Polym. Sci.* **49**: 209-218.
- Haas, M.J. 2005. Improving the economics of biodiesel production through the use of low value lipids as feedstock: vegetable oil, soapstock. *Fuel Processing Technology*. **86**: 1087–1096.
- Han, X.X., Chen, K.K., Yan, W., Hung, C.T., Liu L.L., Wu, P.H., Lin, K.C., Liu, S.B., 2016. Amino acid-functionalized heteropolyacids as efficient and recyclable catalysts for esterification of palmitic acid to biodiesel. *Fuel*. **165**:115–122
- Hanika, J., Smejkal, Q., and Kolena, J. 2001. 2-Methylpropylacetate synthesis via catalytic distillation. *Catalysis Today*. **66**(2-4): 219–223.

- Harmer, M.A. and Sun, Q. 2001. Solid acid catalysis using ion-exchange resins. *Journal Applied Catalysis A: General*. **221**: 45–62.
- Harmsen, G. J. 2007. Reactive distillation: The front-runner of industrial process intensification. *Chemical Engineering and Processing: Process Intensification*. **46**(9), 774–780.
- Hayashi, S., Hirai, T., Hayashi, F., and Hojo, N. 1983. Permeation characteristics of poly(vinyl alcohol) poly(vinyl acetate) composite porous membranes. *Journal Applied Polymer Science*. **28**: 3041-3048.
- Hino, M. and Arata, K. 1981. Synthesis of esters from acetic acid with methanol, ethanol, propanol, butanol and iso-butyl alcohol catalysed by solid superacid. *Chemistry Letter*. 1671–1672.
- Hoechst Celanese Corp. 1992. *Material Safety Data Sheet: 2-Ethylhexyl Acrylate (41)*, Dallas, TX
- Hsiue, G.H., Yang, Y.S., and Kuo, J.F. 1987. Permeation and separation of aqueous alcohol solutions through grafted poly(vinyl alcohol) latex membranes. *Journal Applied Polymer Science*. **34**: 2187–2196.
- Hui Y.H. 1996. *Bailey's Industrial Oil and Fat Products*. Wiley-Interscience, New York.
- Hüls 1995. *Determination of the surface tension*. Unpublished test report (Report No. AN-ASB 0066, 28.06.1995).
- ICB Chemical Profile, 2008, Acrylic Acid Uses and Market Data. <http://www.icis.com/v2/chemicals/9074870/acrylic+acid/uses.html>, (13 October 2013)
- IHS Markit, Acrylic Acid: Process Economics Program Report. October 2015 from <https://ihsmarkit.com/products/chemical-technology-pep-acrylic-acid-2015.html>
- Ingale, M.N. and Mahajani, V.V. 1996. Recovery of Carboxylic Acids, C2-C6, from an Stream using Tributylphosphate (TBP): Effect Aqueous Waste of Presence of Inorganic Acids and their Sodium Salts. *Journal Separation Science Technology*. **6**: 1–7.
- Inoue, K., Iwasaki, M., and Matsui, K. 1993. Process for producing ethyl acetate. USP 5241106
- Iranpoor, N. and Shekarriz, M. 1999. Ring Opening of Epoxides with Sodium Cyanide Catalyzed with Ce(OTf)₄. *Journal Synthetic Communications*. **29**(13): 2249-2254.
- Ishihara, K., Nakayama, M., Ohara, S., and Yamamoto, H. 2001. A green method for the selective esterification of primary alcohols in the presence of secondary alcohols or aromatic alcohols, *SYNLETT*. **7**: 1117-1120

- Ishihara, K., Nakayama, M., Ohara, S., and Yamamoto, H. 2002. Direct ester condensation from a 1:1 mixture of carboxylic acids and alcohols catalyzed by hafnium(IV) or zirconium(IV) salts. *Journal Tetrahedron*. **58**: 8179-8188
- Ishihara, K., Ohara, S., and Yamamoto, H. 2000 Direct condensation of carboxylic acids with alcohols catalyzed by hafnium(IV) salts. *Journal Science*. **290**: 1140-1142.
- Izci, A. and Bodur, F. 2007. Liquid Phase Esterification of Acetic Acid with iso-Butanol Catalyzed by Ion Exchange Resins. *Reactive and Functional Polymers* **67**(12): 1458–1464.
- Izumi Y. 1997 Hydration/hydrolysis by solid acids. *Catalysts Today* **33** 371-409.
- Jagadeeshbabu, P.E., Sandesh, K., and Saidutta, M.B. 2011. Kinetics of Esterification of Acetic Acid with Methanol in the Presence of Ion Exchange Resin Catalysts. *Journal of Industrial Engineering Chemistry. Res.* **50**: 7155–7160.
- Jalbani N, Kazi T G, Arain B M, Jamali M K, Afridi I, and Irfraz R A 2006 Application of factorial design in optimization of ultrasonic-assisted extraction of aluminum in juices and soft drinks. *Talanta* **70** (2) 307–314.
- Jaques, D. and Leisten, J.A. 1964. Acid-catalysed ether fission. Part II. Diethyl ether in aqueous acids. *J. Chem. Soc.* 2683-2689
- Johannessen, T., Larsen, J.H., Chorkendorff, I., Livbjerg, H., and Topsøe, H. 2000. Catalyst dynamics: consequences for classical kinetic descriptions of reactors. *Journal Chemical Engineering Journal*. **82**(1-3): 219- 230.
- Kadaba, P.K. 1974. New compounds: Convenient selective esterification of aromatic carboxylic acids bearing other reactive groups using a boron trifluoride etherate—alcohol reagent. *Journal of Pharmaceutical Sciences*. **63**(8): 1333-1335
- Karakus, S., Sert, E., Buluklu, D., and Atalay F.S. 2014. Liquid phase esterification of acrylic acid with isobutyl alcohol catalyzed by different cation exchange resins. *Ind Eng Chem Res* **53**:4192–4198
- Katz, M.G. and Wydeven, T. 1982. Selective permeability of PVA membranes. II. Heat treated membranes. *Journal Applied Polymer Science*. **27**: 79-87.
- Kienberger, M., Hackl, M., & Siebenhofer, M. 2018. Recovery of acetic acid using esterification of acetic acid with n-octanol in a membrane reactor. *J. of Environmental Chemical Engineering*, **6**(2): 3161–3166.
- Keshav, A., Chand, S., and Wasewar, K.L. 2009. Recovery of propionic acid from aqueous phase by reactive extraction using quarternary amine (Aliquat 336) in various diluents. *Chemical Engineering Journal*. **152**(1), 95–102.
- Khurana, J.M., Sahoo, P.K., and Maitkap, G.C. 1990. Sonochemical Esterification of Carboxylic Acids in Presence of Sulphuric Acid. *Synth. Commun.* **20**(15), 2267.

- Kimura, T. and Ito, Y. 2001. Two bacterial mixed culture systems suitable for degrading terephthalate in wastewater. *Journal Bioscience Bioengineering*. **91**: 416–418.
- Kiss, A.A. 2011. Heat-integrated reactive distillation process for synthesis of fatty esters. *Fuel Processing Technology*. **92**: 1288–1296.
- Kiss, A. A. 2018. Novel Catalytic Reactive Distillation Processes for a Sustainable Chemical Industry. *Topics in Catalysis*.
- Klein, G., Houérou, V.L., Muller, R., Gauthier, C., and Holl, Y. 2012. Friction properties of acrylic-carboxylated latex films. 1. Effects of acrylic acid concentration and pH *Tribology International*. **53**: 142–149.
- Kołodziej, A., Jaroszyński, M., Schoenmakers, H., Althaus, K., Geißler, E., Übler, C., and Kloeker, M. 2005. Dynamic tracer study of column packings for catalytic distillation. *Chem Eng and Processing: Process Intensification*, **44**(6), 661–670.
- Kojima, Y., Fruhata, K.I., and Miyasaka, K. 1985. Sorption and permeation of iodine in water-swollen poly (vinyl alcohol) membranes and iodine complex formation. *Journal Applied Polymer Science*. **30**: 1617-1628.
- Komesu, A., Martinez, P. F. M., Lunelli, B. H., Filho, R. M., and Maciel, M. R. W. (2015). Lactic acid purification by reactive distillation system using design of experiments. *Chem. Eng. and Processing: Process Intensification*. **95**, 26–30.
- Komoń, T., Niewiadomski, P., Oracz, P., and Jamróz, M.E. 2013. Esterification of acrylic acid with 2-ethylhexan-1-ol: Thermodynamic and kinetic study. *Journal Applied Catalysis A: General*. **451**: 127– 136.
- Kozhevnikov, I.V. 1987. Advances in Catalysis by Heteropolyacids. *RUSS CHEM REV.* **56** (9): 811–825
- Kraai, G.N., Winkelman, J.G.M., de Vries, J.G., and Heeres, H. J. 2008. Kinetic studies on the *Rhizomucor miehei* lipase catalyzed esterification reaction of oleic acid with 1-butanol in a biphasic system. *Journal Biochemical Engineering*. **41**(1): 87–94.
- Kudła, S. and Kaledkowska, M. 1998. Production and Use of Acrylic-Acid and It's Esters. *Przemysl Chemiczny*. **77**(3): 86–91.
- Kuila, S. B. and Ray, S. K. 2011. Dehydration of acetic acid by pervaporation using filled IPN membranes, *J. Separation and Purification Technology*. **81**: 295–306.
- Kumar, A., Prasad, B., and Mishra, I.M. 2008. Optimization of process parameters for acrylonitrile removal by a low-cost adsorbent using Box–Behnken design. *Journal of Hazardous Materials*. **150**: 174–182.
- Kumar, M.V.P. and Kaistha, N. 2009. Evaluation of ratio control schemes in a two-temperature control structure for a methyl acetate reactive distillation column. *J. Chemical Engineering Research and Design*. **87**(2): 216–225.

- Kuusik, A. and Faingold, S.I. 1974. Esterification of Acrylic Acid with 1-Octenes. 22(3):212-216. (English language translation included from the Academy of Sciences of the Estonian Soviet Republic, vol. 22, Chemistry; Geology, 1973, No. 3, pp. 1-7.).
- Lam, M.K., Lee, K.T., and Mohamed, A.R. 2010. Homogeneous, heterogeneous and enzymatic catalysis for transesterification of high free fatty acid oil (waste cooking oil) to biodiesel: A review. *J. Biotechnology advances*, **28**(4), 500–18.
- Lee, L.S. and Kuo, M.Z. 1996. Phase and reaction equilibria of the acetic acid-isopropanol-isopropyl acetate-water system at 760 mmHg. *J. Fluid Phase Equilibrium*. **123**: 147–165.
- Lee, M., Chiu, J., and Lin, H. 2002. Kinetics of Catalytic Esterification of Propionic Acid and n-Butanol over Amberlyst. *J. Ind. Eng. Chem. Res.* **35**: 2882–2887.
- Lei, Z., Li, C., Li, Y., and Chen, B. 2004. Separation of acetic acid and water by complex extractive distillation. *J. Separation and Purification Technology*. **36**(2): 131–138.
- Li, S., Zhuang, J., Zhi, T., Chen, H., and Zhang, L. 2008. Combination of complex extraction with reverse osmosis for the treatment of fumaric acid industrial wastewater. *Desalination*. **234**: 362–369.
- Li, S.J., Chen, H.L., and Zhang, L. 2009. Recovery of fumaric acid by hollow-fiber supported liquid membrane with strip dispersion using trialkylamine carrier. *J. Separation and Purification Technology*. **66**: 25–34.
- Liljaja, J., Murzina, D.Y., Salmia, T., Aumoa, J., Mäki-Arvelaa, P., and Sundell, M. 2002. Esterification of different acids over heterogeneous and homogeneous catalysts and correlation with the Taft equation. *Journal of Molecular Catalysis A: Chemical*. **182–183**, 555–563.
- Lotero, E., Liu, Y., Lopez, D.E., Suwannakarn, K., Bruce, D.A. and Goodwin, I.G., Jr. 2005. Synthesis of Biodiesel via acid catalysis. *Industrial and Engineering Chemistry Research*. **44**: 5353-5363.
- Lutze, P., Dada, E.A., Gani, R., and Woodley, J.M.. 2010. Heterogeneous catalytic distillation – a patent review. *Rec. Pat. Chem. Eng.* **3**: 208-229.
- Mahajan, Y. S., Shah, A. K., Kamath, R. S., Salve, N. B., and Mahajani, S. M. 2008. Recovery of trifluoroacetic acid from dilute aqueous solutions by reactive distillation. *J. Separation and Purification Technology*. **59**(1), 58–66.
- Mallaiah, M., and Reddy, G.V. 2016. Optimization studies on a continuous catalytic reactive distillation column for methyl acetate production with response surface methodology. *J. of the Taiwan Institute of Chemical Engineers*. **69**:25–40.
- Malshe, V.C. and Chandalia, S.B. 1977. Kinetics of liquid-phase esterification of acrylic-acid with methanol and ethanol. *J. Chemical Engineering Science*. **32**: 1530–1531.

- Manabe, K., Iimura, S., Sun, X.M., and Kobayashi, S. 2002. Dehydration reactions in water. Brønsted acid-surfactant-combined catalyst for ester, ether, thioether, and dithioacetal formation in water. *J. Am. Chem. Soc.* **124**: 11971–11978.
- Martinec, A., Sentinek, K., Beranek, L. 1978. The effect of cross-linking on catalytic properties of macroporous styrene-divinylbenzene ion exchangers. *J. Catalysis*, **51**:86-95
- Mekala, M., Goli, V.R. 2015. Kinetics of esterification of methanol and acetic acid with mineral homogeneous acid catalyst. *Chinese Journal of Chemical Engineering*. **23**: 100-105
- Merchant, S.Q., Almohammad, K.A., Al Bassam, A.A.M., and Ali, S. H. 2013. Biofuels and additives: Comparative kinetic study of Amberlite IR 120-catalyzed esterification of ethanol with acetic, propanoic and pentanoic acids to produce eco-ethyl-esters. *J. Fuel*. **111**: 140–147.
- Merck Index, 1996. *The Merck Index*. 12th edition. Merck & Co., Inc., Whitehouse Station, NJ. Miller
- Molinero, L., Ladero, M., Tamayo, J.J., García-Ochoa, F. 2014. Homogeneous catalytic esterification of glycerol with cinnamic and methoxycinnamic acids to cinnamate glycerides in solventless medium: Kinetic modeling. *Chemical Engineering Journal*. **247**: 174-182.
- Moraru, M. D., and Bildea, C. S. 2018. Process for 2-Ethylhexyl Acrylate Production Using Reactive Distillation: Design, Control, and Economic Evaluation. *Industrial and Engineering Chemistry Research*. **57**(46):15773–15784.
- Neier W., 1991, *Ion exchangers as catalysts*, in: K. Dorfner (Ed.), *Ion Exchangers*, Walter de Gruyter, p. 981.
- Neumann, R. and Sasoon, Y. 1984. Recovery of dilute acetic acid by esterification in a packed chemorectification column. *J. Ind. Eng. Chem. Process Des. DeV.* **23** (4), 654-659.
- Nowak, P. 1999. Kinetics of The Liquid Phase Esterification of Acrylic Acid With n Octanol and 2-ethylhexanol catalyzed by Sulphuric Acid. *J. React. Kinetic Catalyst Lett.* **66**(2): 375-380.
- Ogawa, T., Hikasa, T., Ikegami, T., Ono N., and Suzuki, H. J. (1994). Selective Activation of Primary Carboxylic Acids by Electron-rich Triarylbismuthanes. Application to Amide and Ester Synthesis under Neutral Conditions. *Chem. Soc., Perkin Trans. 1*, 3473-3478.
- Ohya, H., Matsumoto, K., Negishi, Y., Hino, T., and Choi, H.S. 1992. The separation of water and ethanol by pervaporation with PVA-PAN composite membranes. *J. Memb. Sci.* **68**: 141-148.
- Okuhara T, Kimura M, Kawai T, Xu Z, and Nakato T 1998 Organic reactions in excess water catalyzed by solid acids. *Catalysis Today*. **45** 73–77.

- Okuhara, T. 2002. New catalytic functions of heteropoly compounds as solid acids. *J. Catal. Today.* **73**: 167-176
- Olah, G.A. 1973. *Friedel Crafts Chemistry*, Wiley-Interscience, New York.
- Orjuela, A., Yanez, A. J., Santhanakrishnan, A., Lira, C. T., and Miller, D. J. 2012. Kinetics of mixed succinic acid/acetic acid esterification with Amberlyst 70 ion exchange resin as catalyst. *Chemical Engineering Journal.* **188**: 98–107.
- Osorio-Viana, W., Duque-Bernal, M., Fontalvo, J., Dobrosz-Gómez, I., and Gómez-García, M.Á. 2013. Kinetic study on the catalytic esterification of acetic acid with isoamyl alcohol over Amberlite IR-120. *J. Chemical Engineering Science.* **101**: 755–763.
- Otera J and Nishikido J 2010 *Esterification Methods, Reactions and Applications*, seconded., Wiley-vch verlag GmbH & Co., KGaA, Weinheim,.
- Otera, J.; Dan-oh, N.; and Nozaki, H. 1991. Distannoxane-catalysed transesterification of 1,n-diols. Selective transformation of either of chemically equivalent functional groups. *J. Chem. Soc., Chem. Commun.* 1742-1743.
- Painer, D., Lux, S., and Siebenhofer, M. 2015. Recovery of Formic Acid and Acetic Acid from Waste Water Using Reactive Distillation. *Separation Science and Technology (Philadelphia).* **50**(18):2930–2936.
- Pappu, V.K.S., Kanyi, V., Santhanakrishnan, A., Lira, C.T., and Miller, D.J. 2013. Butyric acid esterification kinetics over Amberlyst solid acid catalysts: The effect of alcohol carbon chain length. *J. Bioresource Technology.* **130**: 793–797
- Pappu, V.K.S., Yanez, A.J., Peereboom, L., Muller, E., Lira, C.T., and Miller, D.J. 2011. A kinetic model of the Amberlyst-15 catalyzed transesterification of methyl stearate with n-butanol. *J. Bioresource technology.* **102**(5): 4270–4272.
- Park, D.W., Haam, S., Ahn, I.S., Lee, T.G., Kim, H.S., and Kim, W.S. 2004. Enzymatic esterification of beta-methylglucoside with acrylic/methacrylic acid in organic solvents. *Journal of biotechnology.* **107**: 151–160.
- Paul, J.M. and Samuel, Y. 1995. *Method of manufacturing secondary butyl acrylate by reaction of acrylic acid and butene isomers*. M. Esch, European Patent, No.745579
- Paumard, E. 1990. *Heteropolyacid catalysts in the preparation of esters of unsaturated carboxylic acids, The preparation of unsaturated carboxylic acid esters by liquid phase trans-esterification using heteropolyacids as catalysts*. French Patent FR PP.007.368.
- Peters, T.A., Benes, N.E., Holmen, A., and Keurentjes, J.T.F. 2006. Comparison of commercial solid acid catalysts for the esterification of acetic acid with butanol *Appl. Catalyst. A: General.* **297**: 182–188.

- Peykova, Y., Lebedeva, O.V., Diethert, A., Müller-Buschbaum, P., and Willenbacher, N. 2012. Adhesive properties of acrylate copolymers: effect of the nature of the substrate and copolymer functionality. *Int. J. Adhes. Adhes.* **34**: 107–116.
- Ping, Z., Nguyen, Q.T., and Neel, J. 1994. Investigation of poly(vinyl alcohol):poly(N-vinyl-2)-pyrrolidone blends. 3. Permeation properties of polymer blend membranes. *Macromol. Chem. Phys.* **195**: 2107-2116.
- Prasad K N, Kong K W, Ramanan R N, Azlan A, and Ismail A 2012 Selection of experimental domain using two-level factorial design to determine extract yield, antioxidant capacity phenolics, and flavonoids from *Mangifera pajang* Kosterm. *Sep. Sci. Technol.* **47 (16)** 2417–2423.
- Qu, Y., Peng, S., Wang, S., Zhang, Z., and Wang, J. 2009. Kinetic Study of Esterification of Lactic Acid with Isobutanol and n-Butanol Catalyzed by Ion-exchange Resins. *Chinese Journal of Chemical Engineering.* **17(5)**: 773–780.
- Rafiee, E., Paknezhad, F., Shahebrahimi, S., Joshaghani, M., Eavani, S., Rashidzadeh, S. 2008. Acid catalysis of different supported heteropoly acids for a one-pot synthesis of β -acetamido ketones. *Journal of Molecular Catalysis A: Chemical.* **282**: 92-98
- Ragaini, V., Bianchi, C.L., Pirola, C., and Carvoli, G. 2006. Increasing the value of dilute acetic acid streams through esterification. *Applied Catalysis B: Environmental.* **64(1-2)**: 66–71.
- Rahmanian, A., and Ghaziaskar, H.S. 2008. Selective extraction of maleic acid and phthalic acid by supercritical carbon dioxide saturated with trioctylamine. *The Journal of Supercritical Fluids.* **46(2)**: 118–122.
- Ram R.N. and Charles, I. 1997. Selective Esterification of Aliphatic Nonconjugated Carboxylic Acids in the Presence of Aromatic or Conjugated Carboxylic Acids Catalysed by $\text{NiCl}_2 \cdot 6\text{H}_2\text{O}$. *J. Tetrahedron.* **53**: 7335.
- Rat, M., Zahedi-Niaki, M.H., and Kaliaguine, S.T.O.D 2008. Sulfonic acid functionalized periodic mesoporous organosilicas as acetalization catalysts. *Microporos Mesoporous Mater.* **112**: 26–31.
- Rattanaphra, D., Harvey, A. P., Thanapimmetha, A., and Srinophakun, P. 2011. Kinetic of myristic acid esterification with methanol in the presence of triglycerides over sulfated zirconia. *J. Renewable Energy.* **36(10)**: 2679–2686.
- Research and Market, Acrylic Acid - Global Market Outlook (2017-2026) .September 2018 from https://www.researchandmarkets.com/research/sfxctt/global_acrylic?w=5
- Reyhanitash, E., Brouwer, T., Kersten, S. R. A., van der Ham, A. G. J., and Schuur, B. 2018. Liquid–liquid extraction-based process concepts for recovery of carboxylic acids from aqueous streams evaluated for dilute streams. *Chemical Engineering Research and Design.* **137**:510–533.

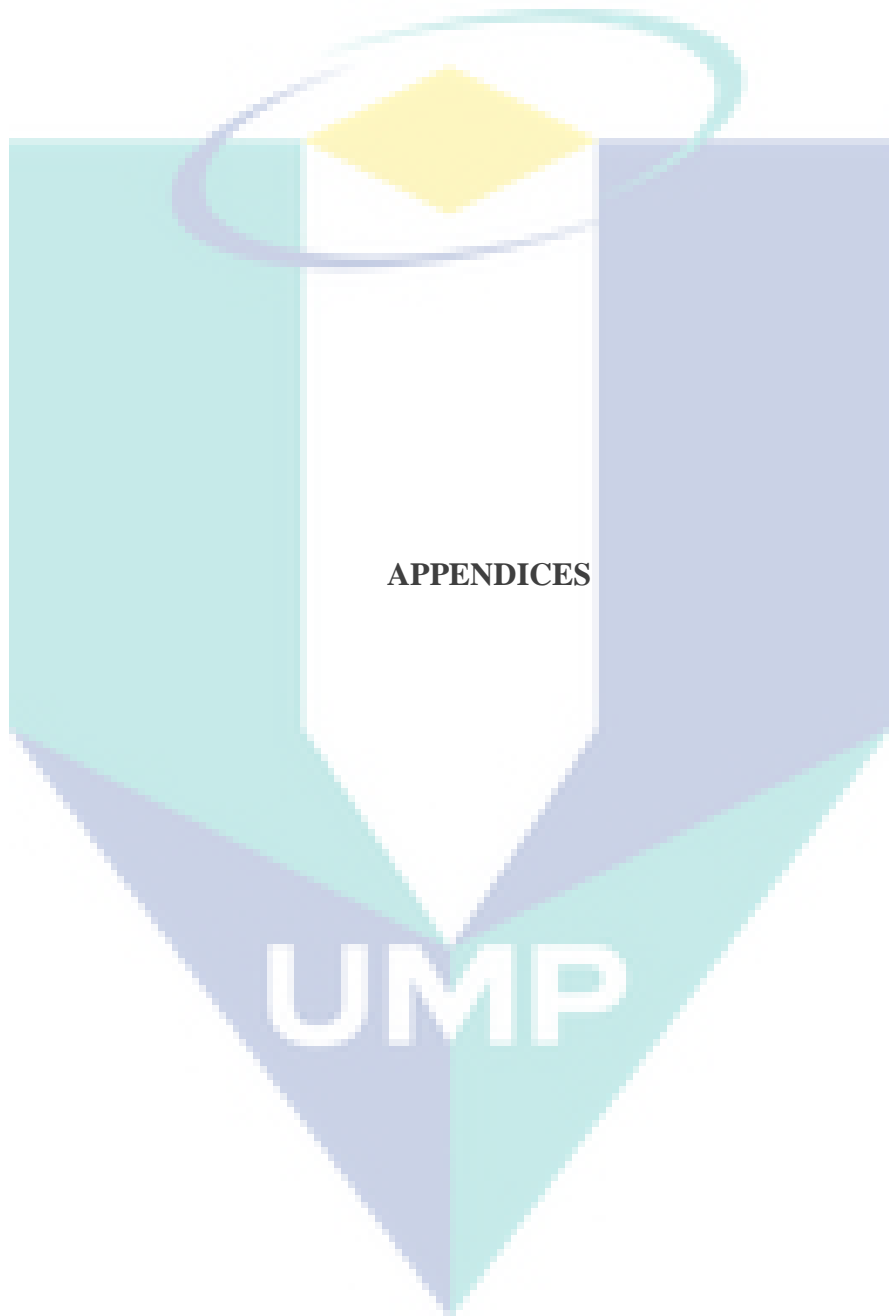
- Rohe, D. 1995. *Märkte und Unternehmen, Acrylsäure, Chemische Industrie* 1-2/95, pp 12-13.
- Rohm, Haas, 2006. *Amberlyst 15 Dry, Product data sheet*. Philadelphia, USA.
- Saha, B. and Sharma, M. 1996. Esterification of formic acid, acrylic acid and methacrylic acid with cyclohexene in batch and distillation column reactors: ion-exchange resins as catalysts. *J. Reactive and Functional Polymers*. **28**(3): 263–278.
- Saha, B. and Streat, M. 1999. Transesterification of cyclohexyl acrylate with n -butanol and 2-ethylhexanol: acid-treated clay, ion exchange resins and tetrabutyl titanate as catalysts. *J. Reactive and Functional Polymers*. **40**: 13–27.
- Saha, B., Chopade, S.P., and Mahajani, S.M. 2000. Recovery of dilute acetic acid through esterification in a reactive distillation column. *J. Catalysis Today*. **60**: 147–157.
- Salem, I.A. (2001). Activation of H₂O₂ by Amberlyst-15 resin supported with copper(II)-complexes towards oxidation of crystal violet. *Chemosphere*, **44**(5), 1109–19.
- Santia, V.D., Cardellina, F., Brinchib, L., and Germani, R. 2012. Novel Brønsted acidic deep eutectic solvent as reaction media for esterification of carboxylic acid with alcohols. *Tetrahedron Letters*. **53**: 5151–5155.
- Sanz, M.T., Murga, R., Beltrán, S., and Cabezas, J.L. 2002. Autocatalyzed and Ion-Exchange-Resin-Catalyzed Esterification Kinetics of Lactic Acid with Methanol, *J. Ind. Eng. Chem. Res.* **41**: 512-517.
- Sarah, C. Allied Market Research, Acrylic Acid Market is expected to garner \$18.8 billion, Globally, by 2020. 2014 <https://www.alliedmarketresearch.com/press-release/acrylic-acid-market-is-expected-to-reach-18-8-billion-globally-by-2020.html>
- Sarkar, A., Ghosh, S. K., and Pramanik, P. 2010. Investigation of the catalytic efficiency of a new mesoporous catalyst SnO₂/WO₃ towards oleic acid esterification. *Journal of Molecular Catalysis A: Chemical*. **327**(1-2): 73–79.
- Sayyed Hussain, S., Mazhar Farooqui, N., and Gaikwad Digambar, D. 2010. Kinetic and Mechanistic Study of Oxidation of Ester By KMnO₄. *International Journal of ChemTech Research*. **2**(1): 242-249.
- Scates, M.O., Parker, S.E., Lacy, J.B., and Gibbs, R.K. 1997. *Recovery of acetic acid from dilute aqueous streams formed during carbonylation process*. US Patent 5,599,976
- Scholz, N. 2003. Ecotoxicity and biodegradation of phthalate monoesters. *J. Chemosphere*. **53**(8): 921-926
- Schwegler, M. A., van Bekkum, H., and de Munck, N. A. 1991. Heteropoly acids as catalysts for the production of phthalate diesters. *Appl. Catal. A*. **74**: 191-204.

- Sejidov, F.T., Mansoori, Y., and Goodarzi, N. 2005. Esterification reaction using solid heterogeneous acid catalysts under solvent-less condition. *Journal of Molecular Catalysis A: Chemical*. **240**: 186–190.
- Sert, E., and Atalay, F. S. (2012). Esterification of acrylic acid with different alcohols catalyzed by zirconia supported tungstophosphoric acid. *Industrial and Engineering Chemistry Research*, **51**(19), 6666–6671.
- Sert, E. and Atalay, F.S. 2012. Determination of Adsorption and Kinetic Parameters for Transesterification of Methyl Acetate with Hexanol Catalyzed by Ion Exchange Resin. *J. Industrial and Engineering Chemistry Research*. **51**: 6350–6355.
- Sert, E., Buluklu, A.D., Karakuş, S., and Atalay, F.S. 2013. Kinetic study of catalytic esterification of acrylic acid with butanol catalyzed by different ion exchange resins. *J. Chemical Engineering and Processing: Process Intensification*. Article in Press
- Shafaei, A., Nikazar, M., and Arami, M. 2010. Photocatalytic degradation of terephthalic acid using titania and zinc oxide photocatalysts: Comparative study. *J. Desalination*. **252**(1-3): 8-16.
- Shah, M., Kiss, A. A., Zondervan, E., and de Haan, A. B. 2012. Influence of liquid back mixing on a kinetically controlled reactive distillation process. *Chemical Engineering Science*, **68**(1), 184–191.
- Shanmugam, S., Vieswanathan, B., and Varadarajan, T.K. 2004. Esterification by solid acid catalysts—a comparison. *J. Mol. Catal. A*. **223**: 143-147.
- Shantora, V. and Huang, R.Y.M. 1981. Separation of liquid mixtures by using polymer membranes. III. Grafted poly(vinyl alcohol) membranes in vacuum permeation and dialysis. *Journal of Applied Polymer Science*. **26**(10): 3223-3243.
- Sharma, M. M. 1995. Some novel aspects of cationic ion-exchange resins as catalysts. *Reactive and Functional Polymers*. **26**(1-3): 3–23.
- Shi, W., He, B., and Li, J. (2011). Esterification of acidified oil with methanol by SPES/PES catalytic membrane. *J. Bioresource technology*. **102**(9): 5389-93.
- Shin, C.H., Kim, J.Y., Kim, J.Y., Kim, H.S., Lee, H.S., Mohapatra, D., and Bae, W. 2009. A solvent extraction approach to recover acetic acid from mixed waste acids produced during semiconductor wafer process. *Journal of hazardous materials*. **162**(2-3): 1278–1284.
- Sigma-Aldrich (2013, July 25). Acrylic acid [Material Safety Data Sheet]. Retrieved from <http://www.sigmaaldrich.com/MSDS/MSDS/DisplayMSDSPage.do?country=MY&language=en&productNumber=147230&brand=ALDRICH&PageToGoToURL=http%3A%2F%2Fwww.sigmaaldrich.com%2Fcatalog%2Fproduct%2Faldrich%2F147230%3Flang%3Den>
- Siirola, J.J. 1995. *An industrial perspective on process synthesis*. In: Biegler, L.T., Doherty, M.F. (Eds.), *A.I.Ch.E. Symposium Series No. 304*, **91**, 222–233.

- Sing, K.S.W. 1982. *Reporting physisorption data for gas/solid systems with special reference to the determination of surface area and porosity (Provisional)*. **54** (11): 2201-2218
- Singh, A., Tiwari, A., Mahajani, S.M., and Gudi, R.D. 2006. Recovery of Acetic Acid from Aqueous Solutions by Reactive Distillation. *J. Industrial & Engineering Chemistry Research*. **45**(6): 2017–2025.
- Singh, N. and Sachan, P.K. 2013. Kinetic Study of Catalytic Esterification of Butyric Acid and Ethanol over Amberlyst 15. *ISRN Chemical Engineering*. **2013**:1–6.
- Siril, P.F., Cross H.E., and Brown D.R. 2008. New polystyrene sulfonic acid resin catalysts with enhanced acidic and catalytic properties. *Journal Mol. Catalyst A Chem*. **279**(1):63–68
- Smitha, B. 2004. Separation of organic–organic mixtures by pervaporation—a review, *Journal of Membrane Science*. **241**: 1–21.
- Song, C., Qi, Y., Deng, T., Hou, X., and Qin, Z. 2010. Kinetic model for the esterification of oleic acid catalyzed by zinc acetate in subcritical methanol. *J. Renewable Energy*. **35**(3): 625–628.
- Staples, C., Murphy, S.R., McLaughlin, J.E., Leung, H.W., Cascieri, T.C., and Farr, C.H. 2000. Determination of selected fate and aquatic toxicity characteristics of acrylic acid and a series of acrylic esters. *Chemosphere*. **40**(1): 29–38.
- Ströhlein, G., Assunção, Y., Dube, N., Bardow, A., Mazzotti, M., and Morbidelli, M. 2006. Esterification of acrylic acid with methanol by reactive chromatography: Experiments and simulations. *Chemical Engineering Science*. **61**(16): 5296–5306.
- Sundmacher, K. and Kienle, A. 2003. *Reactive Distillation*, 1 ed., Wiley-VCH, Weinheim.
- Takegami, S., Yamada, H., and Tsujii, S. 1992. Dehydration of water:ethanol mixtures by pervaporation using modified poly(vinyl alcohol). *Polym. J.* **24** (11): 1239-1250.
- Talnikar, V.D., Deorukhkar, O.A., Katariya, A., and Mahajan, Y.S. 2018. Intensification of the Production of 2-Ethyl-Hexyl Acrylate: Batch Kinetics and Reactive Distillation. *Int Journal of Chem Reactor Engineering*. **16**(7), 1–16.
- Taylor, R. and Krishna, R. 2000. Modelling reactive distillation. *J. Chemical Engineering Science*. **55**(22): 5183–5229.
- Teo, H.T.R. and Saha, B. 2004. Heterogeneous catalysed esterification of acetic acid with isoamyl alcohol: kinetic studies. *Journal of Catalysis*. **228**: 174–182.
- Thil, L., Breitscheidel, B., Disteldorf, W., Dornik K., and Morsbach, 2000. *Mixture of diesters of adipic or phthalic acid with isomers of nonanols*. B. DE 19924339 (2000).

- Tsai, Y.T., Lin, H., and Lee, M.J. 2011. Kinetics behavior of esterification of acetic acid with methanol over Amberlyst 36. *J. Chemical Engineering Journal*. **171**(3): 1367–1372.
- Tsukamoto, J. and Franco, T.T. 2009. Enzymatic esterification of d-fructose with acrylic acid in organic media, *J. New Biotechnology*. **25**: 108-109.
- Tuyun, A.F., Uslu, H., Gökmen, S., and Yorulmaz, Y. 2011. Recovery of Picolinic Acid from Aqueous Streams Using a Tertiary Amine Extractant. *Journal of Chemical and Engineering Data*. **56**(5): 2310–2315.
- Van de Steena E, De Clereq J, Thybaut J.W. 2014. Ion exchange resin catalysed transesterification of ethyl acetate with methanol: gel versus macroporous resins. *Chem Eng J*. **242**:170–179
- Vicente, G., Martinez, M., and Aracil, J. 2004. Integrated biodiesel production: a comparison of different homogeneous catalysts systems. *Bioresource Technology*. **92**, 297–305.
- Wakasugi, K., Misaki, T., Yamada, K., and Tanabe, Y. 2000. Diphenylammonium Triflate (DPAT): Efficient Catalyst for Esterification of Carboxylic Acids and for Transesterification of Carboxylic Esters with Nearly Equimolar Amounts of Alcohols. *Tetrahedron Lett*. **41**: 5249-5252.
- Wang, Q., Cheng, G., and Sun, X. 2006. Recovery of lactic acid from kitchen garbage fermentation broth by four-compartment configuration electro dialyzer. *J. Process Biochemistry*. **41**: 152–158.
- Wang, Y.Z., Liu, Y.P., and Liu, C.G. 2008. Removal of Naphthenic Acids of a Second Vacuum Fraction by Catalytic Esterification. *J. Petrol Sci Technol*. **26**(12): 1424–32.
- Weast, R.C. 1989. *Handbook of Chemistry and Physics*. 69th edition. CRC Press Inc., Boca Raton, FL, C-673.
- Wesslein, M., Heintz, A., and Lichtenthaler, R.N. 1990. Pervaporation of liquid mixtures through poly(vinyl alcohol) (PVA) membranes. II. The binary systems methanol:1-propanol and methanol:dioxane and the ternary system water:methanol:1-propanol. *J. Memb. Sci*. **51**: 181-188.
- Will, B. and Lichtenthaler, R.N. 1992. Comparison of the separation of mixtures by vapor permeation and by pervaporation using PVA composite membranes. II. The binary systems ammonia-water, methylamine-water, 1-propanol-methanol and the ternary system 1-propanol-methanol-water. *J. Memb. Sci*. **68**: 127-131.
- Wu, L.G., Zhu, C.L., and Liu, M. 1994. Study of a new pervaporation membrane, Part 1. Preparation and characteristics of the new membrane. *J. of Membrane Science* **90**: 199-205.
- Xiang, S., Zhang, Y.L., Xin, Q., and Li, C. 2002. Enantioselective epoxidation of olefins catalysed by Mn (salen)/MCM-41 synthesized with a new anchoring method. *J. Chem. Commun*. **22**: 2696-2697.

- Xu, T.W. and Yang, W.H. 2002. Citric acid production by electro dialysis with bipolar membranes. *Chem. Eng. Process.* **41**: 519–524.
- Xu, X., Lin, J., and Cen, P. 2006. Advances in the Research and Development of Acrylic Acid Production from Biomass. *Chinese J. Chem. Eng.* **14**(4): 419-427.
- Xu, Z.P., Afacan, A., and Chuang, K.T. 1999. Removal of Acetic Acid from Water by Catalytic Distillation. Part 1. Experimental Studies. *Can. J. Chem. Eng.* **77**: 676
- Yadav, G.D., and Rahuman, M.S.M.M. 2003. Synthesis of fragrance and flavour grade esters: activities of different ion exchange resins and kinetic studies. *J. Clean Tech. Environ. Policy.* **5**: 128–135.
- Yin, P., Chen, W., Liu, W., Chen, H., Qu, R., Liu, X., and Xu, Q. 2013. Efficient bifunctional catalyst lipase/organophosphonic acid-functionalized silica for biodiesel synthesis by esterification of oleic acid with ethanol. *J. Bioresource technology.* **140**: 146–151.
- Yu, L., Lin, T., Guo, Q., and Hao, J. 2003. Relation between mass transfer and operation parameters in the electro dialysis recovery of acetic acid. *J. Desalination.* **154**(2): 147–152.
- Yu, W., Hidajat, K., and Ray, A.K. 2004. Determination of adsorption and kinetic parameters for methyl acetate esterification and hydrolysis reaction catalyzed by Amberlyst 15. *Applied Catalysis A: General.* **260**: 191–205.
- Yuzhong, Z., Keda, Z., and Jiping, X. 1993. Preferential sorption of modified PVA membrane in pervaporation. *J. Memb. Sci.* **80**: 297-308.
- Zhang, X., Li, C., Wang, Y., Luo, J., and Xu, T. 2011. Recovery of acetic acid from simulated acetaldehyde wastewaters: Bipolar membrane electro dialysis processes and membrane selection. *Journal of Membrane Science.* **379**(1-2): 184–190.
- Zhicai, Y., Xianbao, R.C., and Jings, G. 1998. Esterification – distillation of butanol and acetic acid, *J. Chemical Engineering Science.* **53**(11): 2081-2088.
- Zhong, S., Xixin, D., Jing, Z., Xiaohong, W., Zijiang, J. 2015. Homogeneous borotungstic acid and heterogeneous micellar borotungstic acid catalysts for biodiesel production by esterification of free fatty acid. *Biomass and Bioenergy.* **76**: 31-42
- Zundel, G. 1969. Hydration and Intramolecular Interaction: Infrared Investigations with Polyelectrolytic Membranes, Academic Press, New York. Abrahams, P. W.; T



Appendix A

Standard Curve of AA

Figure A.1-A.6 shows the chromatogram of standard AA with various concentrations.

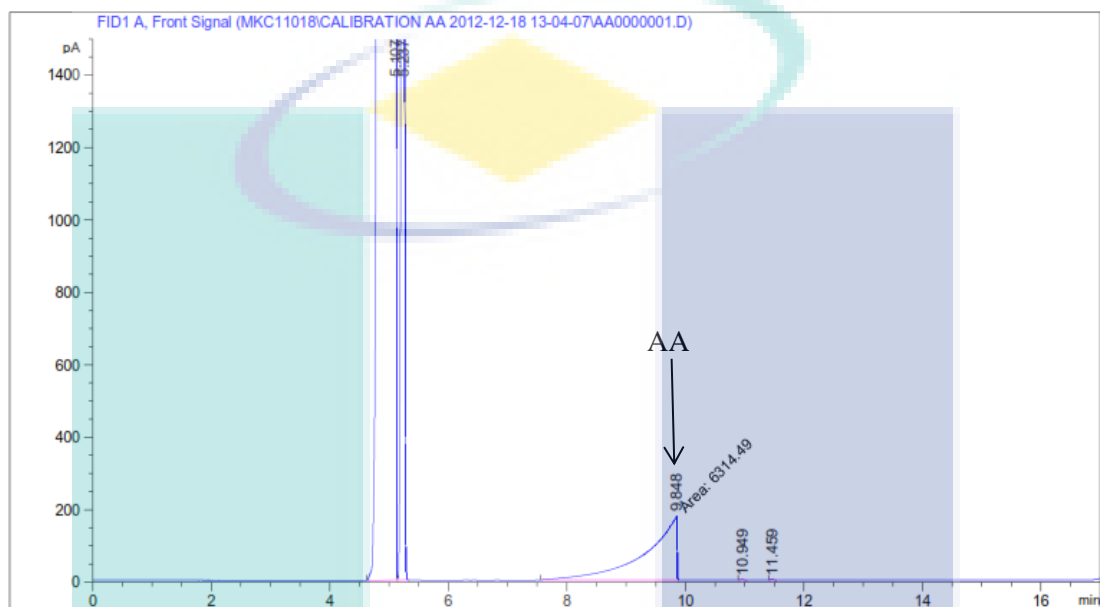


Figure A.1 GC-FID spectrometry of 6,393.27 ppm AA

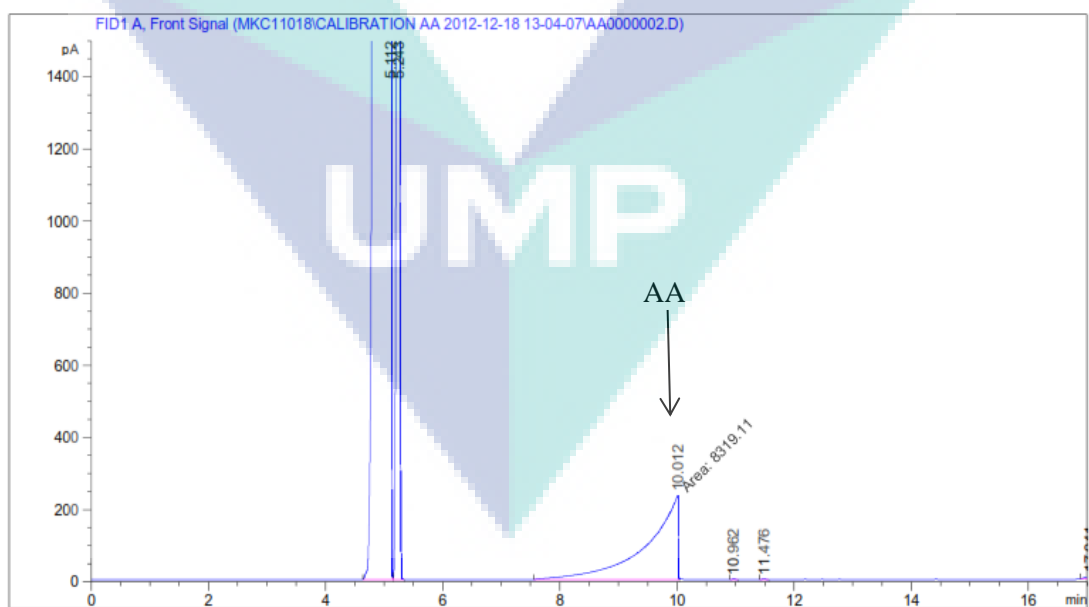


Figure A.2 GC-FID spectrometry of 12,786.55 ppm AA

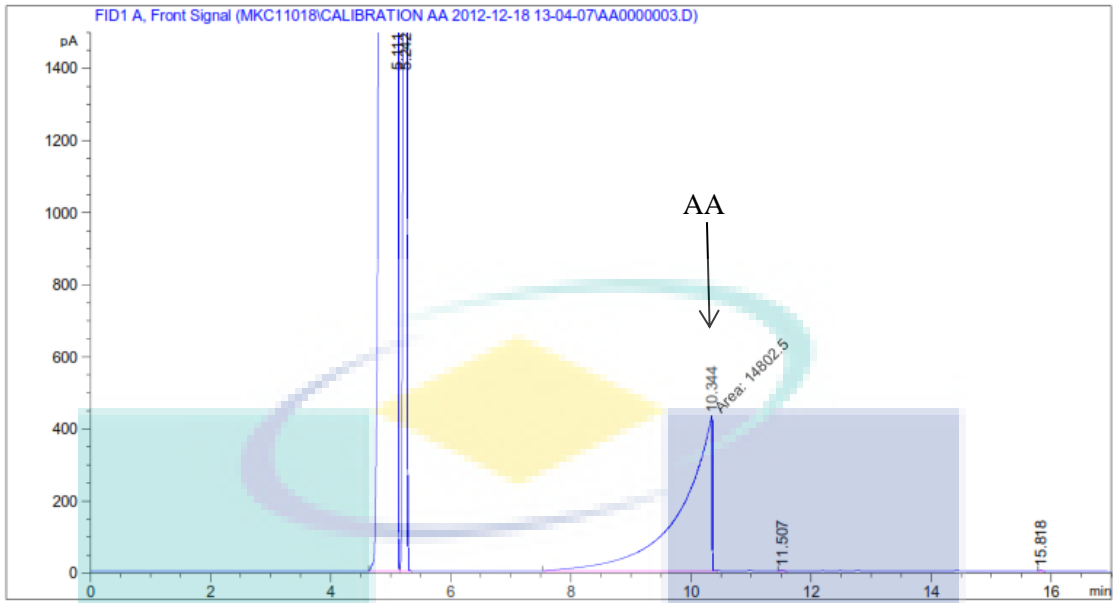


Figure A.3 GC-FID spectrometry of 25,573.10 ppm AA

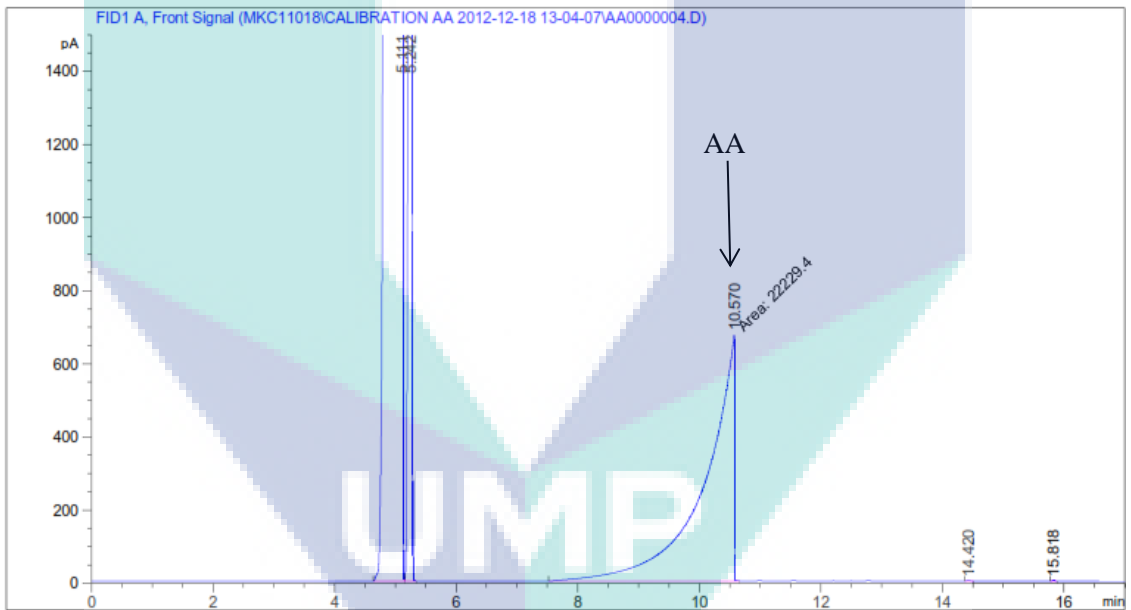


Figure A.4 GC-FID spectrometry of 38,359.64 ppm AA

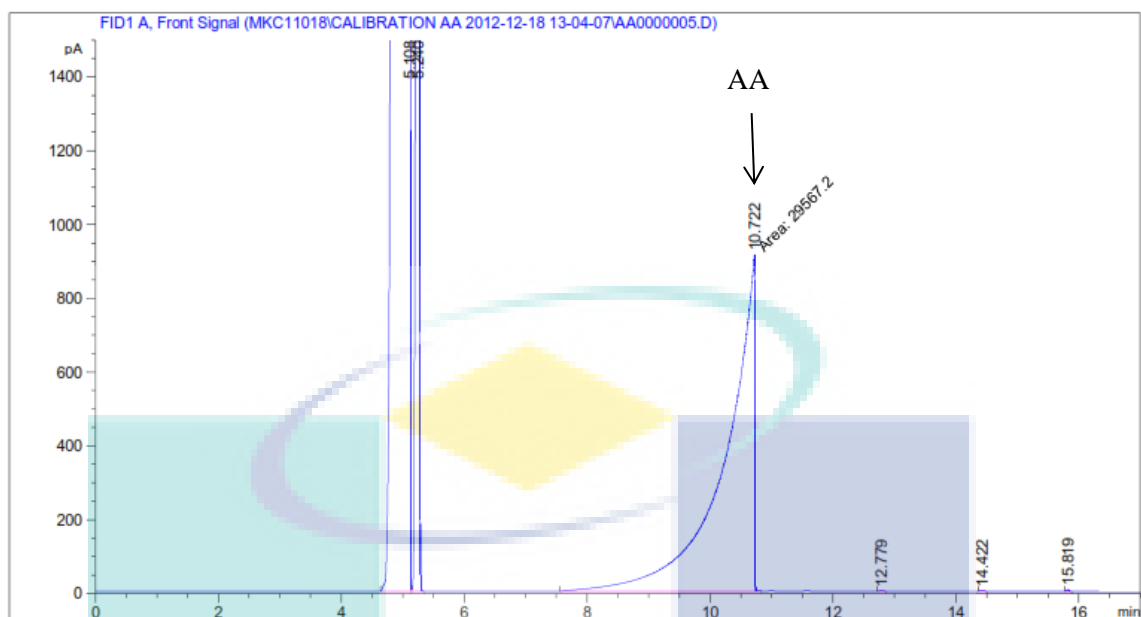


Figure A.5 GC-FID spectrometry of 51,146.19 ppm AA

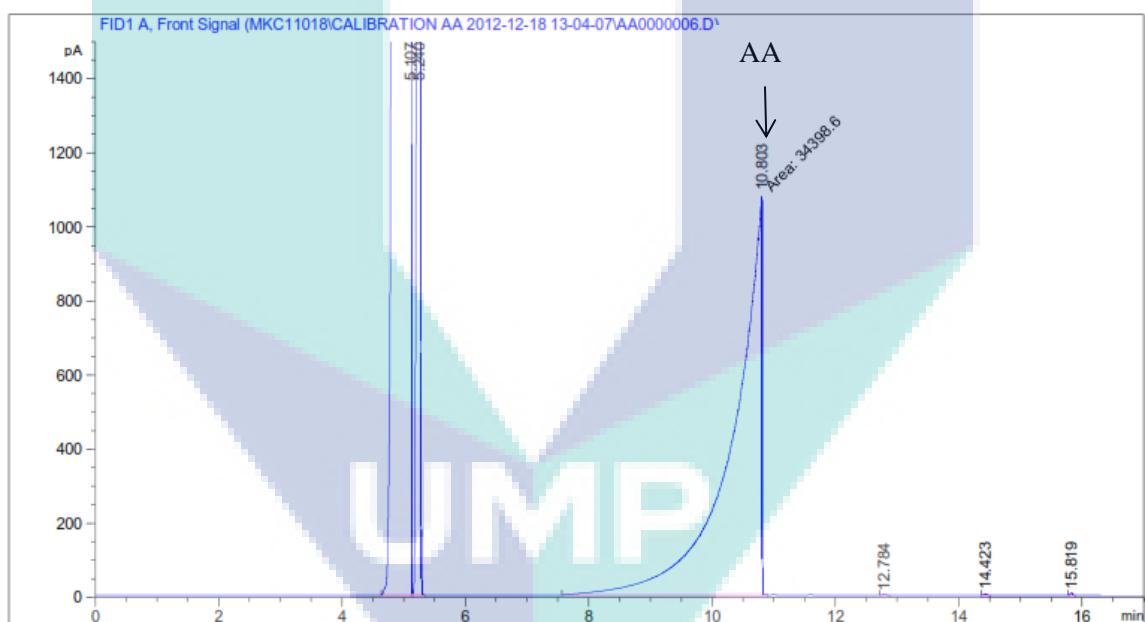


Figure A.6 GC-FID spectrometry of 63,932.74 ppm AA

The retention time for AA was detected at 10 min. The ABS-concentration data of standard calibration curve was included in Table A.1 and plotted in Figure A.7.

Table A.1 Concentration versus ABS for standard calibration curve plot of AA.

| concentration (ppm) | ABS (pA*s) |
|---------------------|------------|
| 0.00 | 0.000 |
| 6,393.27 | 6,314.490 |
| 12,786.55 | 8,319.110 |
| 25,573.10 | 14,802.500 |
| 38,359.64 | 23,229.400 |
| 51,146.19 | 29,567.200 |
| 63,932.74 | 34,398.600 |

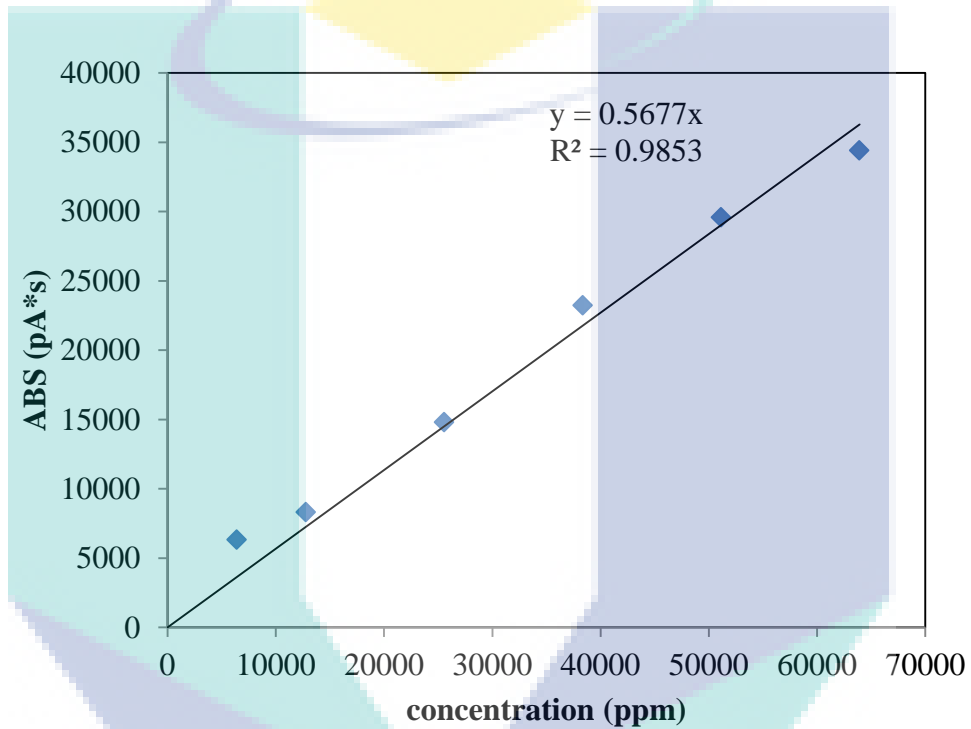


Figure A.7 Calibration curve for AA using GC-FID

The following equation was developed to calculate the unknown concentration of AA for each sample using the absorbance given by GC-FID analysis base on Figure A7,:

$$ABS_{AA} = m \times C_{AA} \quad (A1)$$

$$C_{AA} = \frac{ABS_{AA}}{m} \quad (A2)$$

$$C_{AA} = \frac{ABS_{AA}}{0.5677} \quad (A3)$$

$$C_{AA} = 1.76 \times ABS_{AA} \quad (A4)$$

APPENDIX B

Standard Curve of 2EHA

Figure B.1-B.8 shows the chromatogram of standard 2EHA with various concentrations.

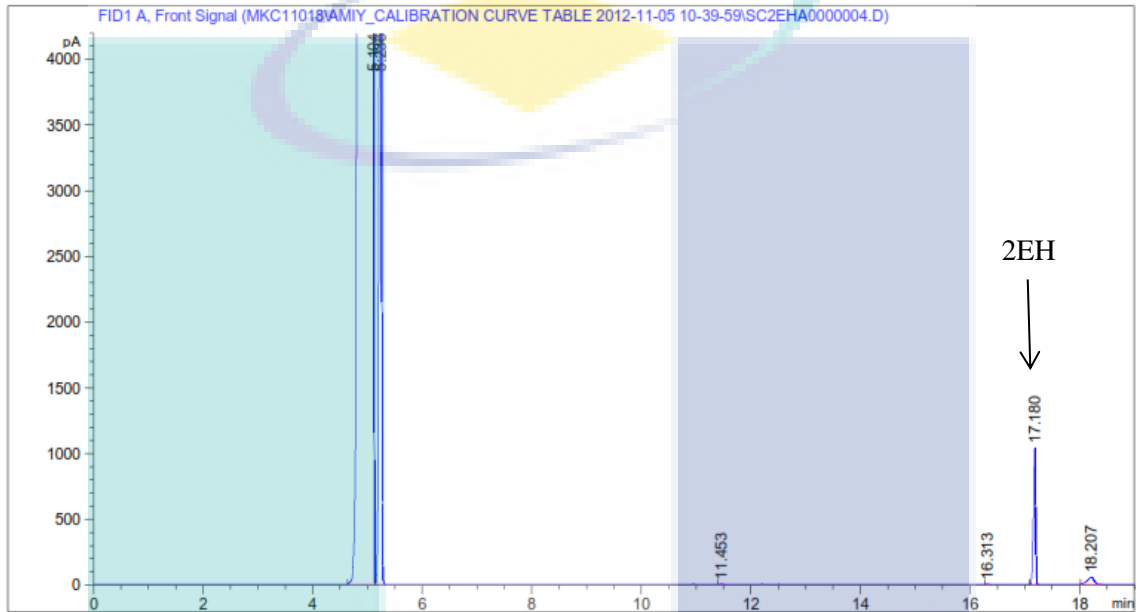


Figure B.1 GC-FID spectrometry of 2,000 ppm 2EHA

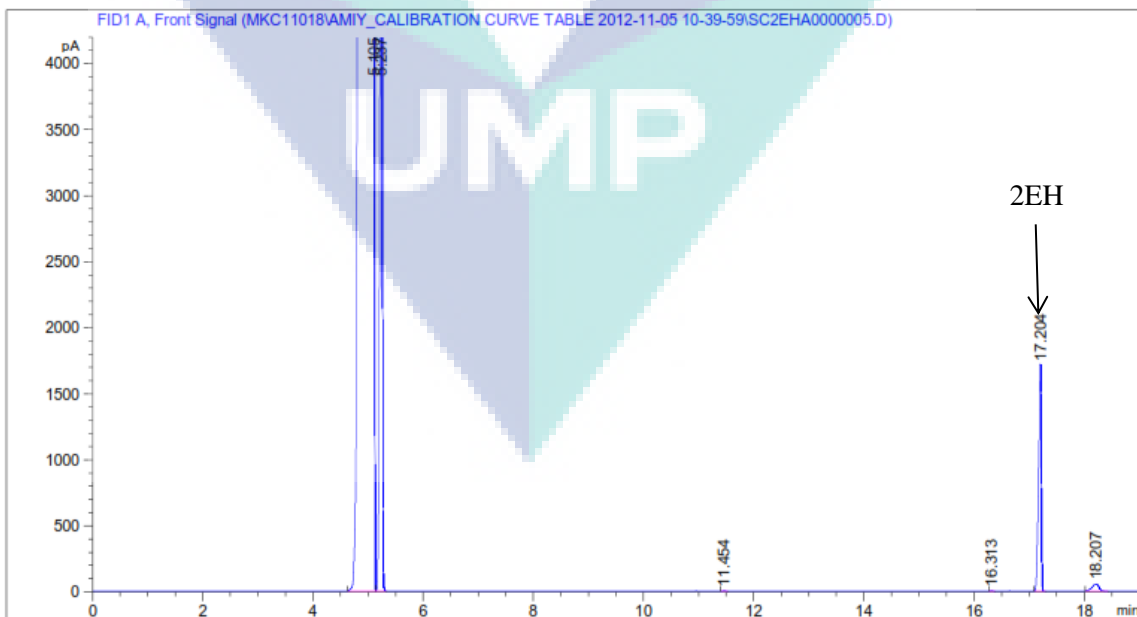


Figure B.2 GC-FID spectrometry of 4,000 ppm 2EHA

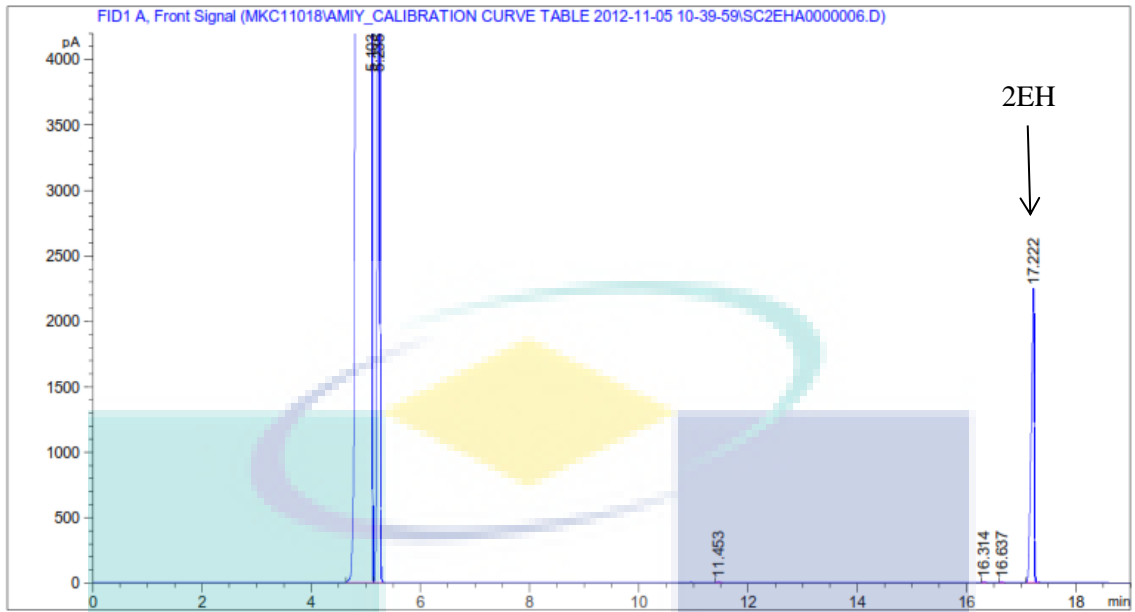


Figure B.3 GC-FID spectrometry of 6,000 ppm 2EHA

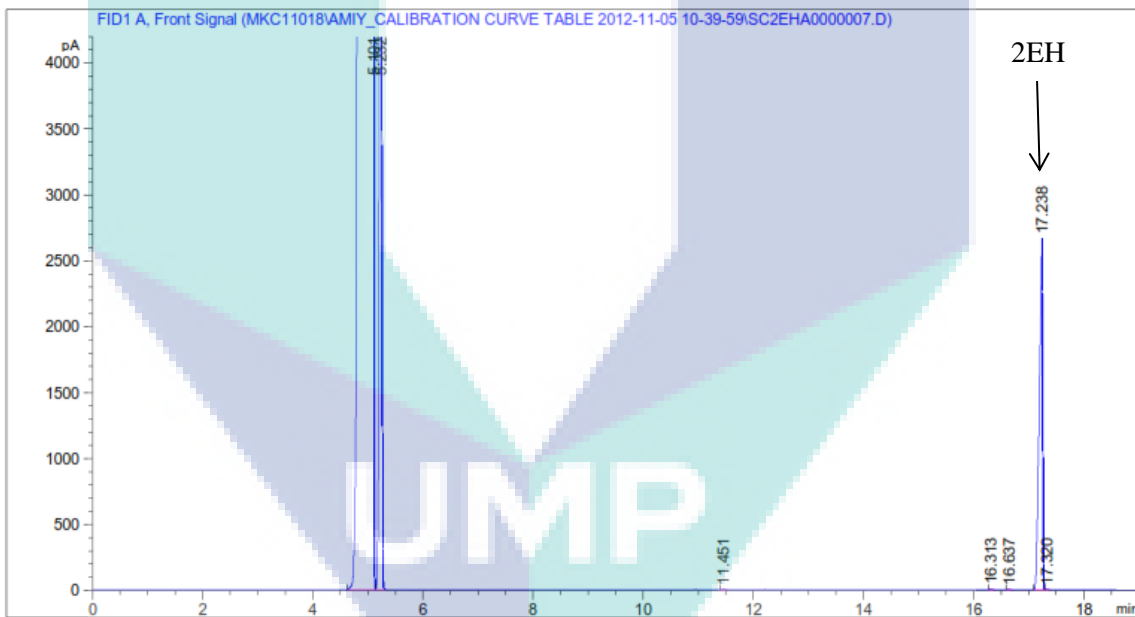


Figure B.4 GC-FID spectrometry of 8,000 ppm 2EHA

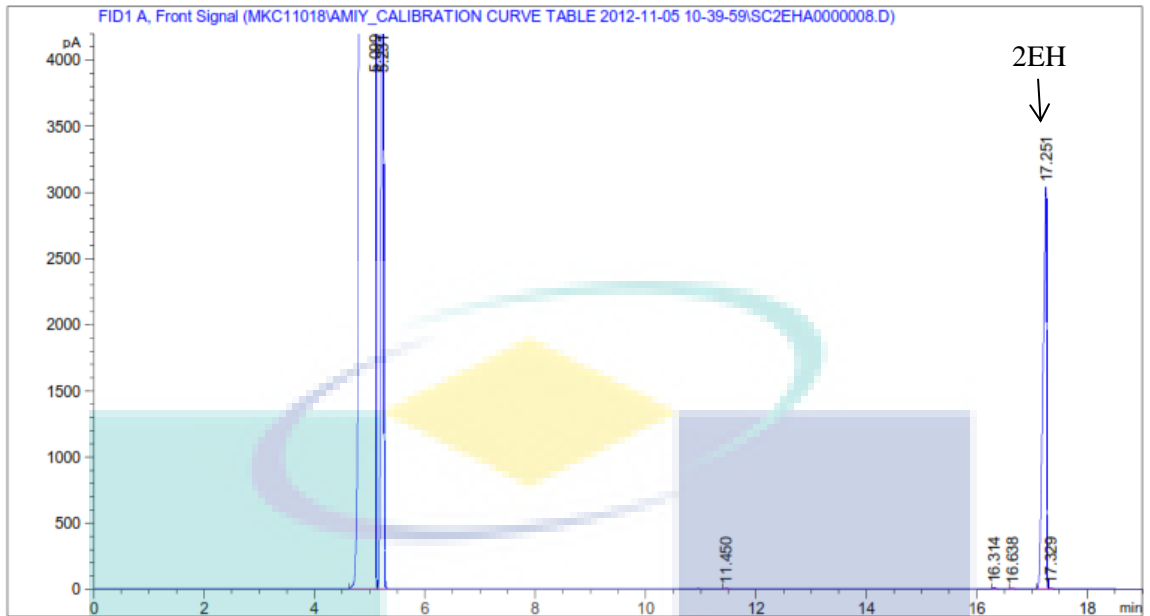


Figure B.5 GC-FID spectrometry of 10,000 ppm 2EHA

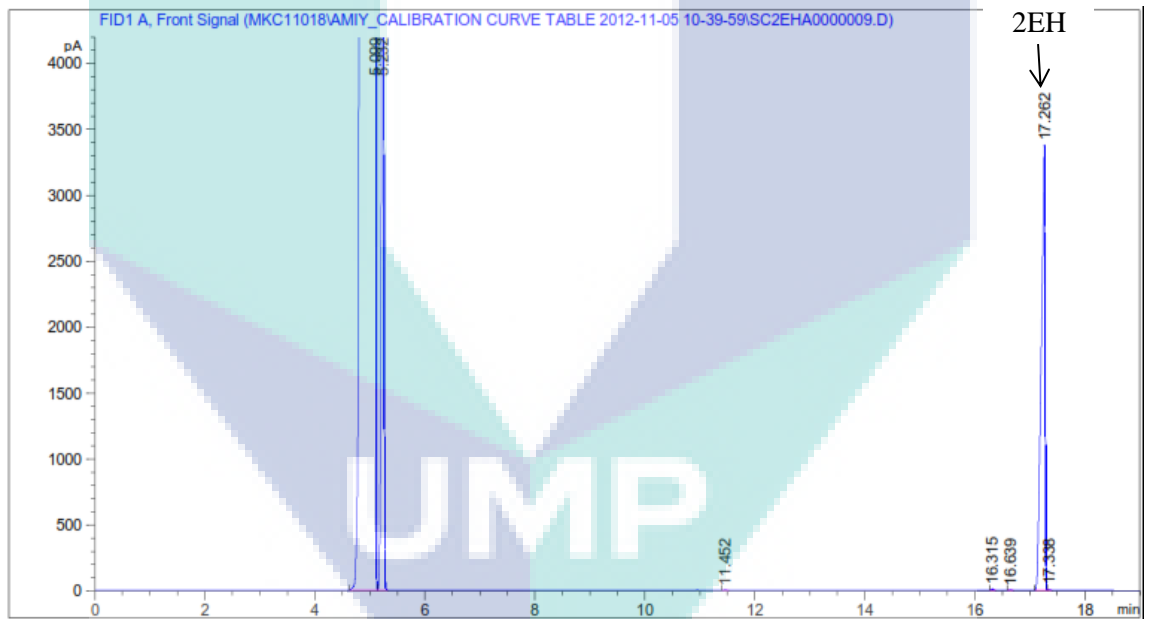


Figure B.6 GC-FID spectrometry of 12,000 ppm 2EHA

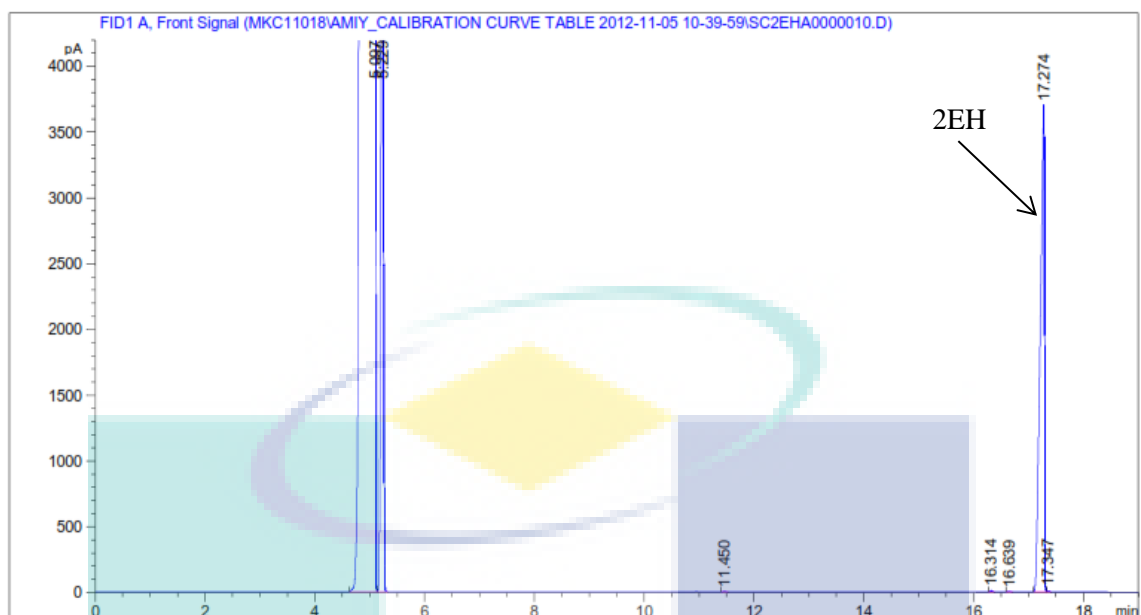


Figure B.7 GC-FID spectrometry of 14,000 ppm 2EHA

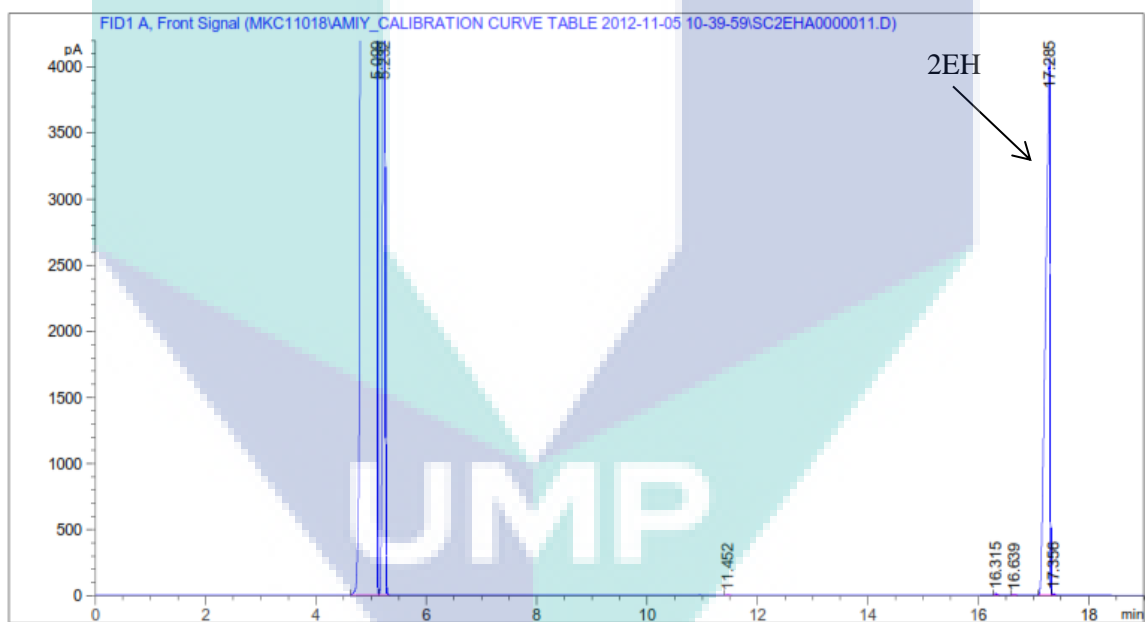


Figure B.8 GC-FID spectrometry of 16,000 ppm 2EHA

The retention time for 2EHA was detected at 17.2 min. The ABS-concentration data of standard calibration curve was included in table B1 and plotted in Figure B9.

Table B1: Concentration versus ABS for standard calibration curve plot of 2EHA

| concentration (ppm) | ABS (pA*s) |
|---------------------|------------|
| 0 | 0.000 |
| 2000 | 2921.603 |
| 4000 | 5844.755 |
| 6000 | 8702.682 |
| 8000 | 11464.200 |
| 10000 | 14178.100 |
| 12000 | 16817.200 |
| 14000 | 19797.600 |
| 16000 | 22472.300 |

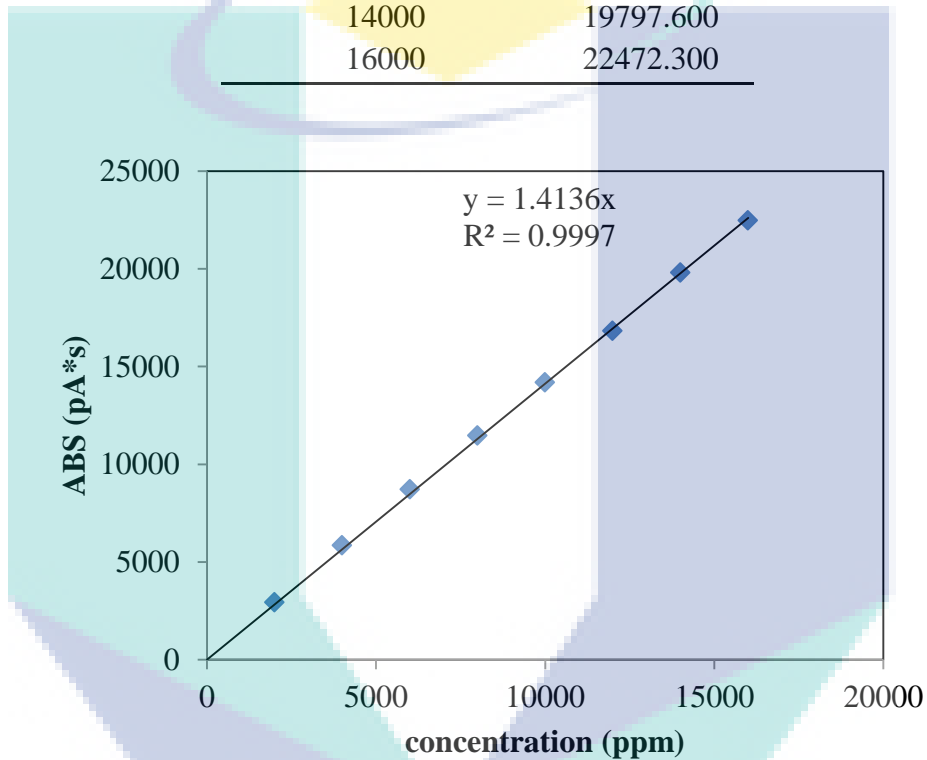


Figure B.9 Calibration curve for 2EHA using GC-FID

From the Figure B9, the following equation was developed to calculate the unknown concentration of 2HA for each sample using the absorbance given by GC-FID analysis:

$$ABS_{2EHA} = m \times C_{2EHA} \quad (B1)$$

$$C_{2EHA} = \frac{ABS_{2EHA}}{m} \quad (B2)$$

$$C_{2EHA} = \frac{ABS_{2EHA}}{1.4136} \quad (B3)$$

$$C_{2EHA} = 0.707 \times ABS_{2EHA} \quad (B4)$$

$$Yield_{2EHA} = \frac{C_{2EHA}}{C_{AA\ initial} - C_{AA\ final}} \times 100\% \quad (B5)$$

Appendix C

UNIFAC (VLE) for Esterification AA with 2EH

| | | |
|--------|----------|------|
| P= | 111.0182 | mmHg |
| T(°C)= | 100 | °C |

As distributed, this cell has a formula to calculate the bubble pressure.

Table 1. Antoine Coefficients (mmHg) $\log_{10}(P^{sat})=A-B/(T+C)$ where T[=] °C

| | comp1 | comp2 | comp3 | comp4 | comp5 |
|------------------|-----------|-----------|---------|----------|-----------|
| A | 8.87829 | 8.07131 | | 8.1122 | 6.87632 |
| B | 2010.33 | 1730.63 | | 1592.864 | 1075.78 |
| C | 252.636 | 233.426 | | 226.184 | 233.205 |
| P^{sat} [mmHg] | 1504.6159 | 760.08637 | | 1693.832 | 4443.6208 |
| y_i | 1.00000 | 10.81294 | 0.00000 | 9.59272 | 0.00000 |

Enter Antoine constants or vapor pressures if you want bubble P and vapor phase concentrations calculated automatically.

Table 2. Component Structure Information and Activity Coefficient Calculation.

| | comp1 | comp2 | comp3 | comp4 | comp5 |
|------------------------|-----------|--------|---------|---------|---------|
| x_i | AA | Water | 2EH | 2EHA | |
| γ_i | 0.727 | 3.963 | 1.213 | 1.578 | 0.951 |
| SubGroup | | | | | |
| 1 | CH3 | | 2 | 2 | 1 |
| 2 | CH2 | | 5 | 4 | 1 |
| 3 | CH | | 1 | 1 | |
| 5 | CH2=CH | 1 | | 1 | |
| 10 | AC | | | | |
| 11 | ACCH3 | | | | |
| 12 | ACCH2 | | | | |
| 14 | OH | | 1 | | |
| 15 | CH3OH | | | | |
| 16 | H2O | | 1 | | |
| 17 | ACOH | | | | |
| 18 | CH3CO | | | | |
| 20 | CHO | | | | |
| 21 | CH3COO | | | | |
| 22 | CH2COO | | | 1 | |
| 36 | ACNH2 | | | | |
| 42 | COOH | 1 | | | |
| 49 | CCL2 | | | | |
| 51 | CCL3 | | | | |
| 99 | CON(CH2)2 | | | | |
| $\sum_k v_k^{(i)} x_i$ | 0.203 | 0.3985 | 0.9135 | 3.5865 | 2E-20 |
| N groups | 2 | 1 | 9 | 9 | 2 |
| q | 2.4000 | 1.4000 | 5.8240 | 6.6800 | 1.3880 |
| r | 2.6467 | 0.9200 | 6.6211 | 7.9685 | 1.5755 |
| θ_i | 0.0601 | 0.1376 | 0.1458 | 0.6565 | 0.0000 |
| Φ_i | 0.0599 | 0.0818 | 0.1499 | 0.7084 | 0.0000 |
| $\ln \gamma^C$ | -0.1173 | 0.0135 | -0.0756 | -0.1034 | -0.3947 |
| $\ln \gamma^{R0}$ | 1.2029 | 0.0000 | 1.9433 | 0.9151 | 0.0000 |
| $\ln \gamma^R$ | 1.0013 | 1.3636 | 2.2118 | 1.4744 | 0.3441 |

Vapor phase mole fractions calculated automatically.

Liquid phase mole fractions. Enter a very small number like 1E-20 or smaller for absent compounds - don't use zero.

Enter the number of occurrences of a chemical structure in this table for each component. Residual group interaction parameters are not available for all groups, and are treated as zero if unavailable. Check Table 1 on sheet "ajj-UNIFAC (VLE)".

The sub-groups available in this table may be changed in this column by changing the SubGroup number. If you change a sub-group here, be sure to edit the component structure information in the table. Available subgroups and subgroup numbers are in Table 2 of sheet "ajj-UNIFAC (VLE)".

Note that columns H:AS are hidden. They contain intermediate calculations. Unprotect the sheet and unhide them to see the calculations.

Appendix D

Sample of Calculation For Mears Criterion

$$C_M = \frac{r_{A,obs} \times \rho_b R_c \times n}{K_c \times C_{Ab}} < 0.15 \quad (D.1)$$

Where:

- $r_{A,obs}$: Reaction rate
- ρ_b : Bulk density of catalyst
- R_c : Catalyst radius
- n : Reaction order
- C_{ab} : Bulk concentration of limiting reactant

Reaction rate, $r_{A,obs}$

$$r_{A,obs} = \frac{\text{moles of limiting reactant in reaction time, } t \text{ (mol)}}{\text{catalyst loading (gcat)} \times \text{reaction time, } t \text{ (s)}} \quad (D.2)$$

Table D.1 Reaction rate, $r_{A,obs}$

| Mol AA at time, t | Catalyst loading (g) | $r_{A,obs}$ (kmol/kg.s) |
|-------------------|----------------------|-------------------------|
| 0.161602 | 3 | 0.0539 |
| 0.150145 | 3 | 0.0501 |
| 0.142996 | 3 | 0.0477 |
| 0.141241 | 3 | 0.0471 |

Mass transfer coefficient, K_c

$$K_c = \frac{2D_{AB}}{d_p} + 0.31 N_{Sc}^{-2/3} \left(\frac{\Delta\rho\mu_c g}{\rho_c^2} \right)^{1/3} \quad (D.3)$$

Diffusivity, D_{AB}

Obtain from multi component diffusivity correlation from Perkin and Geankoplis method as shown below:

$$D_{Am}\mu_m^{0.8} = \sum_{\substack{j=1 \\ j \neq A}}^n x_j D_{Aj} \mu_j^{0.8} \quad (D.4)$$

Where

- D_{Am} : Dilute diffusion coefficient of A through mixture
- μ_m : Mixture viscosity
- D_{Aj} : Dilute binary diffusion of A in j
- X_j : Mole fraction

D_{Aj} is obtain from Wilke-Chang correlation from Perry Handbook

$$D_{AB}^o = 1.173 \times 10^{-8} (\Phi_B M_B)^{1/2} \frac{T}{\mu_B V_A^{0.6}} \quad (D.5)$$

Where,

- Φ : Association parameter of solvent
- M_B : Molecular weight of solvent B, kg/mol
- T : Temperature, K
- μ_B : Viscosity of B, kg/m.s
- V_A : Specific molar volume of limiting reactant, m³/kg mol

Atomic volume (m³/kg mol) values are shown in Table below (from Geankoplis)

Table D.2 Atomic volume for each compound

| Compound | Atomic volume (m ³ /kg mol) |
|----------|--|
| C | 14800 |
| H | 3700 |
| O | 7400 |

The atomic volume for butanol (C₄H₁₀O) is 192400 m³/kg mol

The viscosity of mixture:

$$\ln \mu_m = \sum_{i=1}^n x_i \ln \mu_i \quad (D.6)$$

Where:

- μ_m : Viscosity mixture
- x_i : Mole fraction
- μ_i : Viscosity of fraction

From Yaw's Handbook, the viscosities of i^{th} component

Table D.3 Viscosity of ith component

| Comp | A | B | C | D | T | log ₁₀ (μ liq) | μ liq (cp) | μ (kg/m.s) |
|------|---------|--------|--------|----------|--------|------------------------------|---------------|---------------|
| AA | -15.418 | 2354.1 | 0.0336 | -2.74E-5 | 353.15 | -0.298 | 0.5040 | 5.04E-4 |
| 2EH | -5.397 | 1325.6 | 0.0062 | -5.51E-6 | 353.15 | -0.141 | 0.7236 | 6.24E-4 |

The viscosity of mixture is 0.000564 kg/ms

The $D_{Aj}=D_{AB}^0$

Table D.4 Calculated value for each parameter

| Parameter | Value |
|-------------------------------------|-------------|
| Φ | 1 |
| M (kg/kmol) | 72.06 |
| x _j | 0.5 |
| T (K) | 353.15 |
| Mm(kg/m.s) | 0.000603854 |
| DA _j (m ² /s) | 4.75793E-05 |

So, the diffusivity of A through mixture is 2.7493×10^{-5} m²/s

Density calculation:

From Albright Handbook and assume the liquid mixture is ideal

$$v^{id} = \sum_i x_i v_i \quad (D.7)$$

Where V is molar volume (m³/mol). The density of component are calculated based on Yaw's Handbook

$$\rho \text{ (g/cm}^3\text{)} = A(B^{-(1-T/T_c)^n}) \quad (D.7)$$

Table D.5 Calculated density and molar volume based on Yaw's Handbook

| | A | B | n | T _c | T | ρ (g/cm ³) | V (m ³ /mol) |
|-----|--------|--------|--------|----------------|--------|------------------------|----------------------------|
| AA | 0.3322 | 0.2515 | 0.2946 | 498 | 353.15 | 0.37391 | 0.000192731 |
| 2EH | 0.2689 | 0.2667 | 0.2457 | 562.93 | 353.15 | 0.303491 | 0.000344235 |

Molar volume is 0.0002184

Molar mass of mixture

$$M = \sum_i x_i MW_i \quad (D.8)$$

M= 0.07309kg/mol

So, the density of liquid mixture is 334.55 kg/m³

Schmidt number, N_{sc}

$$N_{Sc} = \frac{\mu_c}{\rho_c D_{AB}} \quad (D.8)$$

Where

μ_c : Viscosity of mixture (kg/m.s)

ρ_c : Density of mixture (g/ml)

D_{AB} : Diffusivity (m²/s)

So, the Schmidt number is 0.01717

Mears Criterion for different stirring rate:

Table D.6 Calculated Mears Criterion from 2 factorial experimental studies

| Experiment | Mears Criterion (C _M) |
|------------|-----------------------------------|
| 1 | 0.077 |
| 2 | 0.092 |
| 3 | 0.091 |
| 4 | 0.103 |
| 5 | 0.099 |
| 6 | 0.087 |
| 7 | 0.099 |
| 8 | 0.079 |
| 9 | 0.075 |
| 10 | 0.089 |
| 11 | 0.094 |
| 12 | 0.089 |
| 13 | 0.077 |
| 14 | 0.079 |
| 15 | 0.082 |
| 16 | 0.101 |
| 17 | 0.080 |
| 18 | 0.083 |
| 19 | 0.079 |

Appendix E

Sample of Calculation of Weisz-Prater Criterion (C_{WP})

$$C_{WP} = \frac{-r_{A,obs} \rho_c R_c^2}{D_{eff} C_{li}} < 1 \quad (E.1)$$

Where:

- $-r_{A,obs}$: Reaction rate at given time, t
- ρ_c : Catalyst density
- R_c : Effective radius of catalyst
- D_{eff} : Effective diffusivity
- C_{li} : Concentration of limiting reactant in mixture

Effective diffusivity

$$D_{eff} = D_{AA} \left(\frac{\varepsilon}{\tau} \right) = D_{AA} \times \varepsilon^2 \quad (E.2)$$

$$\varepsilon_p = \frac{V_{pore}}{V_p} = \frac{\rho_s - \rho_p}{\rho_s} \quad (E.3)$$

The porosity is 0.279 and effective diffusivity is 0.03704cm²/s.

True radius

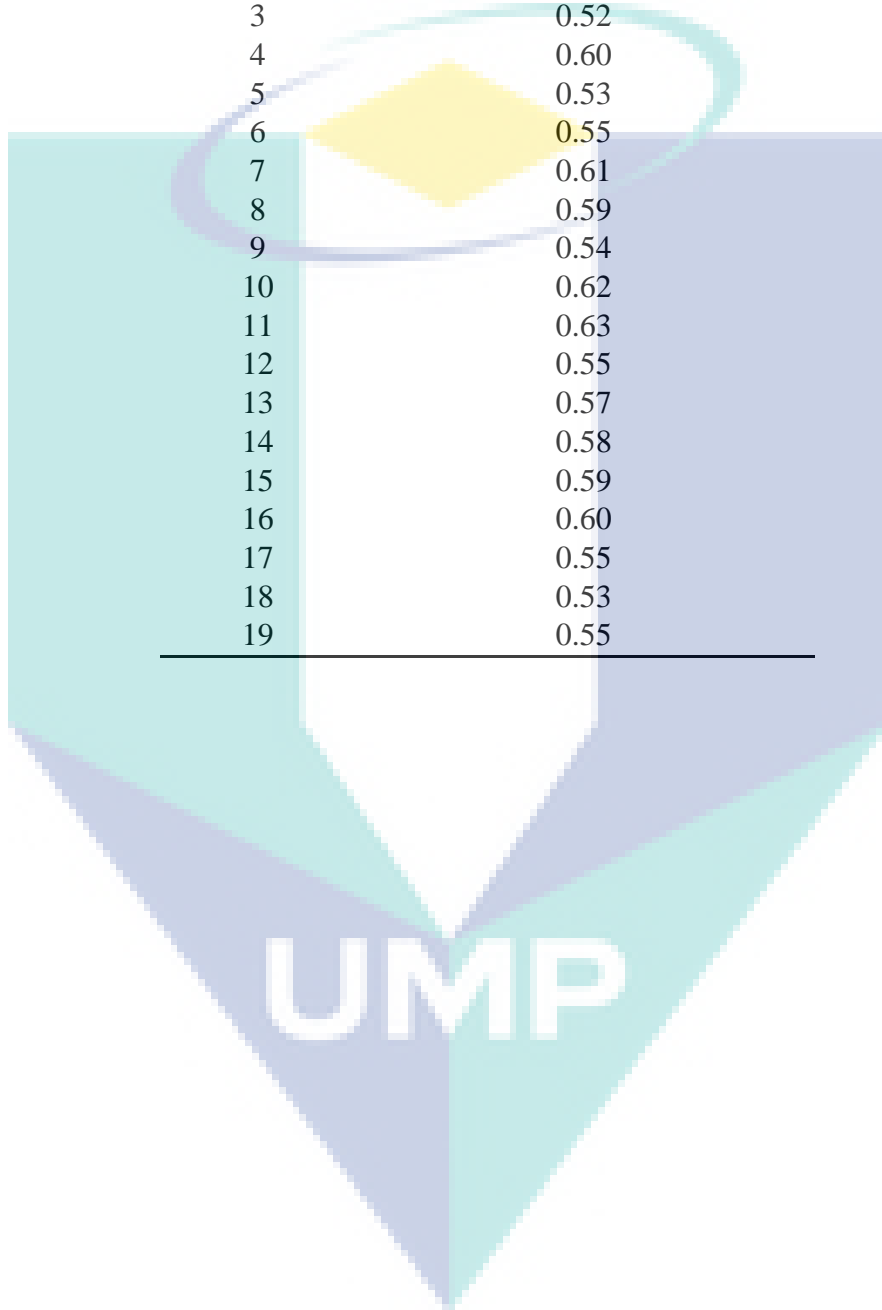
The 'true radius' calculated based on equation below and assumed that SK1B is sphere.

$$R = \sqrt[3]{\frac{\text{swelling in mixture (\%)}}{\text{swelling in BuOH (\%)}}} \times \text{mean radius} \quad (E.4)$$

The SK1B swell in reaction mixture is 280% and in BuOH is 240%. The radius is 0.55mm and the 'true' radius is 0.5540mm. The density of catalyst is 1.279 g/cm³. The C_{WP} is calculated and values shows below:

Table E.1 Calculation of Weisz-Prater Criterion (C_{WP}) from 2 factorial experimental studies

| Experiment | Weisz - Prater parameters (C_{WP}) |
|------------|---|
| 1 | 0.55 |
| 2 | 0.59 |
| 3 | 0.52 |
| 4 | 0.60 |
| 5 | 0.53 |
| 6 | 0.55 |
| 7 | 0.61 |
| 8 | 0.59 |
| 9 | 0.54 |
| 10 | 0.62 |
| 11 | 0.63 |
| 12 | 0.55 |
| 13 | 0.57 |
| 14 | 0.58 |
| 15 | 0.59 |
| 16 | 0.60 |
| 17 | 0.55 |
| 18 | 0.53 |
| 19 | 0.55 |



Appendix F

List of Publication

- Chin, S. Y., Ahmad, M. A. A., Kamaruzaman, M. R., & Cheng, C. K. (2015). Kinetic studies of the esterification of pure and dilute acrylic acid with 2-ethyl hexanol catalysed by Amberlyst 15. *Chemical Engineering Science*, **129**, 116–125.
- Chin, S. Y., Kamaruzaman, M. R., & Ahmad, M. A. A. (2016). Synthesis and Characterization of Dealuminated Ultra-Stable Zeolite Y Supported Cesium Salt of Phosphotungstic Acid for the Esterification of Acrylic Acid with Butanol. *Chemical Engineering Communications*, **203**(11), 1515–1522.
- Ahmad, M. A. A., & Chin, S. Y. (2017). Screening of Catalyst and Important Variable for the Esterification of Acrylic Acid with 2 Ethylhexanol. *IOP Conference Series: Materials Science and Engineering*, **206**(1).
- Sim Yee Chin, Nurwadiyah Azizan, Mohd Amirul Asyraf Ahmad and Muhammad Ridzuan Kamaruzaman (2019). Ion Exchange Resins Catalysed Esterification for the Production of Value Added Petrochemicals and Oleochemicals. *Applications of ion exchange materials in chemical and food industries. Applications of Ion Exchange Materials in Chemical and Food Industries*. Springer International Publishing. 75-98.
- Ahmad, M. A. A. Bin, Chin, S. Y., & Abidin, S. B. Z. (2019). Kinetic studies of the esterification of acrylic acid with 2-Ethyl hexanol catalysed by diaion resins. *Journal of Chemical Engineering of Japan*, **52**(4), 342–348.